To the Graduate Council:

I am submitting herewith a thesis written by Kurt Allison Boyd entitled "Compressive Strength and Constitutive Behavior of Structural Clay Tile Prisms". I have examined the final copy of this thesis for form and content and recommend that it be accepted in partial fulfillment of the requirements for the degree of Master of Science, with a major in Civil Engineering.

Richard M. Bennett

Dr. Richard M. Bennett, Major Professor

We have read this thesis and recommend its acceptance:

W. Goodpasture

Edwin G. Burdette

Accepted for the Council:

C. W. Minkel

Associate Vice Chancellor
and Dean of the Graduate School

STATEMENT OF PERMISSION TO USE

In presenting this thesis in partial fulfillment of the requirements for a Master's degree at the University of Tennessee, Knoxville, I agree that the library shall make it available to borrowers under rules of the Library. Brief quotations from this thesis are allowable without special permission, provided that accurate acknowledgement of the source is made.

Permission for extensive quotation from or reproduction of this thesis may be granted by my major professor, or in his absence, by the Head of Interlibrary Services when, in the opinion of either, the proposed use of the material is for scholarly purposes. Any copying or use of the material in this thesis for financial gain shall not be allowed without my written permission.

Signature Kurt Burl

Date 3/10/93

COMPRESSIVE STRENGTH AND CONSTITUTIVE BEHAVIOR OF CLAY TILE PRISMS

A Thesis

Presented for the

Master of Science

Degree

The University of Tennessee, Knoxville

Kurt Allison Boyd

May 1993

DEDICATION

This thesis is dedicated to my parents Mr. Gene Boyd and Mrs. Mary Ann Boyd. Their love and support has provided me with invaluable educational opportunities.

ACKNOWLEDGEMENTS

This thesis could not have been completed without the help from a large number of people. I would like to express my appreciation to my major professor, Dr. Richard M. Bennett, for his guidance and tolerance. I would also like to thank Dr. Edwin Burdette for taking time to oversee the testing and answering the numerous questions that confronted me. I want to thank Dr. David Goodpasture for serving on my committee and Roger Flanagan, who supplied an abundance of valuable information. I want to thank Dr. Francis Oluokun, Jim Bernardi, George Barclay, Chris Columber, and Joele Fowler for their essential contributions. Finally, I want to thank Martin-Marietta Energy Systems for their financial support. Their funding and personnel allowed the project to continue without interruption.

ABSTRACT

Thirty - one structural clay tile prisms were tested in uniaxial compression. Twenty - three of these prisms were 8" thick, and the remainder were 13" thick. The prisms were constructed with running bond, a full bed joint, and face shell bedding for the head joint. The 8" prisms were tested at various angles to bed joint. The 13" prisms were tested with the bed joint either horizontal or vertical. The prism failure pattern depended on the bed joint angle. The failures were the result of slipping along the bed joint, cracks along principal stresses, or a combination of the two.

The stress - strain relations were determined by linear variable displacement transducers over gage lengths that included mortar joints. The stress - strain curve was approximately linear up to about 33% of ultimate stress. From 33% of ultimate to ultimate, an exponential fit was more appropriate to model the curve. This non-linear behavior in the upper portion of the stress - strain curve was influenced by mortar joint deformations.

Several of the prisms were loaded, unloaded, and reloaded during the test to observe the effect of the cycling load. There appeared to be little difference in the results with this loading pattern and the monotonically loaded prisms. Beyond ultimate stress, plastic deformations were apparent in

the prisms under a cyclic load. When the prism was reloaded, the strain increased dramatically from what it had been at unloading.

The testing program showed the wide variation that can exist in prism testing. Many factors, including construction practices, affect the results.

TABLE OF CONTENTS

CHAPTER		PAGE
1.	INTRODUCTION AND PURPOSE	1
2.	LITERATURE REVIEW	4
	Introduction	4
	The Effects of Testing Variables on the Behavior of Masonry Prisms	4
	Typical Results for Compressive Testing of Masonry Prisms	9
	Current Code Provisions for Masonry Design	23
3.	TESTING PROCEDURE FOR STRUCTURAL CLAY TILE PRISMS	25
	Introduction	25
	Prism Construction	25
	Testing Apparatus	31
	Instrumentation Description	33
	Testing Procedure	34
	Pre-Test Events	36
	Test Events	39
	Post-Test Events	39
4.	STRUCTURAL CLAY TILE PRISM STRENGTH	40
	Introduction	40
	Tile Strength	40
	Prism Strength Test Results	41
	Prism Mode of Failure	44

Discussion of Strength Tests.....50
Comparison of Results with Previous Research.....54
5. CONSTITUTIVE BEHAVIOR OF STRUCTURAL CLAY TILE PRISMS...57
Introduction.....57
Prism Stress - Strain Curves.....57
Prism Elastic Behavior.....58
Constitutive Behavior During Load - Unload Cycling.....74
Logarithmic Relationship of Stress - Strain Curve.....79
6. CONCLUSIONS.....85
BIBLIOGRAPHY.....89
APPENDICES.....96
Appendix A (Sample Data Sheets).....97
Appendix B (Fortran Program for Control Data Modification).....110
Appendix C (Photographs).....113
VITA.....123

LIST OF TABLES

TABLE		PAGE
2-1	ASTM-C270 Required Mortar Strength	8
2-2	Effect of Varying Sand on the Compressive Strength	8
2-3	Effect of Mortar Strength on Prism Strength	10
2-4	Effect of Mortar Joint Thickness on Prism Strength	10
2-5	Prism Compression Test Results (Johnson and Matthys,1973)	16
2-6	Results of Prism Compression Tests (SCPRF,1967)	18
2-7	Prism Compression Test (Hamid and Drysdale,1980)	20
2-8	Prism Compression Test (Khattab and Drysdale,1980)	22

LIST OF FIGURES

FIGURE		PAGE
2.1.1	Variation of Compressive Strength with Shape of Specimen (Krefeld,1938)	6
2.2.1	Compression Test Results (Whittemore and Hathcock,1923)	12
2.2.2	Compression Strength Results (Stang et al.,1926)	14
2.2.3	Tile Block Dimensions (SCPRF,1967)	17
3.1.1	Cross-Sectional Dimensions of SCT Tile	26
3.1.2	Group A SCT Prisms	27
3.1.3	SCT Prisms in Group B	29
3.1.4	Frame for Angled Prism Construction	30
3.1.5	Template Layout on Existing Wall	31
3.2.1	Testing Frame for Prism Uniaxial Compression Test.	32
3.3.1	LVDT Location on Test Specimen	33
3.3.2	Instrumentation and Control Schematic for Prism Test	35
3.4.1.1	Strapping for Transporting of Prisms	37
4.1.1	Description of Unit Tiles	41
4.2.1	Description of Clay Tile Prisms	42
4.2.2	Prism Strength Results	43
4.2.3	Prism Net Strength	45
4.2.4	Net Areas Used in Strength Calculations	46
4.3.1	Prism Cracking Pattern at Failure	47

4.3.2 Cracking Pattern of 13" Prisms.....50
4.4.1 Average Gross Strength of Tested Prisms.....51
4.4.2 Strength Variation Due to Bed Joint Angle.....52
4.5.1 Comparison of Similar Uniaxial Compression Tests..55
5.1.1 Stress - Strain Curve for UT8-0-1.....59
5.1.2 Stress - Strain Curve for UT8-90-1.....60
5.1.3 Stress - Strain Curve for UT8-22-1.....61
5.1.4 Stress - Strain Curve for UT8-45-1.....62
5.1.5 Stress - Strain Curve for UT13V-1.....63
5.1.6 Stress - Strain Curve for UT8V-4.....64
5.1.7 Stress - Strain Curve for UT8-90-3.....65
5.1.8 Stress - Strain Curve for UT13V-3.....66
5.2.1 Modulus of Elasticity for Clay Tile Prisms.....67
5.2.2 Average Elastic Modulus for Clay Tile Prisms.....69
5.2.3 Modulus of Elasticity from Past Research.....70
5.2.4 Strain at Maximum Stress from Stress-Strain Curves.....72
5.2.5 Poisson's Ratio at 33% and 50% of Ultimate Stress.....73
5.3.1 Location of Pre-Peak Rebound Moduli for Prism UT8-90-3.....76
5.3.2 Location of Post-Peak Rebound Moduli for Prism UT8-90-3.....77
5.3.3 Pre-Peak Rebound Modulus.....78
5.3.4 Post-Peak Rebound Modulus.....78

5.4.1 Least-Squared Linear Fit of UT8V-3 (Standard Space).....80
5.4.2 Least-Squared Linear Fit of UT8V-3 (Log - Log Space).....82
5.4.3 Results of Least-Squared Linear Fit for Clay Tile Prisms.....83
5.4.4 Average Coefficients for Log-Log Plot.....84

Chapter 1

INTRODUCTION AND PURPOSE

A recent interest has developed concerning the strength capabilities of structures consisting of structural clay tile. Before the 1940's, clay tile in frame structures was simply viewed as dead weight, ignoring the structural potential of tile infilled frames. Research in the area of clay tile has increased with the need to conserve material cost and labor. As a result of the research, empirical formulae were developed to determine the racking load strengths of infilled frames. The empirical equations required that the unit compressive strength of the structural clay tile be known.

As early as 1923, researchers examined the most appropriate manner to determine the compressive strength of clay tile. It was found that the unit strength based on tests using individual tile units was highly unconservative because of end restraint and the absence of mortar joints. Prisms of various sizes were then constructed in order to determine their effectiveness in predicting strength. It was determined that a large number of variables can affect the results of the uniaxial compression test. Therefore, the construction of the prisms should be performed in the same manner as the actual construction so that a valid compressive strength can be determined.

In 1991, the University of Tennessee, Knoxville under contract with Martin - Marietta Energy Systems began research on the racking strength of masonry infilled frames subjected to in-plane loading. As part of the testing program, thirty-one prisms were constructed and tested under a uniaxial compressive load.

The purpose of this thesis is to describe the procedure for making prisms and performing uniaxial compression tests and to present the findings of these tests. The ultimate strength and behavior of the prisms were measured and analyzed.

Seven different types of prisms were constructed. The prisms were 2-ft. x 4-ft. with thicknesses of 8 and 13 inches. The 8 inch prisms were single wythe construction, and the 13 inch prisms were double wythe construction. The 8 inch prisms were tested with bed joint angles of 0°, 22.5°, 45°, 67.5°, and 90° to a horizontal plane. The 13 inch prisms had a bed joint angle of either 0° or 90°.

The uniaxial compression tests were conducted on each prism noting the ultimate load and the mode of failure. Prisms were tested under either a monotonic load or a loading - unloading pattern. Deformations were obtained from a control linear variable displacement transducer (LVDT) and 8 panel LVDTs mounted to the prism. Six of the panel LVDTs were placed vertically so that the vertical displacement could be

monitored. The remaining two LVDTs were placed horizontally to measure the lateral expansion of the prism.

The data collected were used to produce stress - strain curves for all the prisms. Representative constitutive parameters were obtained from the stress - strain curves.

The thesis is divided into four major sections. The first section describes the findings of previous research involving uniaxial tests of structural clay tile or concrete block prisms. The next section details the program followed for the prism tests carried out at The University of Tennessee. The third section presents the compressive strength results along with a detailed description of the modes of failure. The final section examines the constitutive behavior of the prisms under both monotonic load and a load-unload pattern.

Chapter 2

LITERATURE REVIEW

Introduction

The following sections are a brief look at the pertinent research that has been conducted on clay tile, brick, and concrete masonry prisms. Attempts to develop universal equations to describe the compressive behavior of masonry prisms have not been very successful. A large number of variables can cause a wide variation in test results. The first section examines these variables and discusses their effect on the behavior of the prism. The next section is a summary of the results of various tests that have been performed in the past. The final section discusses current code provisions for the design of masonry structures using prism test results.

2.1 The Effects of Testing Variables on the Behavior of Masonry Prisms

Early tests conducted on masonry prisms indicated that results were highly susceptible to testing variables. Factors that affect prism strength include material properties and testing parameters. Kingsley et al. (1992) report that the most important of these parameters include prism slenderness, number of courses, end restraint, capping configuration and

materials, mortar bedding and thickness, bonding pattern, bearing plate thickness, and workmanship in the prism construction.

According to Monk (1967), the most significant factor that affects the strength of the masonry prism is the slenderness ratio. If a specimen with a very low height to thickness ratio (h/t) is tested, the resulting failure mode will be a shear failure rather than the compressive failure that is desired. One of the earliest works investigating the impact of the slenderness ratio on compressive strength was conducted by Krefeld (1938). He found that the effect on the compressive strength, f'_m, was dramatic for very low h/t ratios (see figure 2.1.1). The effect on the strength was reduced as the slenderness ratio was increased. Krefeld concluded that an h/t ratio less than 6 would result in an unconservatively high strength. He suggested the use of strength correction factors that could be applied to smaller ratios to correct for this situation. Krefeld's findings were later verified by Francis et al. (1971). Instead of advocating the use of correction factors, they advised that a minimum of 4 courses be used in the standard prism test. Watstein and Allen (1971) observed that the relationship between strength and slenderness was similar for both high and low strength mortars.

Platen restraint and bearing plate thickness can have a dramatic effect on test results. Platen restraint is caused by

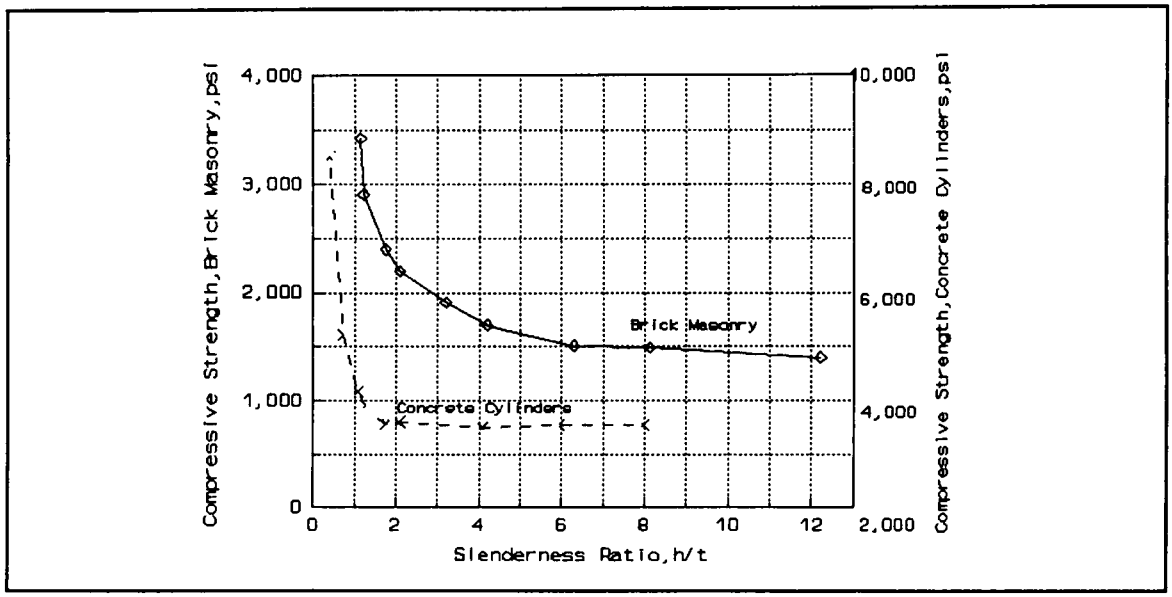


FIGURE 2.1.1 Variation of Compressive Strength with Shape of Specimen (Krefeld,1938)

a capping compound with a higher modulus than the masonry, or by friction between the prism and platen. Platen restraint can cause an overestimation of the compressive strength of the prism. Hegemier (1978) advises that either a capping compound with a low shear modulus or a prism with at least 4 courses be utilized. According to Page and Shrive (1988) it is very important to cap in the same configuration as the tile bedding. Their studies indicated that for hollow concrete masonry prisms, full capping has been observed to reduce the strength of face-shell bedded specimens by up to 50 percent. Therefore, for face shell bedded prisms, face shell capping should be used. Mayes and Clough (1975) note, however, that the effects of capping can be virtually ignored by using a large h/t ratio.

The bearing plate thickness will determine if the load is uniformally applied to the prism. A thin plate may result in a concentrated stress area at the top. Because of the smaller area, larger tensile stresses may form in the top portion and result in premature failure. Hamid and Chukwunenye (1986), based on analysis, advised using 4 inches as a minimum plate thickness, with a thicker plate being desirable.

Attempts have been made to correlate the strength of the masonry unit block to that of the masonry tile prism or wall. The most comprehensive testing was done by the U. S. Department of Commerce (1926) where 708 individual tests were analyzed. Their findings showed no corresponding relationship between unit strength and masonry strength. Mayes and Clough (1975) attribute this lack of correlation to the different modes of failure. The single unit is a shear failure, while the wall or prism is a tensile failure.

Mortar composition is very succeptible to variation. ASTM C-144 designates minimum properties and diameters for the sand-cement mix. The mix is based on the amount of cement required to fill voids in the sand. ASTM C-270 prescribes the required strengths for standard mortars given in Table 2-1.

Tests run by the Structural Clay Products Research Foundation (SCPRF) (1964) varied the ratio of the sand-cement mix to determine the effects on the mortar strength. Table 2-2 shows the results where the sand was varied between 2 1/4 to

Table 2-1 ASTM-C270 Required Mortar Strength

ASTM Mortar Type	28-day Strength
M(1C:1/4L:3S)	2500 psi
S(1C:1/2L:4 1/2S)	1800 psi
N(1C:1L:6S)	750 psi
O(1C:2L:9S)	350 psi
K(1C:4L:15S)	75 psi

Table 2-2 Effect of Varying Sand on the Compressive Strength

ASTM Mortar	28-day Compressive Strength	
Type	MIX 1:2 1/4	MIX 1:3
M	7392 psi	5358 psi
N	3663 psi	2479 psi
K	643 psi	363 psi

3 parts by volume. The slight increase in sand had a major impact on the compressive strength of the mortar. The SCPRF (1965) issued a report on the effect of mortar strength on the compressive strength of prisms (see Table 2-3). The prisms were 4 by 8 by 16 inches, and were constructed using a single type brick. Going from type-M mortar to type-O mortar reduced the prism strength by approximately one-half, while the mortar strength was 1/12 as great. Therefore, it is apparent that mortar type does affect the prism strength, but not directly.

As with the mortar mixture, the joint thickness can affect the compressive strength of the prisms. Data obtained from the SCPRF (1965) using type-S mortar on prisms confirm this fact. Table 2-4 shows how the strength is decreased as the joint thickness is increased.

It is evident that a large number of factors can contribute to the tested strength of masonry prisms. Because of the range of variables, it is difficult to derive a formula or recommend a constant value for the strength of masonry prisms for masonry design. Many researchers have recommended that if a prism is used to determine the compressive strength of walls using similar construction is very important.

2.2 Typical Results for Compressive Testing of Masonry Prisms

Some of the earliest tests performed on hollow clay tile masonry walls were done by Whittemore and Hathcock (1923). The tiles were Ohio fire clay. The walls were 4 feet long and 12

Table 2-3 Effect of Mortar Strength on Prism Strength

Mortar Type	Mortar Prop. by Volume	Mortar Strength,psi	Prism Strength,psi
M	1C:1/4L:3S	2503	5805
S	1C:1/2L:4 1/2S	1292	5497
N	1C:1L:6S	579	3900
O	1C:2L:9S	262	2905

Table 2-4 Effect of Mortar Joint Thickness on Prism Strength

Mortar Joint Thickness,in.	Prism Compressive Strength,psi	Strength Ratio
1/4	6550	1.00
3/8	5850	0.89
1/2	4900	0.75
5/8	4050	0.62
3/4	3150	0.48

feet high. Plaster of Paris was used for capping the walls. Tiles were laid with the cores vertical or horizontal during construction. Figure 2.2.1 gives the results of the uniaxial compressive tests on the walls. The initial portion of the stress-strain curve was used to calculate the modulus of elasticity. Whittemore and Hathcock (1923) determined that there was no apparent correlation between the ultimate strength of the wall and the load observed at the first crack. They also found that walls built with cells laid vertically had approximately twice the strength of those having horizontal cells.

The mode of failure was either a crushing at the top or the emergence of vertical cracks through the joints. It was concluded that failure at the top resulted from the plaster cap having a weaker strength than the mortar joints.

Stang et al. (1926) performed tests similar to those done earlier by Whittemore and Hathcock. Tests, including uniaxial compressive tests, were run on 70 walls. Fifteen types of tile were considered including the ones listed below. The walls were 6 feet long and 9 feet high and were as follows:

Tile A : 6-Cell 8"x12"x12" Ohio Fire Clay

Tile B : 6-Cell 8"x12"x12" New Jersey Fire Clay

Tile C : 6-Cell 12"x12"x12" Ohio Fire Clay

Tile D : 3-Cell 3-¾"x12"x12" Ohio Fire Clay

The capping was done using plaster of Paris. The results obtained by Stang et al. (1926) were based on the nominal

Wall Thickness	Kind of Tile	Tile Size	Cell Orientation	Strength at 1st Crack net area (psi)	Mod of Elasticity net area (ksi)	Avg Strength gross area (psi)	Avg Strength net area (psi)
8"	Ohio Fire Clay	6-cell 12"x12"x12"	vertical	1790	1970	933	2260
8"	Ohio Fire Clay	4-cell 8"x12"x12"	vertical	1000	2640	1045	2310
8"	Ohio Fire Clay	4-cell 8"x12"x12"	vertical	930	1480	1022	2220
8"	Ohio Fire Clay	6-cell 12"x12"x12"	horizontal	430	3180	375	1670
8"	Ohio Fire Clay	4-cell 8"x12"x12"	horizontal	430	3770	393	1795
8"	Ohio Fire Clay	4-cell 8"x12"x12"	horizontal	400	3625	697	2570

Figure 2.2.1 Compression Test Results (Whittemore and Hathcock, 1923)

dimensions of the wall. The results found for the walls using the tiles listed above are given in figure 2.2.2. Results using the net area were calculated from the ratio of the net area and gross area of the individual tile.

Stang et al. (1926) observed that failure in the walls with vertical cells began by a crushing of the mortar and was followed by spalling of the tiles at the joints, and later by the appearence of cracks in the tiles. Failure in walls with horizontal cells also began with a crushing of the mortar. As the load was increased, cracks formed in the horizontal shells of the tiles. The cracks gradually extended vertically through the horizontal webs on the interior of the tiles.

Whittemore et al. (1938) extended his previous research and tested tile and brick masonry walls. Compression tests were run on 4′-2" by 8′-4" masonry walls constructed from Ohio fire clay. The tiles were 8" by 12" by 12" and had 6 cells. The mortar mix was 1 part cement, 1 part lime, and 6 parts sand (1C:1L:6S) by volume. Three walls were constructed with the cells laid vertically, and three with cells laid horizontally. The strength of the vertically and horizontally celled walls were found to be 496 and 271 psi, respectively. These were based on the gross area of the wall. The walls with horizontal cells failed by the crushing of one or more of the bed joints near the inside face. Whittemore et al. (1938) noted the appearance of vertical cracks through some of the tiles and joints on the outside face. Walls with horizontal

Wall Thickness	Tile Description	Cell Orientation	Mortar Ratio	Mod of Elasticity net area (ksi)	Avg strength gross area (psi)	Avg Strength net area (psi)
8"	A	vertical	1 1/4L:3S	368	90	221
8"	A	vertical	1C:1 1/4L:6S	1618	275	674
8"	A	vertical	1C:1 1/4L:4S	1701	460	1127
8"	A	vertical	1C:3S	2074	355	870
8"	A	horizontal	1 1/4L:3S	1225	165	727
8"	A	horizontal	1C:1 1/4L:6S	1829	285	1256
8"	A	horizontal	1C:1 1/4L:4S	2477	405	1785
8"	A	horizontal	1C:3S	2014	360	1587
8"	B	vertical	1C:1 1/4L:6S	1358	295	591
8"	B	horizontal	1C:1 1/4L:4S	2011	230	1012
12"	C	vertical	1C:1 1/4L:6S	2255	335	889
12"	A and D	vertical	1C:1 1/4L:6S	2033	320	748
12"	C	horizontal	1C:1 1/4L:6S	3054	385	1724

Figure 2.2.2 Compressive Strength Results (Stang et al., 1926)

cells failed by breaking of the tiles in the two courses at the upper end of the specimen.

Johnson and Matthys (1973) tested prisms constructed from six types of hollow clay tile. The prisms had a slenderness ratio of five. The horizontally celled prisms were laid with full bed joints, and the vertically celled prisms had face shell bedding with type-S mortar. Eleven specimens were built with each type of tile. Five specimens each were tested under a uniaxial compressive load. Tests results for the uniaxial load is given in Table 2-5. The modulus of elasticity is the secant modulus based on 50% ultimate strength.

The mode of failure for the horizontally celled prisms was observed to be the horizontal cracking at the junction of the web walls and side wall. The vertically celled prisms failed by tension cracks emerging on the ends of the specimens.

The Structural Clay Products Research Foundation (SCPRF) (1967) carried out tests on 4" structural clay tile prisms. Three prisms were built from each of six types of clay blocks (see figure 2.2.3). The prisms were laid in stack bond with type-S mortar. Each prism consisted of three stacked blocks laid with horizontal cores for a nominal slenderness ratio of four. The mode of failure under compressive loading was a horizontal splitting of the units through the cross webbing. Many times the face shells would fall exposing the web. Table 2-6 shows the results of the uniaxial compressive tests. The

Table 2-5 Prism Compression Test Results (Johnson and Matthys, 1973)

Tile Type (in)	Compressive Strength,psi		Modulus of Elasticity,ksi	
	Gross Area	Net Area	Gross Area	Net Area
4x12x12 horizontal	1045	3040	1470	4280
4x12x12 Vertical	1337	3740	1400	3730
6x12x12 horizontal	545	2190	760	3060
6x12x12 vertical	1270	3920	890	2740
8x12x12 horizontal	629	2200	720	2040
8x12x12 vertical	569	3140	830	4560

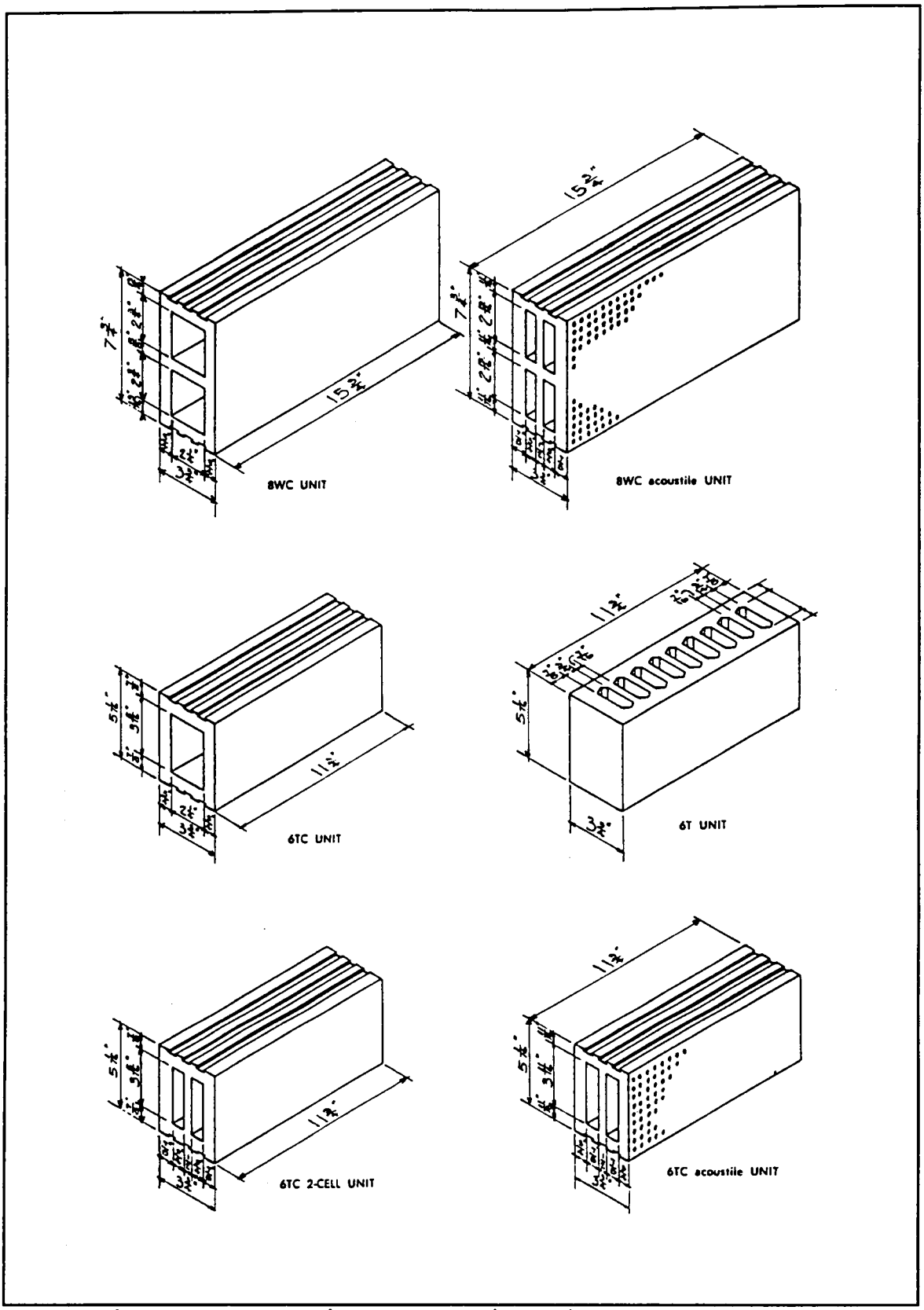


Figure 2.2.3 Tile Block Dimensions (SCPRF,1967)

Table 2-6 Results of Prism Compression Tests (SCPRF,1967)

Block Type	Compressive Strength (gross area)	Compressive Strength (net area)
6T	4457 psi	6600 psi
6TC(2-cell)	3675 psi	6120 psi
8WC(acoustile)	3191 psi	6070 psi
6TC(acoustile)	3043 psi	6900 psi
6TC	2561 psi	6430 psi
8WC	2487 psi	6260 psi

strength computed with the gross area varied depending on the block geometry. Based on the net area, the compresive strength was uniform, averaging between 6000 and 7000 psi.

Walls may experience combined shear and compressive stresses, as in the case of an earthquake, as well as gravity loads. In order to determine the effect of combined stresses on the strength of masonry walls, Hamid and Drysdale (1980) tested prisms at bed joint angles of 0°, 15°, 45°, 75°, and 90°. Concrete masonry prisms were built using type-S mortar. An angle of zero degrees meant that the cores were vertical. The horizontal prisms (90°) and vertical prisms (0°) were three courses high and constructed by placing half blocks flatwise and endwise, respectively. Prisms with bed joint angles of 15°, 45°, and 75° were cut from small panels. The prisms were capped with a sulfur compound. Test results (Table 2-7) were determined using the gross area.

The prisms with vertical cores (0°) exhibited a splitting failure along the block - mortar interface. Hamid and Drysdale (1980) suggest that as the compressive strength of the mortar is reached, the blocks must confine the mortar through the development of lateral tensile stresses. Failure results because of the combined compression - tension state of stress.

The horizontal core prisms (90°) failed by a vertical splitting across the intermediate webs. This failure was due to the lateral tensile stresses developed in the blocks caused by the different lateral strain characteristics of the block

Table 2-7 Prism Compression Test (Hamid and Drysdale,1980)

Bed Joint Angle	Mortar Strength, psi	Prism Strength	
		Mean Strength, psi	Mod. of Elasticity, ksi
0°	2625	1392	622
15°	2625	609	967
45°	2625	1204	791
75°	2625	1334	1243
90°	1958	1479	1024

and mortar. The failure resulted at the web which had the minimum cross-section.

Prisms at 15° appeared to fail in shear along the bed joint. A slip failure occurred at the block - mortar interface. At 75°, a splitting mode of failure occurred near the head joints. This was the result of high tensile stresses in this area. The prisms with a bed joint angle of 45° possessed equal shear and tensile stresses acting on the bed and head joints. The mode of failure was somewhere between the shear - slip failure in the 15° prisms and the shear - tension failure in the 75° prisms.

A similar testing program was conducted by Khattab and Drysdale (1992). An attempt to study the shear transfer mechanism of masonry walls included the uniaxial compressive testing of concrete masonry grouted prisms at bed joint angles of 0°, 22.5°, 45°, 67.5°, and 90°. Test results (Table 2-8) were very similar to those found by Hamid and Drysdale. Drysdale noted that the modes of failure appeared to be the same as those observed by Hamid. There was little difference in the strengths of the ungrouted prisms tested by Hamid and the grouted prisms tested by Khattab except in the 90° prisms. Drysdale attributed the increase in strength in the 90° prisms to the ease in applying the grout. Because of the core orientation, it was easy to grout the "frogged" ends in the head joints of the prisms. Under inspection, it was discovered

Table 2-8 Prism Compression Test (Khattab and Drysdale,1980)

Bed Joint Angle	Mortar Strength,psi	Avg. Prism Strength,psi
0°	1189	1603
22.5°	1189	2828
45°	1189	1133
67.5°	1189	910
90°	1189	2250

that the grout did not fully fill these locations in the prisms cut from the panels.

2.3 Current Code Provisions for Masonry Design

Current U.S. code provisions rely heavily on the modulus of elasticity in the design of masonry structures. In working stress design, the modulus of elasticity of masonry is used in the determination of the modular ratio for flexural stress calculations and the distribution of loads between elements in the structure. Therefore an accurate prediction of masonry modulus values is necessary to correctly estimate stress distribution in a structure in the elastic range (Atkinson and Yan, 1990).

In the Uniform Building Code, the modulus is estimated as 750 times the prism compressive strength. The UBC bases f'_m on the net area for hollow clay tiles. The prism strength is modified using correction factors found in UBC Standard 24-26 to a strength corresponding to a slenderness ratio of two. The UBC also allows the estimation of the design strength based on the unit block compressive strength and the mortar type using Table 24-C of the code.

The ACI 530-88/ASCE 6-88 Standard allows the designer to base the design strength on the mortar type and the unit compressive strength computed from the net area. Correction factors in sections 5.5.1.2 and 5.5.1.3 are used for concrete and clay masonry. ACI 530.1-88/ASCE 6-88 specification allows

for the estimation of design strength based on prism compression tests. For concrete masonry, the test value is corrected to a slenderness ratio of two, while clay masonry is corrected to a slenderness ratio of five. Atkinson and Yan (1990) indicate that the difference in ratios is based on historical data and practical problems in prism testing. It is not reflective of any fundamental difference in material behavior.

As noted above, correction factors are widely used in design practices. Foster and Bridgeman (1973) noted that while different codes may use a different slenderness ratio as unity in their conversion factors, the ratio of the factors between slenderness ratios is almost constant between codes. It is apparent that the codes used a common source to develop their correction factors. Hegemier et al. (1978) believe that these factors are based on Krefeld's research done in 1936. Krefeld's tests were done on a single brick and mortar type, and he concluded that other factors including brick and mortar strength, bond configuration, and prism cross-sectional dimensions required further investigation. Foster and Bridgeman (1973) indicated that Krefeld's results have been accepted as being of general validity by the codes, which Krefeld advised against.

Chapter 3

TESTING PROCEDURE FOR STRUCTURAL CLAY TILE PRISMS

Introduction

The following sections outline the setup for the uniaxial compressive tests performed on structural clay tile prisms at The University of Tennessee. Compression tests were performed on 13" and 8" prisms. The 13" prisms tested had bed joint angles of 0° and 90°. The 8" prisms were tested at various angles to the bed joint. The first section explains the prism construction. The second section describes the testing frame and the means for applying the load. Linear variable displacement transducers (LVDTs) were used to measure the deformation of the prism. The final section outlines the testing procedure from setting the prism into the testing frame to running the actual test.

3.1 Prism Construction

The prisms were constructed with structural clay tile having nominal dimensions shown in figure 3.1.1 (Flanagan and Bennett, 1992). Light red clay (terra cotta) masonry units manufactured by D'Hanis Brick and Tile Company, San Antonio, Texas were used in the construction. Two groups of prisms were built with nominal dimensions of 2′ high by 4′ wide. Group A consisted of four prism types shown in figure 3.1.2. The first

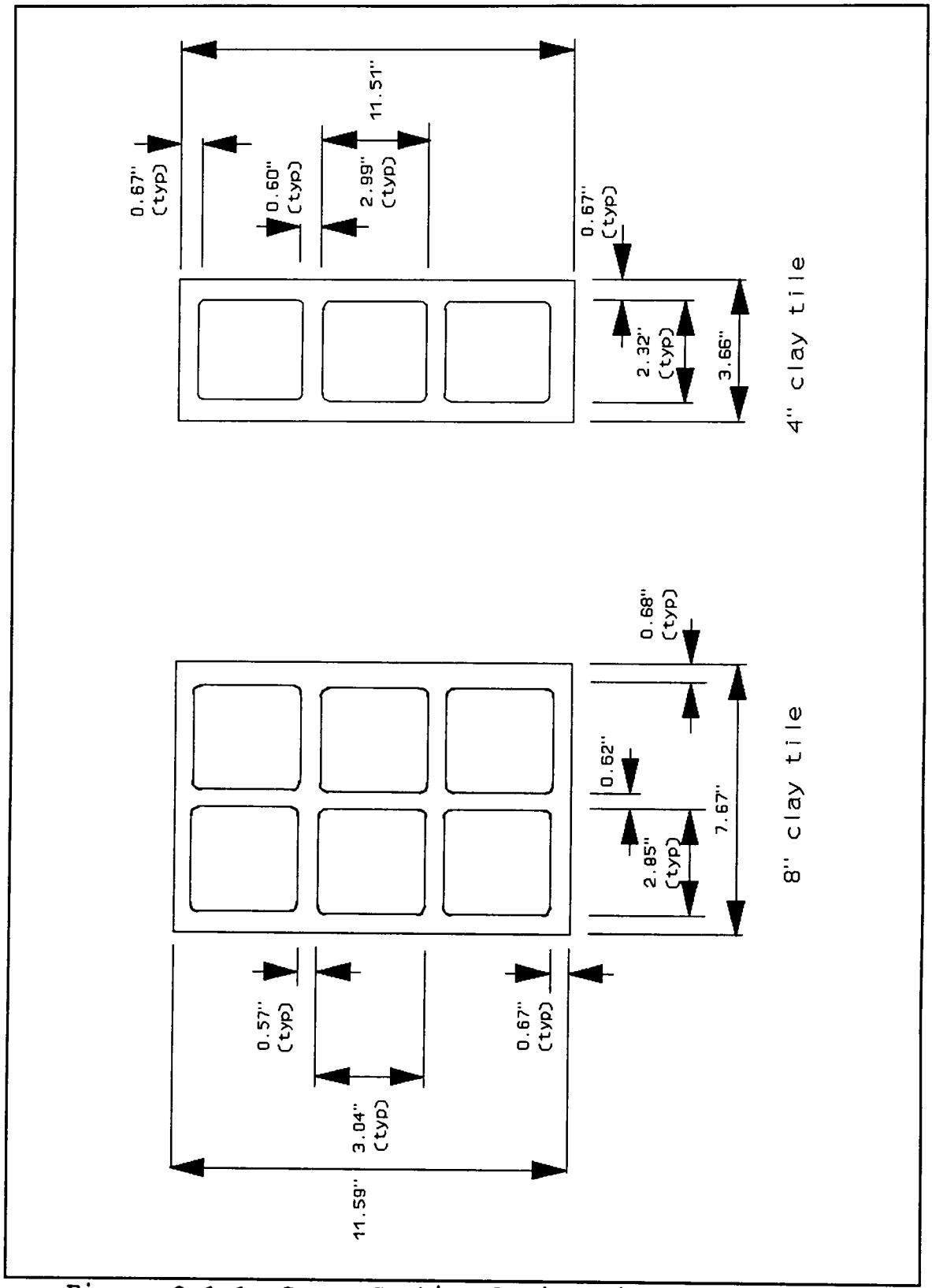


Figure 3.1.1 Cross-Sectional Dimensions of SCT Tile (Flanagan and Bennett, 1992)

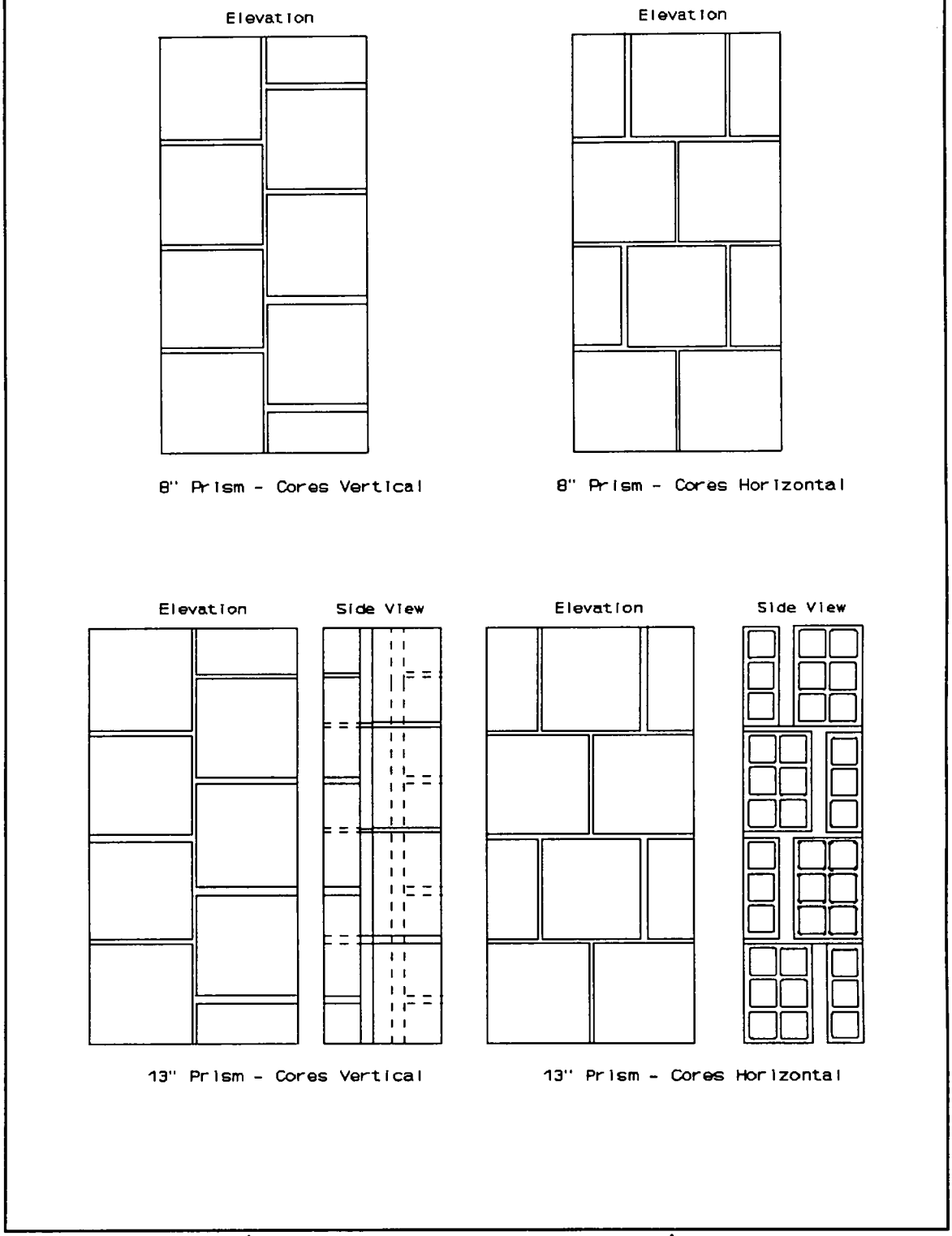
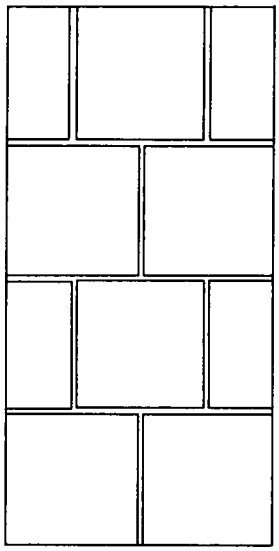


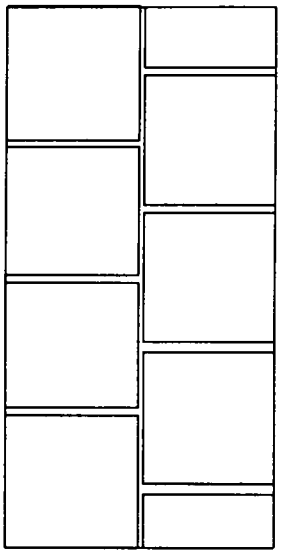
Figure 3.1.2 Group A SCT Prisms

type was 8" thick with the cores laid horizontally. The bottom course had two whole tiles and the next course had half tiles on the ends with a whole tile in the center. These two courses were repeated to complete the four courses of the prism. The second type was 8" thick with the cores vertical. The prism was built on its side to maintain a horizontal bed joint, and then rotated 90° for testing. A staggered full and half tile configuration resulted along the height of the prism with a vertical mortar joint running through the center. The third type of prism was 13" thick using double wythe construction with 8" and 4" tiles and an approximately 1" collar joint. The cores were horizontal. The final type of prism in the group was the 13" prism with cores vertical. These prisms were built on their side and rotated 90°. These prisms were also double wythe construction.

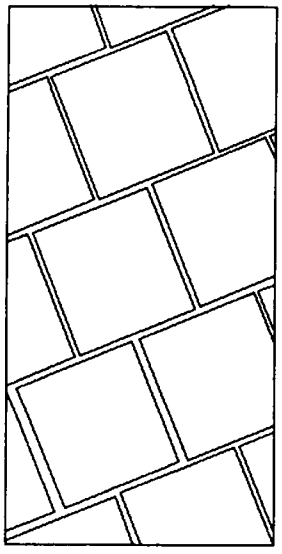
Three sets of group B prisms were built and tested. Each set was constructed at the same time. This group of prisms was built with a varying bed joint angle (figure 3.1.3). The angle was measured from the horizontal. The 8" prisms with cores vertical and horizontal (90° and 0° respectively) were constructed similar to those in group A. The prisms built with angles of 22.5°, 45°, and 67.5° were constructed on frames that would allow the mortar to set with the bed joint remaining in the horizontal position (figure 3.1.4). The prisms were constructed from pieces of tile that were cut using a diamond tip saw. Templates were made for each tile



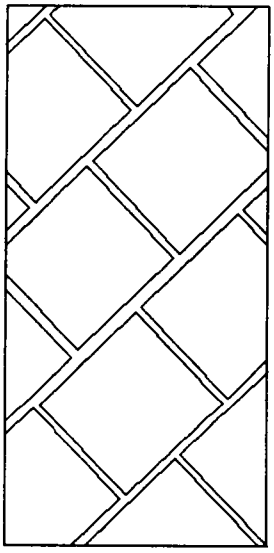
0° Bed Joint Angle



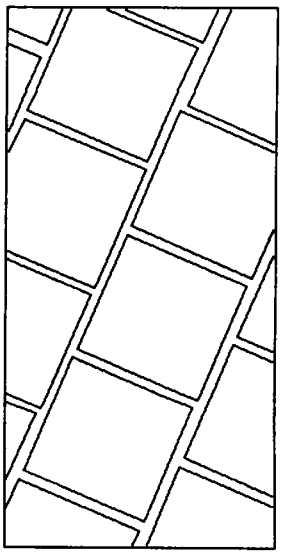
90° Bed Joint Angle



22.5° Bed Joint Angle



45° Bed Joint Angle



67.5° Bed Joint Angle

Figure 3.1.3 SCT Prisms in Group B

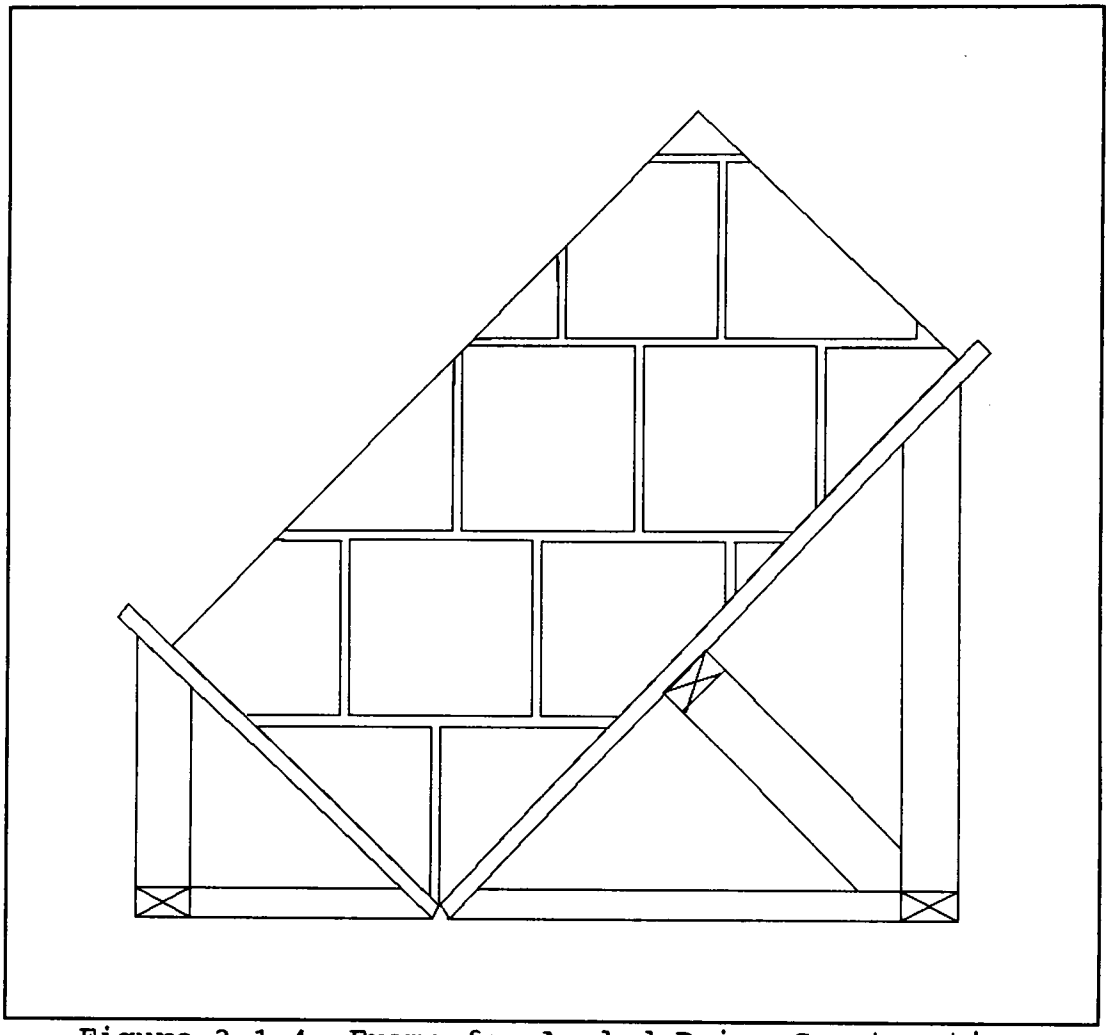


Figure 3.1.4 Frame for Angled Prism Construction

piece by placing a 2′ by 4′ board on the side of an existing wall at the required angle (figure 3.1.5). An outline was drawn around the board and a piece of cardboard the size of a whole tile was placed on each wall tile inside the outline. The cardboard was then cut to match the size of the tile. These cardboard pieces were used as templates for the cuts on the prism tiles in each set of group B.

The mortar mix consisted of ½ bag of type N mortar throughly mixed with seven shovelfuls of sand. Water was added

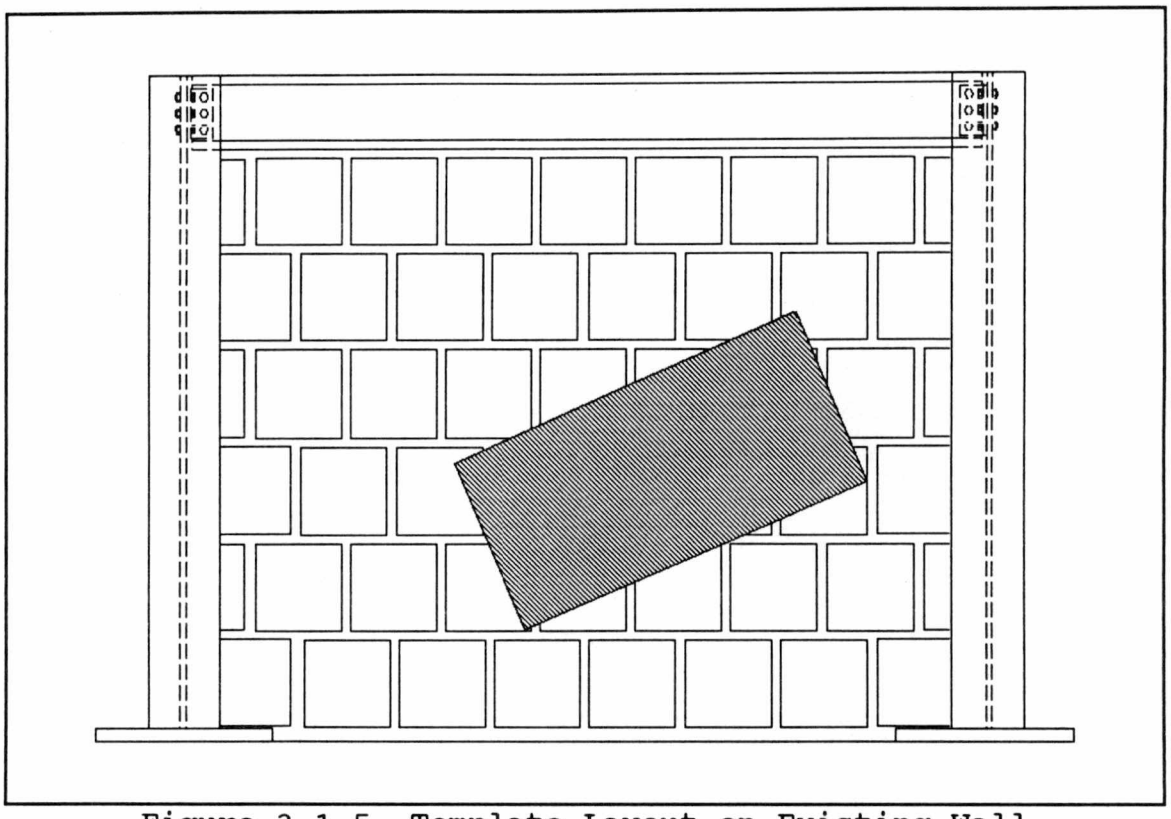


Figure 3.1.5 Template Layout on Existing Wall

to establish workability. Each prism was built from a separate mortar batch with three mortar samples made from each batch. One sample was tested in compression at thirty days and the other two were tested the day of the prism test according to ASTM C780 (1987). The prisms were built by an experienced mason with approximately ¾" head and bed joints.

3.2 Testing Apparatus

The prism testing frame shown in figure 3.2.1 was used for the uniaxial compressive test performed on all the prisms. A BLH Electronics C2P1 200 kip load cell was connected to a

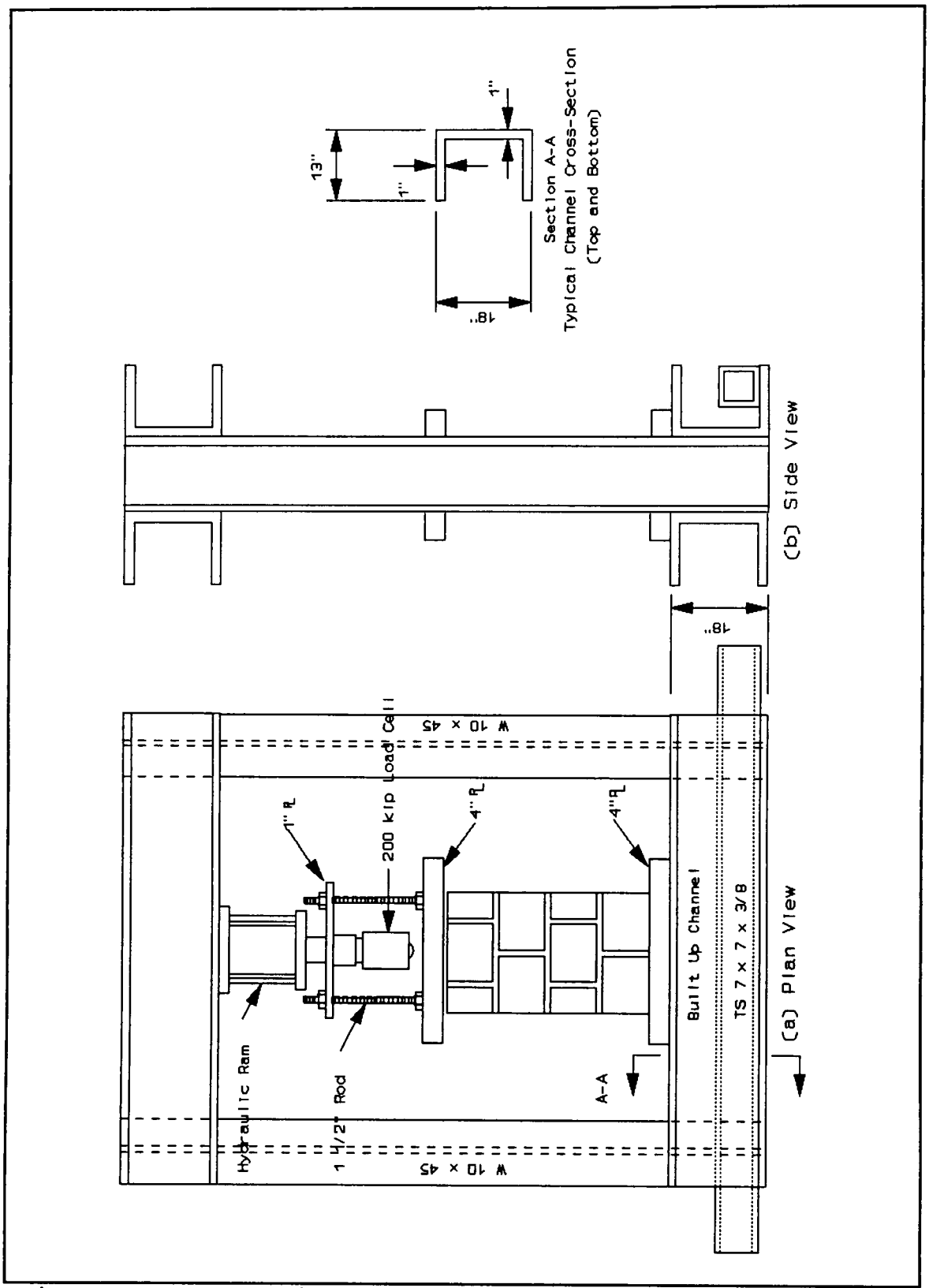


Figure 3.2.1 Testing Frame for Prism Uniaxial Compression Test

Milwaukee Cylinder H-22 hydraulic ram. The hydraulics were controlled by a Moog servo valve 76-1024 through an MTS servo-hydraulic test system.

The steel tube was placed on the back channel to provide additional stability to the frame. Expansion anchors were used to tie the tube to the concrete floor in the lab.

3.3 Instrumentation Description

Linear variable displacement transducers (LVDTs) were located in various positions (figure 3.3.1) to measure the

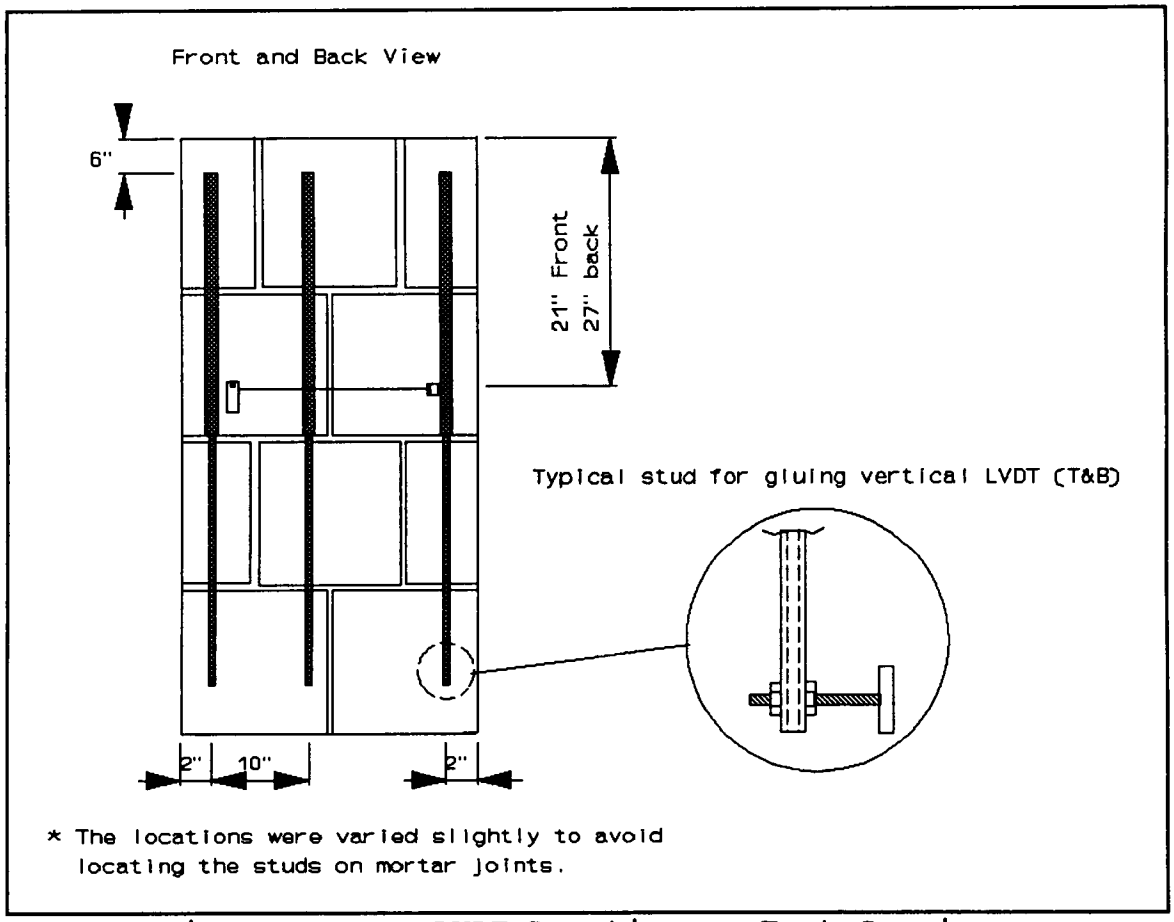


Figure 3.3.1 LVDT Location on Test Specimen

deformations of the prism. Figure 3.3.1 shows the location of the LVDTs on the 8" prism with cores horizontal. The locations for the angled prisms were set as close as possible to these locations without setting the stud on a mortar joint. The studs were applied to the prisms with a hot glue gun. The vertical and horizontal LVDTs had travel ranges of ±1" and ±0.1", respectively. The control LVDT was mounted to the lab wall with the armature set on the 1" plate connected to the RAM.

Load and displacement measurements were collected through a central data acquisition system. The schematic diagram in figure 3.3.2 shows the setup for the typical prism uniaxial compression test. The LVDTs were connected to a STB 884/SCV terminal block. The LVDTs were excited by an external power supply and run into the Megadac 3008 data collection system. The Megadac data collection system ran into an IBM PS/2 via an IEEE 488 interface. Digital monitors or various real time plots could be viewed on the computer during testing. The sampling rate was 2 samples/second for the first prism. This rate was increased to 10 samples/second during the later tests.

3.4 Testing Procedure

The uniaxial compression tests run on the prisms can be divided into several activities. Pre-Test events include the prism construction, transporting the prism, and making several

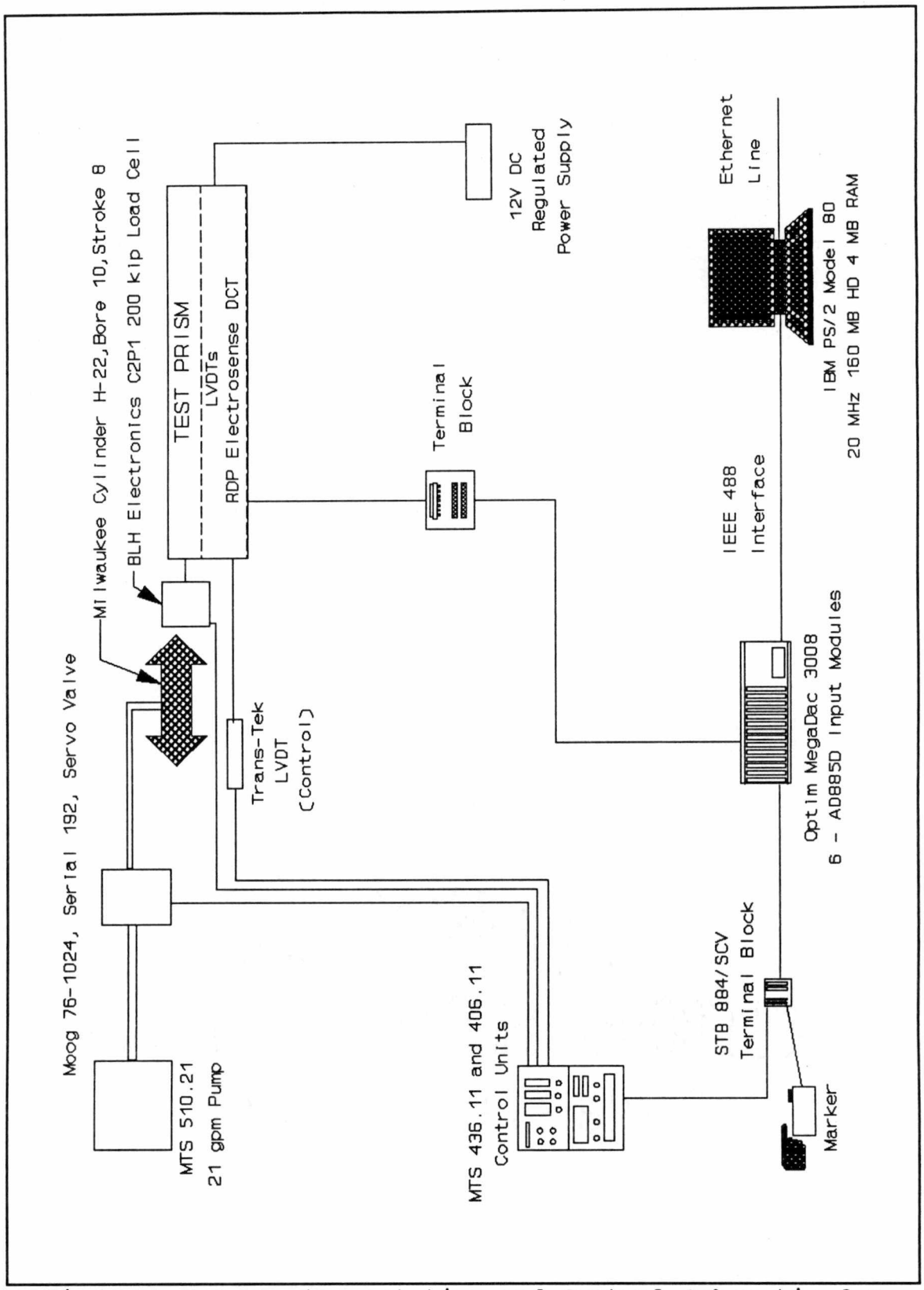


Figure 3.3.2 Instrumentation and Control Schematic for Prism Test

pertinent measurements of the prism. The actual prism testing could then proceed. The following will describe these events in detail.

3.4.1 Pre-Test Events

Testing was not performed on the prisms until at least 30 days after construction. One week after construction, the core voids present on the top of the prism were filled with an expanding foam. The prisms with horizontal cores did not require any foam since the tile face on top was solid. The foam was required to contain the capping material. Hydrostone was used to cap the prism top and bottom. Once the foam dried, a knife was used to cut the foam level with the tile.

The prisms were banded with ½" metal strapping so that the prisms could be moved (figure 3.4.1.1). The lifting of each prism was done with a forklift. The forks were fitted into a frame made of 2x4s that was strapped to the top of each prism with openings provided for the forks. The 13" prisms with the cores vertical required a wood frame on each side to provide stability in its movement. These frames were strapped to the prism in order to prevent the collapse of the 4" tile section due to the collar joint spacing.

Prior to the test, several measurements were taken on the prism. The weight, including the tare, was recorded. Following the test, the tare was weighed and the true prism weight was obtained. Average measurements were taken on the prism height,

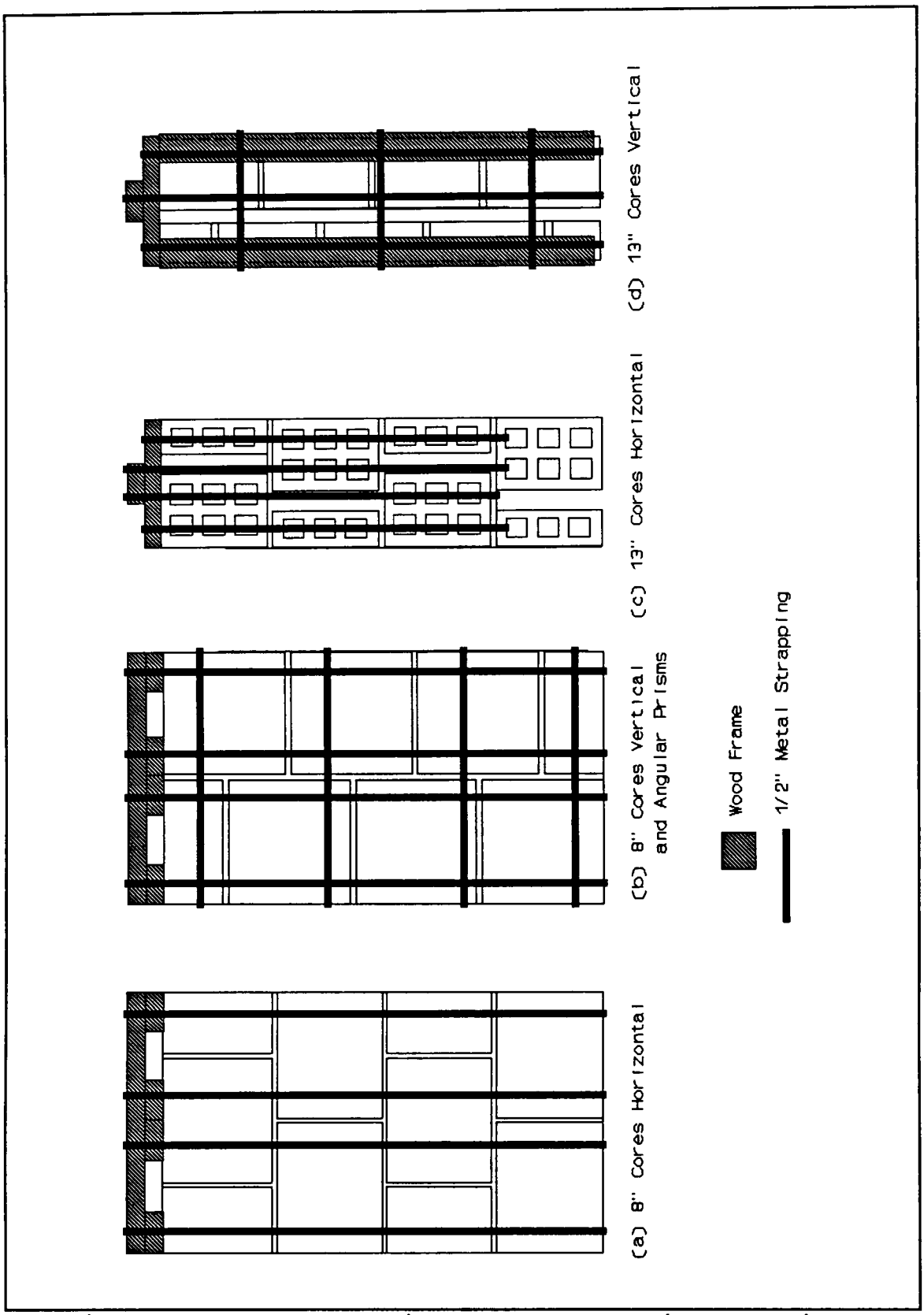


Figure 3.4.1.1 Strapping for Transporting of Prisms

width, and thickness. A sample data sheet is shown in Appendix A.

The prism was carefully placed on the bottom 4" plate of the loading frame with a forklift. Several prisms required shims (small pieces of clay tile) in order to level the top and sides. These shims were glued to the bottom of the prism, and the prism was lifted several inches above the bearing plate. One-half inch weather stripping was placed around the area where the prism would sit. Hydrostone was poured into this area and the prism was lowered into the hydrostone. Once the bottom cap hardened, the straps were cut and the lifting frame removed. The prism was then aligned under the load cell by moving the bottom bearing plate with a hydraulic jack.

The most difficult procedure was the capping of the top of the prism. The prism top was wrapped with the weather stripping leaving about ⅛" above the top of the prism. Aluminum tape was then wrapped around the stripping. The tape was carefully applied to the clay tiles, making sure no voids were present where the hydrostone might leak. The hydrostone was poured into the confined area. Once the area was full, the top bearing plate was lowered to contact the hydrostone. The plate was lowered until it was possible to loosen the nuts on the 1" plate. The top bearing plate was therefore resting completely on the prism. Once the top cap dried, the tape and stripping were removed and the cap inspected.

A crack map was made of the prism in order to locate possible weaknesses in the tiles and mortar joints. The LVDTs were then attached to the prism in their designated locations. The LVDT's gage lengths were adjusted so that they could be balanced within the data acquisition system. These gage lengths were recorded so that the strain could later be calculated.

3.4.2 Test Events

Several people were required during the uniaxial conpressive test on the prism. The loading was controlled by the MTS operator. A loading rate of approximately 60 kips per minute was maintained. Because of the explosive behavior of the clay tiles, the LVDTs were removed at 50-75% of the expected ultimate load to prevent damage. The load at the first major cracking sound and the ultimate load were recorded. During the test, the developing cracks were mapped, and several pictures and videos were made.

3.4.3 Post-Test Events

Once the prism had failed, the top and bottom caps were again checked and measured. The final event for each prism was the testing of the two remaining mortar samples.

Chapter 4

STRUCTURAL CLAY TILE PRISM STRENGTH

Introduction

This chapter presents the results of tests to determine the uniaxial compressive strength of structural clay tile prisms. Results of the compressive strengths are given along with illustrations of the typical modes of failure. A discussion of the probable cause of the failure is followed by a comparison of results obtained in other research.

4.1 Tile Strength

Tests on individual tile units were performed earlier at The University of Tennessee and are presented in the Martin Marietta Energy Systems technical report Y/EN-4536. The tile areas and rates of absorption were averaged for 40 tiles. Twenty tiles each of both 4" and 8" blocks were averaged for their compressive strength and splitting tensile strength. A summary of the results is given in figure 4.1.1.

The compressive and splitting strengths for all but a few of the tiles were found using a Forney 350-kip capacity testing machine. The strengths of the individual 8" tiles tested with cores vertical were determined from tests at the Singleton Laboratory using a 600-kip capacity testing machine. Tests consistent with ASTM C 1006-84 were used to determine

Parameter	Structural Clay Tile Size			
	4 Inch		8 Inch	
	Mean	V (%)	Mean	V (%)
Length (inch)	11.47	0.5	11.54	0.4
Width (inch)	3.66	1.0	7.67	0.4
Height (inch)	11.51	0.4	11.59	0.3
Weight (lbs)	17.87	1.4	31.07	1.7
Gross Area (in)	42.17	1.3	88.90	0.8
Gross Density (pcf)	63.85	1.7	52.35	1.4
Coring (%)	47.73	1.7	57.07	0.9
Net Area Cores Vertical (in)	21.91	1.9	38.15	1.7
Net Area Cores Horizontal (in)	15.42	0.9	22.88	2.2
Ultimate Compressive Load - Cores Horiz. (kips)	138.6	8.7	190.4	5.2
Ultimate Compressive Load - Cores Vert. (kips)	244.4	25.2	457.7	18.2
Gross Compressive Strength - Cores Horiz. (ksi)	3.30	8.6	2.14	5.6
Gross Compressive Strength - Cores Vert. (ksi)	5.84	24.8	5.16	18.7
Net Compressive Strength - Cores Vert. (ksi)	11.29	24.0	12.10	19.7
Net Compressive Strength - Cores Horiz. (ksi)	8.96	8.8	8.22	6.8
Splitting Tensile Load - Cores Horiz. (kips)	12.55	35.7	17.72	21.9
Splitting Tensile Load - Cores Vert. (kips)	11.58	47.0	16.14	30.0

V = Coefficient of Variation (100*standard deviation/mean)

Figure 4.1.1 Description of Unit Tiles

the splitting tensile strength. Hydrocal was used to cap all the specimens.

4.2 Prism Strength Test Results

A compilation of descriptive data for all prisms tested is presented in figure 4.2.1. The 8" and 13" prisms had average densities of 53.9 pcf and 49.0 pcf, respectively. The results of the uniaxial compression tests are presented in figure 4.2.2. The notation for the prism number is based on the prism nominal thickness and the mortar bed joint angle. The first number relates the prism thickness while the next number is the bed joint angle in either rounded degrees or 'H'

Prism Number	Bed Joint Angle (deg.)	Average Width (in.)	Average Thickness (in.)	Average Height (in)	Weight (lbs.)
UT8H-1	0	23.927	7.719	48.438	280
UT8H-2	0	24.063	7.625	48.469	283
UT8H-3	0	24.146	7.729	47.896	274
UT8H-4	0	23.844	7.656	47.740	276
UT8V-1	90	23.500	7.656	48.094	264
UT8V-2	90	23.698	7.583	48.000	258
UT8V-3	90	23.729	7.656	48.375	271
UT8V-4	90	23.917	7.635	48.188	277
UT8-0-1	0	24.208	7.708	48.688	285
UT8-22-1	22.5	24.271	7.750	47.021	---
UT8-45-1	45	24.479	7.688	48.000	282
UT8-67-1	67.5	23.958	7.708	47.688	289
UT8-90-1	90	23.750	7.708	47.896	260
UT8-0-2	0	24.333	7.729	48.188	275
UT8-22-2	22.5	23.583	7.688	47.146	276
UT8-45-2	45	24.000	7.708	48.000	285
UT8-67-2	67.5	24.646	7.708	47.875	302
UT8-90-2	90	23.771	7.708	47.688	260
UT8-0-3	0	23.979	7.771	48.063	261
UT8-22-3	22.5	23.479	7.688	47.125	271
UT8-45-3	45	23.917	7.729	47.084	274
UT8-67-3	67.5	24.521	7.729	47.875	294
UT8-90-3	90	23.938	7.729	48.083	271
UT13H-1	0	24.073	13.042	48.146	459
UT13H-2	0	24.010	13.042	47.813	451
UT13H-3	0	23.833	13.167	47.917	---
UT13H-4	0	23.854	13.292	47.854	430
UT13V-1	90	23.729	13.042	48.396	395
UT13V-2	90	23.646	12.958	48.396	417
UT13V-3	90	23.500	12.979	47.938	411
UT13V-4	90	23.792	13.063	48.063	409

Figure 4.2.1 Description of Clay Tile Prisms

Prism Number	Mortar Strength (psi)		Load at 1st Crack (kips)	Ultimate Load (kips)	Gross Area Stress (psi)	
	30 Day	Test Date			First Crack	Ultimate
UT8H-1	2375	3415	45	164.4	243.6	890.1
UT8H-2	3325	3500	50	143.7	272.5	783.2
UT8H-3	1813	1992	51	154.5	273.3	827.9
UT8H-4	1813	1992	77	139.5	421.8	764.2
UT8V-1	1713	1791	---	77.4	----	430.2
UT8V-2	1713	1718	---	69.8	----	388.4
UT8V-3	2225	2186	---	59.7	----	328.6
* UT8V-4	2225	2365	---	106.6	----	583.8
UT8-0-1	1825	2150	123	170.0	659.2	911.1
UT8-22-1	2250	2494	69	80.8	366.8	429.3
UT8-45-1	2150	2399	30	42.6	159.4	226.4
UT8-67-1	2300	2310	27	39.6	146.2	214.4
UT8-90-1	1850	2019	45	84.8	245.8	463.0
* UT8-0-2	2088	2019	103	136.6	547.7	726.3
* UT8-22-2	2153	2310	90	105.0	496.4	579.1
* UT8-45-2	2175	2144	51	61.8	275.7	334.1
* UT8-67-2	2295	2156	20	20.3	105.3	106.9
* UT8-90-2	2225	2325	15	84.8	81.9	462.8
* UT8-0-3	2030	1925	100	142.8	536.7	766.3
* UT8-22-3	1853	2119	80	105.4	443.2	583.9
* UT8-45-3	1903	1934	35	42.6	189.3	230.5
* UT8-67-3	1175	1275	15	20.8	79.1	109.7
* UT8-90-3	1000	1114	35	73.5	189.2	397.3
UT13H-1	1500	1981	51	131.7	162.4	419.5
UT13H-2	1500	1981	50	114.8	159.7	366.6
* UT13H-3	1949	1949	65	91.0	207.1	290.0
* UT13H-4	1315	1315	65	79.2	205.0	249.8
UT13V-1	1525	1544	30	148.4	96.9	479.5
UT13V-2	1950	2044	25	103.7	81.6	338.4
* UT13V-3	1783	1783	40	98.9	131.1	324.3
* UT13V-4	1500	1519	---	107.7	----	346.5

Figure 4.2.2 Prism Strength Results

for horizontal bed joint and 'V' for vertical bed joint. An angle of 0° indicates horizontal cores. The last number indicates the order in which the prisms were tested. The gross areas were used to calculate the compressive strength in all the prism types in figure 4.2.2. Figure 4.2.3 presents the uniaxial compressive strengths based on the net area in prisms with vertical and horizontal cores. The net areas used in the strength calculations are the hatched sections shown in figure 4.2.4. For the horizontal cored prism, this was the location of the bed joints. For the verical cored prism, this was the location of the head joints. The net areas did not consider the area of the mortar joint. The net area for angled prisms has no practical definition except where the load is applied perpendicular to the mortar joints (Hamid and Drysdale, 1980).

The prisms in figures 4.2.2 and 4.2.3 marked with an asterick were subjected to a load - unload pattern while the others underwent a monotonic loading. The load - unload pattern consisted of 2 to 10 cycles with loads up to between 60 and 90 percent of ultimate.

4.3 Prism Mode of Failure

The mode of failure of the prisms was a function of the orientation of the mortar joints with respect to the direction of load application. Figure 4.3.1 shows the cracking patterns that occurred prior to collapse of the prism. The cracks shown were present in a majority of the particular prism types.

	Prism Number	Net Area (in^2)	Net Compressive Strength (psi)
HORIZONTAL CORE	UT8H-1	45.70	3597.4
	UT8H-2	45.70	3144.4
	UT8H-3	45.70	3380.7
	UT8H-4	45.70	3052.5
	UT8-0-1	45.70	3719.9
	* UT8-0-2	45.70	2989.0
	* UT8-0-3	45.70	3124.7
	UT13H-1	76.44	1722.9
	UT13H-2	76.44	1501.8
	* UT13H-3	76.44	1190.5
	* UT13H-4	76.44	1036.1
VERTICAL CORE	UT8V-1	31.52	2455.5
	UT8V-2	31.52	2214.4
	UT8V-3	31.52	1893.9
	* UT8V-4	31.52	3381.9
	UT8-90-1	31.52	2690.3
	* UT8-90-2	31.52	2690.3
	* UT8-90-3	31.52	2331.8
	UT13V-1	62.37	2379.3
	UT13V-2	62.37	1662.7
	* UT13V-3	62.37	1585.6
	* UT13V-4	62.37	1726.8

* Load – Unload Pattern

Figure 4.2.3 Prism Net Strength

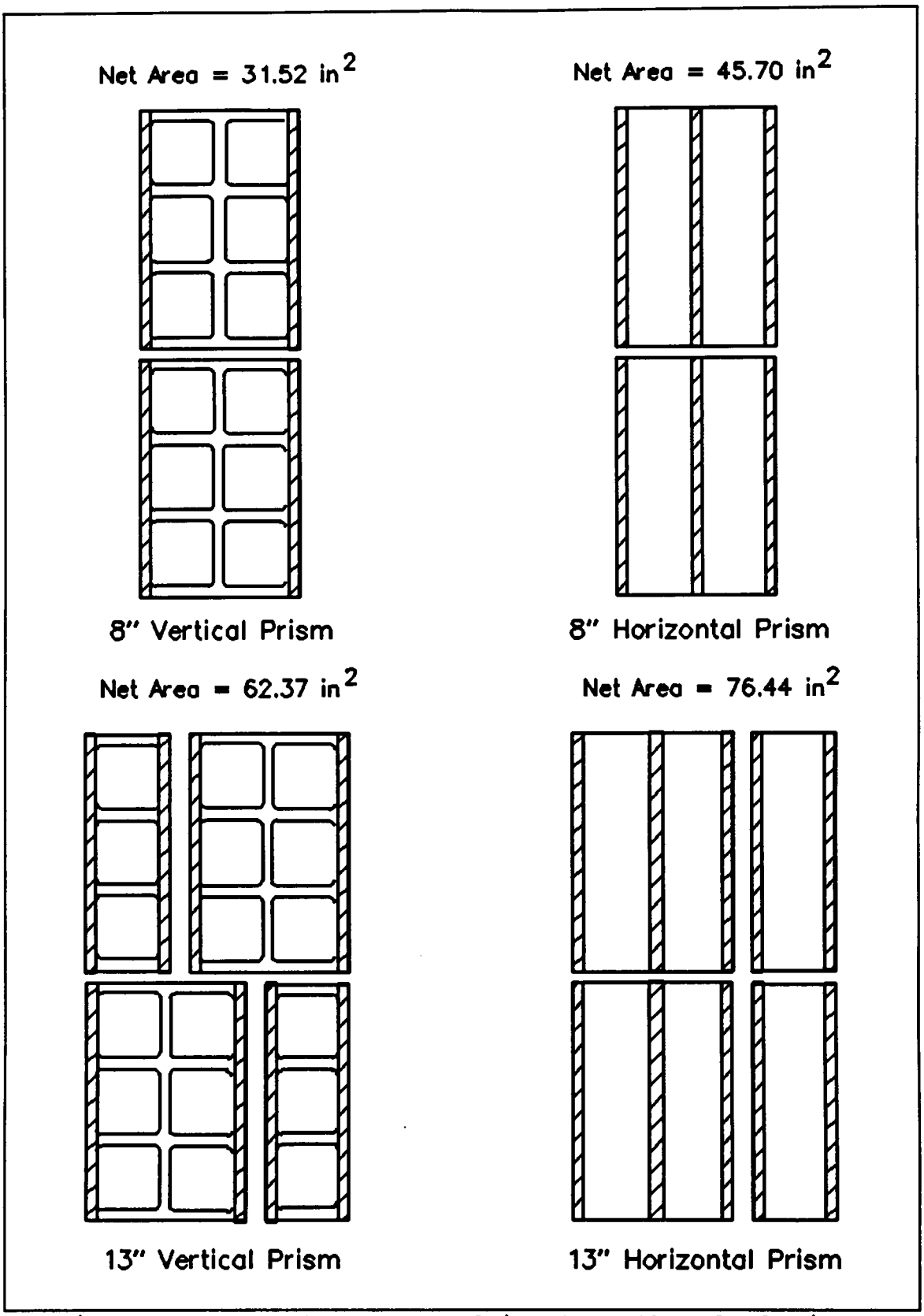


Figure 4.2.4 Net Areas Used in Strength Calculations

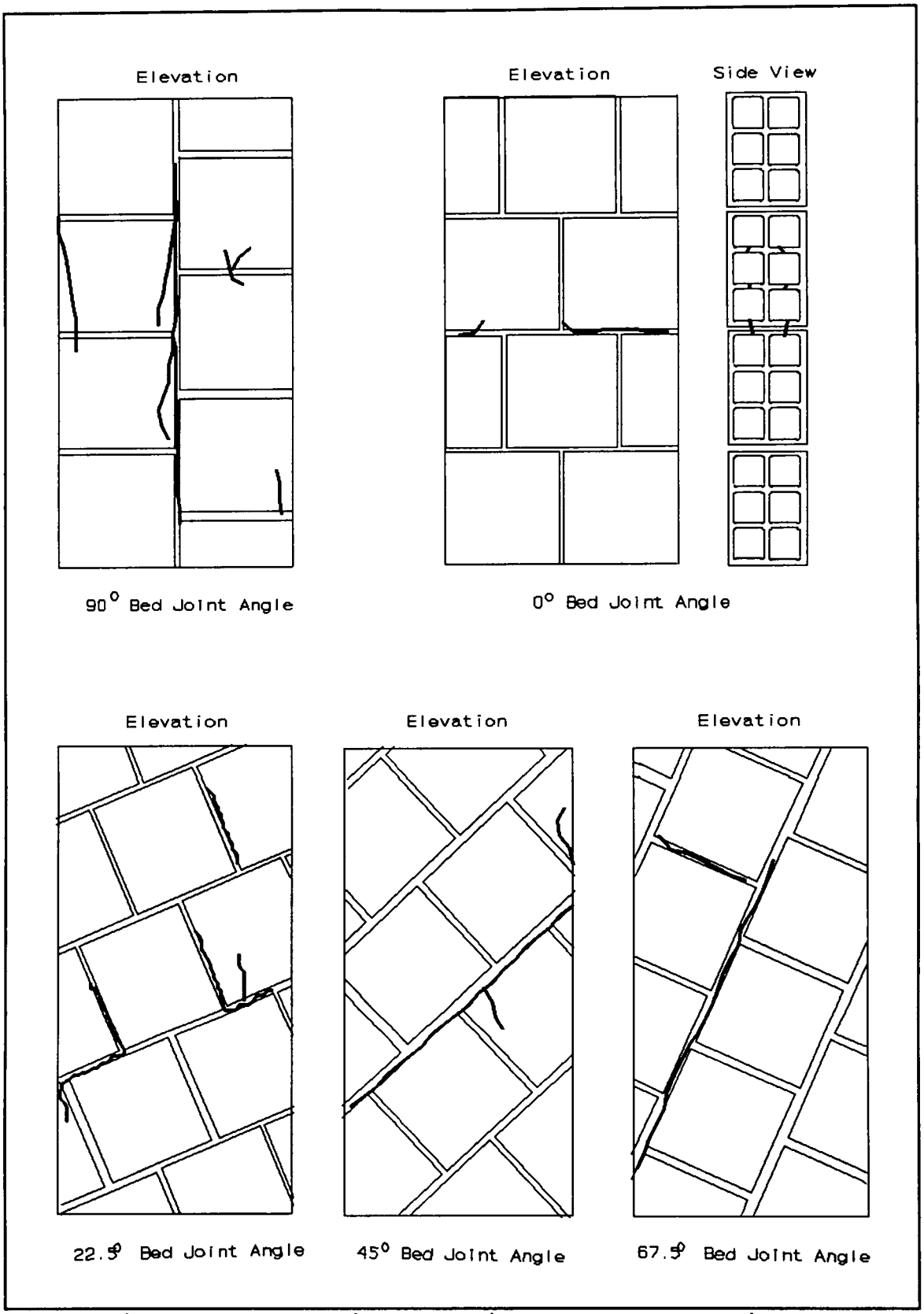


Figure 4.3.1 Prism cracking Pattern at Failure

The 8" prisms with the bed joint at 0° (cores horizontal) exhibited a cracking pattern along the interior web. The first sign of distress was the crushing of mortar along the bed joint. Splitting cracks would then form along the block-mortar interface. As these cracks widened, cracks would progress in adjacent webs at the minimum cross section in the interior of the tiles. Khattab and Drysdale (1992) attribute the formation of the cracks to the different lateral strain characteristics of the mortar and tile. Failure occurs as the faceshells are left to deform individually with a high slenderness ratio which leads, finally, to an explosive reaction. In most cases, the two middle courses were reduced to rubble.

The 8" prisms with a bed joint angle of 90° (cores vertical) failed in a less explosive manner. The first major crack formed along the vertical bed joint that ran along the length of the prism. This crack was followed by the spalling of faceshells at the mortar-tile interface. Finally, vertical cracks formed along the 8" sides and in several tile faceshells. Hamid and Drysdale (1980) suggest that these cracks result from the confinement of the mortar as it reaches its unconfined strength. This results in the formation of lateral tensile stresses in the faceshells. These stresses, in combination with the normal stresses, cause the spalling and subsequent failure of the prism.

Prisms with a bed joint angle of 67.5° from horizontal exhibited a shear failure. A shear plane formed along the bed

joint at the crack shown in figure 4.3.1. The relatively low frictional coefficient between the mortar and tile at the bed joint allowed a major portion of the prism to simply slide free.

Prisms having a bed joint angle of 22.5° appeared to have a shear-tension mode of failure. Minor slippage occured on the head joints resulting in cracking. The normal stresses caused the formation of vertical cracks on the faceshells. The combination of slippage and faceshell cracks resulted in the failure of the prism.

Prisms with a bed joint angle of 45° had equal shear and tensile stresses along the bed and head joints. Small cracks first formed in the bed joint. These cracks were followed by the formation of small cracks in the faceshell of the tiles at the mortar tile interface. Finally, a shear plane formed along the third bed joint. Khattab and Drysdale (1992) noted this failure as being a combination of the failures observed in the 22.5° and the 67.5° prisms.

The cracking patterns for the 13" prisms are shown in figure 4.3.2. The prisms with horizontal cores appeared to progress toward failure in the same manner as the 8" prisms. After the initial crushing of the mortar, cracks began to emerge in the webs of the 8" tiles in the second course. Cracks progressed through the third course 8" tile and then through the 4" tiles in the second and third course. The 13" vertically cored prisms had the same failure pattern as the 8"

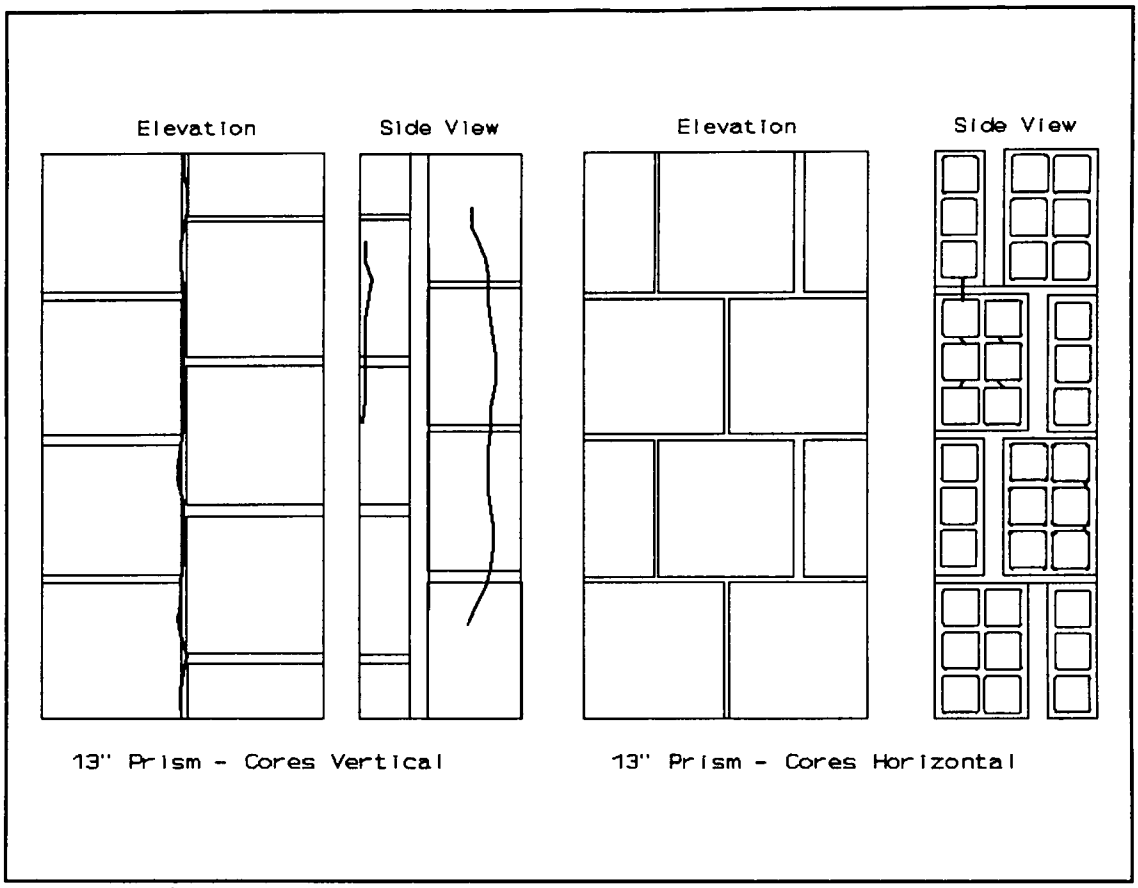


Figure 4.3.2 Cracking Pattern of 13" Prisms

vertically cored prisms. A vertical crack formed along the front and rear bed joints. This was followed by the formation of vertical cracks down the 8" column sections. With the formation of these cracks, the prism tended to rotate allowing the 4" column to collapse.

4.4 Discussion of Strength Tests

Average strength results are presented in figure 4.4.1. The prisms with a horizontal bed joint had a lower variation than other prisms. This lower variability is possibly the result of the ease in construction of the horizontally cored

Prism Type	Number of Prisms	Prism Strength (psi)		Mortar Strength (psi)	
		Mean	V (%)	Mean	V (%)
8" (0 bed joint)	7	809.9	8.5	2428	29.1
8" (22.5 bed joint)	3	530.8	16.6	2308	8.1
8" (45 bed joint)	3	263.7	23.2	2159	10.8
8" (67.5 bed joint)	3	143.7	42.6	1914	29.2
8" (90 bed joint)	7	436.3	18.4	1931	22.7
13" (0 bed joint)	4	331.5	23.0	1807	18.2
13" (90 bed joint)	4	372.2	19.4	1723	14.2

V = Coefficient of Variation (100*standard deviation/mean)

Figure 4.4.1 Average Gross Strength of Tested Prisms

prisms. The load path during the test could be more easily repeated in these prisms. The construction of the angled prisms involved the placing of saw cut tile pieces that could be slightly altered from prism to prism. As a result, the load path could also be slightly changed. The difference in the mortar strengths apparently had very little effect on the prism strength.

Figure 4.4.2 is a plot of the compressive strength based on the gross area versus the bed joint angle. The plot demonstrates the nonisotropic behavior of the masonry tile prisms. The strength of the prisms with a horizontal bed joint was dramatically greater than any of the other prism types.

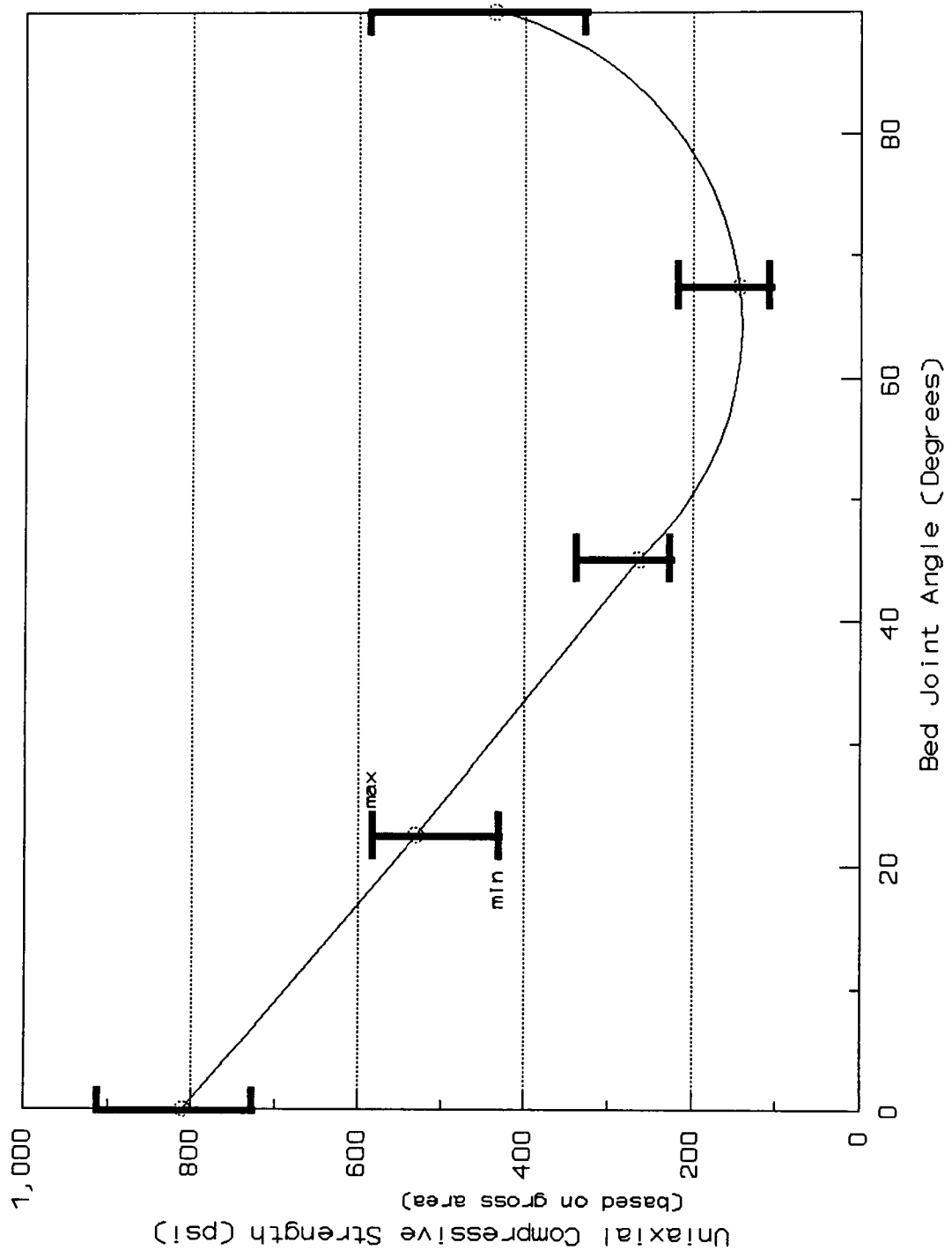


Figure 4.4.2 Strength Variation Due to Bed Joint Angle

The curve shows how the strength is minimum at a bed joint angle of 67.5° and maximum at bed joint angles of 0° and 90°. The relative importance of the mortar joint may account for this behavior. As demonstrated in the previous chapter, the mortar joint plays a major part in the failure in all the prisms except for the 0° prism. In the 45° and 67.5° prisms, slippage occured along the block - mortar interface resulting in a premature failure. The 22.5° prism reacted similarly to the 0° prism; thus the strength was relatively high. The 90° prism had a vertical crack form along the bed joint leaving the tiles to react as columns subject to buckling as the head joint was crushed.

It was found that the compressive strengths of the 8" prisms were greater than the strengths of the 13" prisms. This lower strength is due to the construction practice of alternating the rows of 8" and 4" blocks. The load path creates large stresses as the load is forced to turn at the 8" block - 4" block interface along the height of the prism.

The load - unload pattern appeared to have little effect on the compressive strengths. It would be expected that a reduction in the strengths might occur, but this could not be verified. Because the load was cycled sometimes up to as high as 90% of ultimate, one would expect the formation of minute cracks in the tiles which would result in a lower strength, as with concrete. However, the test results showed no pattern of

strength variation in prisms with monotonic load versus those with load - unload cycles.

4.5 Comparison of Results with Previous Research

Figure 4.5.1 compares the current results with past research involving the uniaxial compressive strength of similar structural clay tile prisms or walls. The first two columns show the strengths of the individual tiles. Although no direct correlation has been made between the tile strength and the prism strength, it is obvious that as the tile strength increases, so would the prism strength. Based on the net area, the current tested tile strengths were noticibly larger than the previous units tested. Flanagan and Bennett (1992) attribute this increase partially to the improvements in the grinding and firing processes of the clay tiles.

Whittemore and Hathcock (1923) reported that the walls with vertical cores had approximately twice the strength of the walls built with horizontal cores. Johnson and Matthys (1973) also found the net strength was greater for the vertical cored prism. They noted that the mode of failure appeared to be cracking at the ends of the prisms. This cracking pattern could be caused by platen restraint, or it might be due to the paster of Paris capping compound having a lower elastic modulus than the mortar. If platen restraint is the cause of the failure pattern, the results would be unconservatively high. The current results show that the

Source	Gross Unit Tile Str. (psi)		Net Unit Tile Str. (psi)		Prism Gross Area Str. (psi)		Prism Net Area Str. (psi)	
	8" Horiz.	8" Vert.	8" Horiz.	8" Vert.	8" Horiz.	8" Vert.	8" Horiz.	8" Vert.
Current Results	2140	5160	8220	12100	810	436	3283	1042
Whittemore and Hathcock 1923	1240	2320	5460	5010	393	1045	1795	2310
Stang et al., 1926 Tile A	500	1830	2210	4470	360	355	1587	870
Stang et al., 1926 Tile B	330	1270	1290	2740	230	295	1012	591
Johnson and Matthys 1973	1181	2762	4100	5900	629	569	2200	3140

Figure 4.5.1 Comparison of Similar Uniaxial Compression Tests

vertically cored prisms had approximately half the strength of the horizontally cored prisms. The results of Stang et al. (1926), based on the prism net area, support this observation.

In all the cases mentioned above, the compressive load was applied perpendicular to the bed joint. The vertical prisms were constructed by laying the tiles with the cores vertical. Thus, the running bed joint existed on the end of the tiles. In the present case, the prisms were constructed with the tiles placed in the horizontal direction with a running bond along the sides of the tiles. Before testing, the prism was rotated in order to achieve the correct orientation. Therefore, the compressive load was applied perpendicular to the head joint. Because of the small face shell thickness, it was difficult to get a good solid head joint. This would result in comparatively lower strengths in the vertically cored prisms. This difference is evident when comparing the net strengths of the current results and those found by Whittemore and Hathcock (1923) and Johnson and Matthys (1973).

Stang reported higher strengths for Ohio fire clay (tile A) than New Jersey fire clay (tile B). In the research reported herein, Escondido fire clay was used, which had a dramatically higher net unit tile strength than those reported by Stang. The current prism strengths were also higher than Stangs' results, but were not directly proportional to the difference in unit tile strengths.

Chapter 5

CONSTITUTIVE BEHAVIOR OF STRUCTURAL CLAY TILE PRISMS

Introduction

An investigation of the constitutive behavior of clay tile prisms is described in this chapter. Stress - strain curves were developed for all the prisms, and representative parameters (moduli of elasticity, Poisson's ratio, strain at peak load, unload-reload moduli) were generated from these curves. The final section examines the stress - strain curve in log-log space since it has been suggested that masonry follows an exponential relationship.

5.1 Prism Stress - Strain Curves

Stress - strain curves, consisting of 800 to 16,000 points, were developed for all the tested prisms using DADISP. The LVDT resting on the RAM had to be adjusted to account for machine flexibility and the machine take-up. The program used to adjust the original data is listed in Appendix B. The first section of the program adjusts the machine take-up, or initial offset, of the curves. A slope was calculated based on loads between 20% and 50% of ultimate. From this modulus a straight line was generated from zero to 20% of ultimate. The strains were then reduced by the zero load strain. The effect was to shift the stress - strain curve to the left to account for the

lowering of the top bearing plate onto the prism and the seating of the prism. To account for the machine takeup, the strains from 0% to 20% of ultimate were recalculated using the calculated control LVDT modulus of elasticity.

The correction due to the machine stiffness was accomplished using the correction factor recommended by Priestley and Elder (1982). The stiffness of the testing machine (EMACH) was calculated from the apparent prism stiffness (ERAM) measured by the RAM and the actual stiffness measured by the panel LVDTs (ELVDT). The strain caused by the machine flexibility was then subtracted from the RAM strains.

Figures 5.1.1 through 5.1.8 are typical corrected stress - strain curves. The first five figures are for monotonically loaded prisms. The remaining figures demonstrate the effect of loading - unloading - reloading cycles. The first unload was at approximately 25% of the ultimate strength and the second at approximately 70% of ultimate. The point of unload varied because of the unpredictability of the prism strength.

5.2 Prism Elastic Behavior

Figure 5.2.1 is a summary of the moduli of elasticity for all the clay tile prisms. A least-squares linear fit was made from 5% to 33% and 5% to 50% of ultimate stress to obtain the elastic modulus. In most cases, the elastic modulus was obtained from the average of the six panel LVDTs. Several of the prisms had the panel LVDTs removed before 33% and 50% of

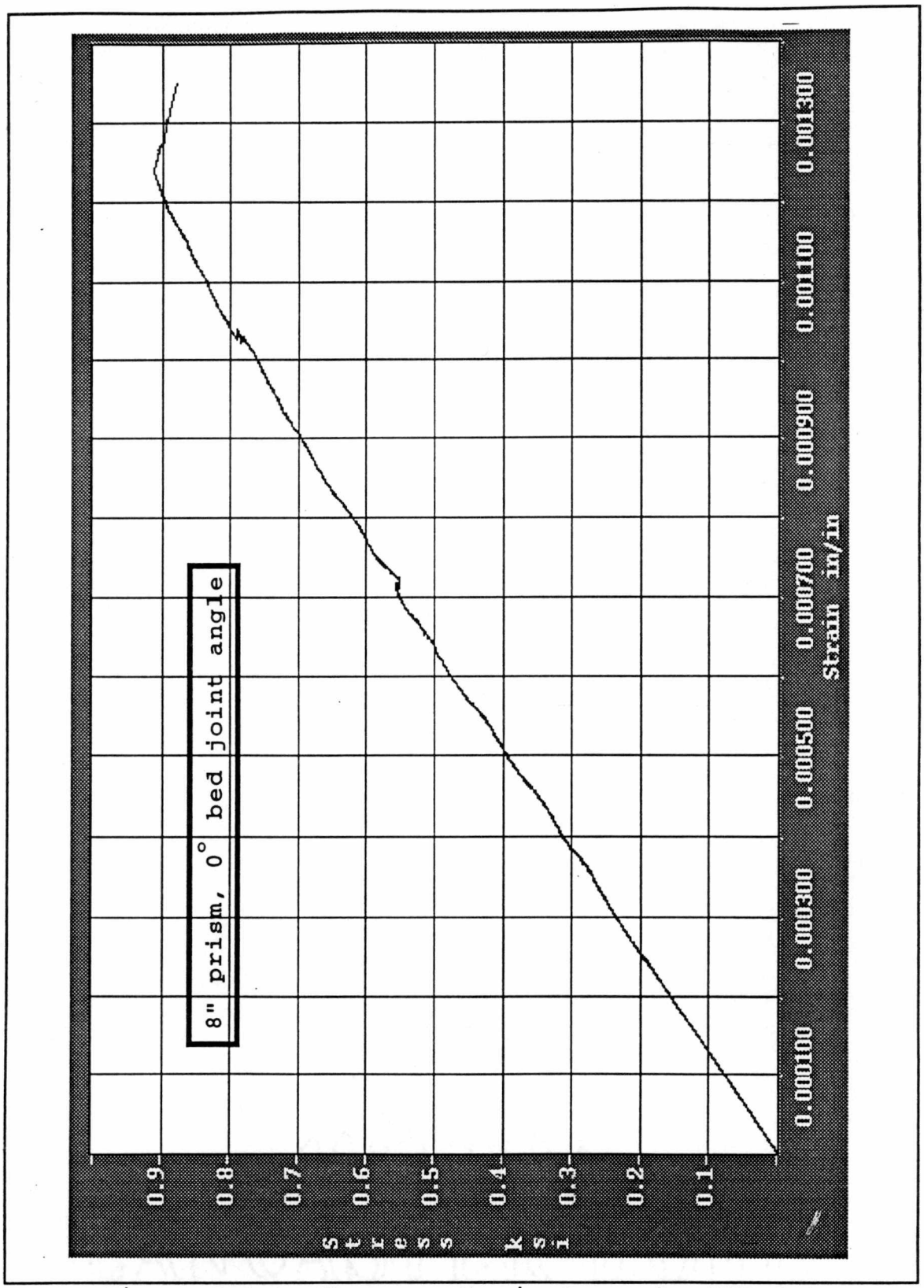


Figure 5.1.1 Stress - Strain Curve for UT8-0-1

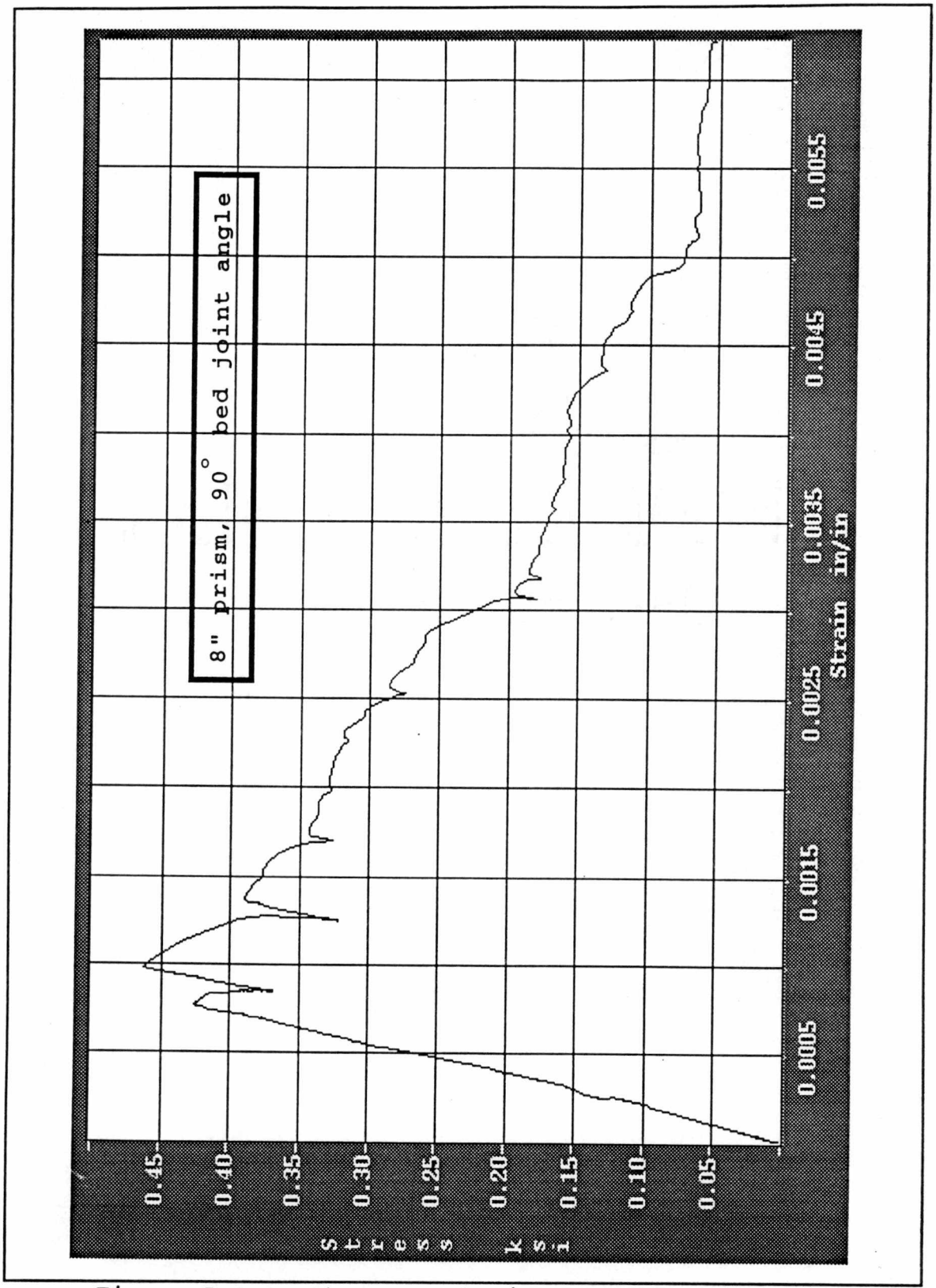


Figure 5.1.2 Stress - Strain Curve for UT8-90-1

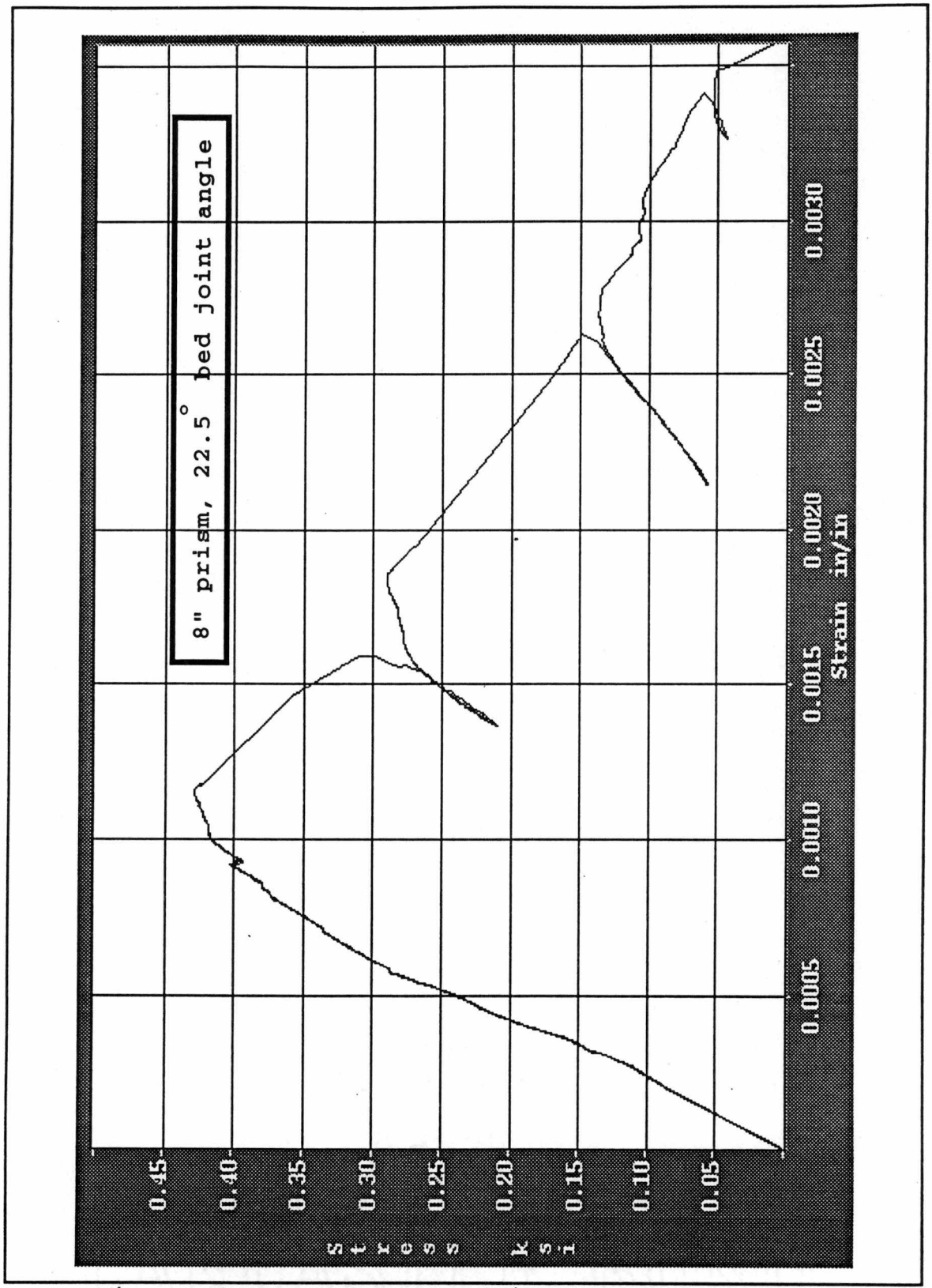


Figure 5.1.3 Stress - Strain Curve for UT8-22-1

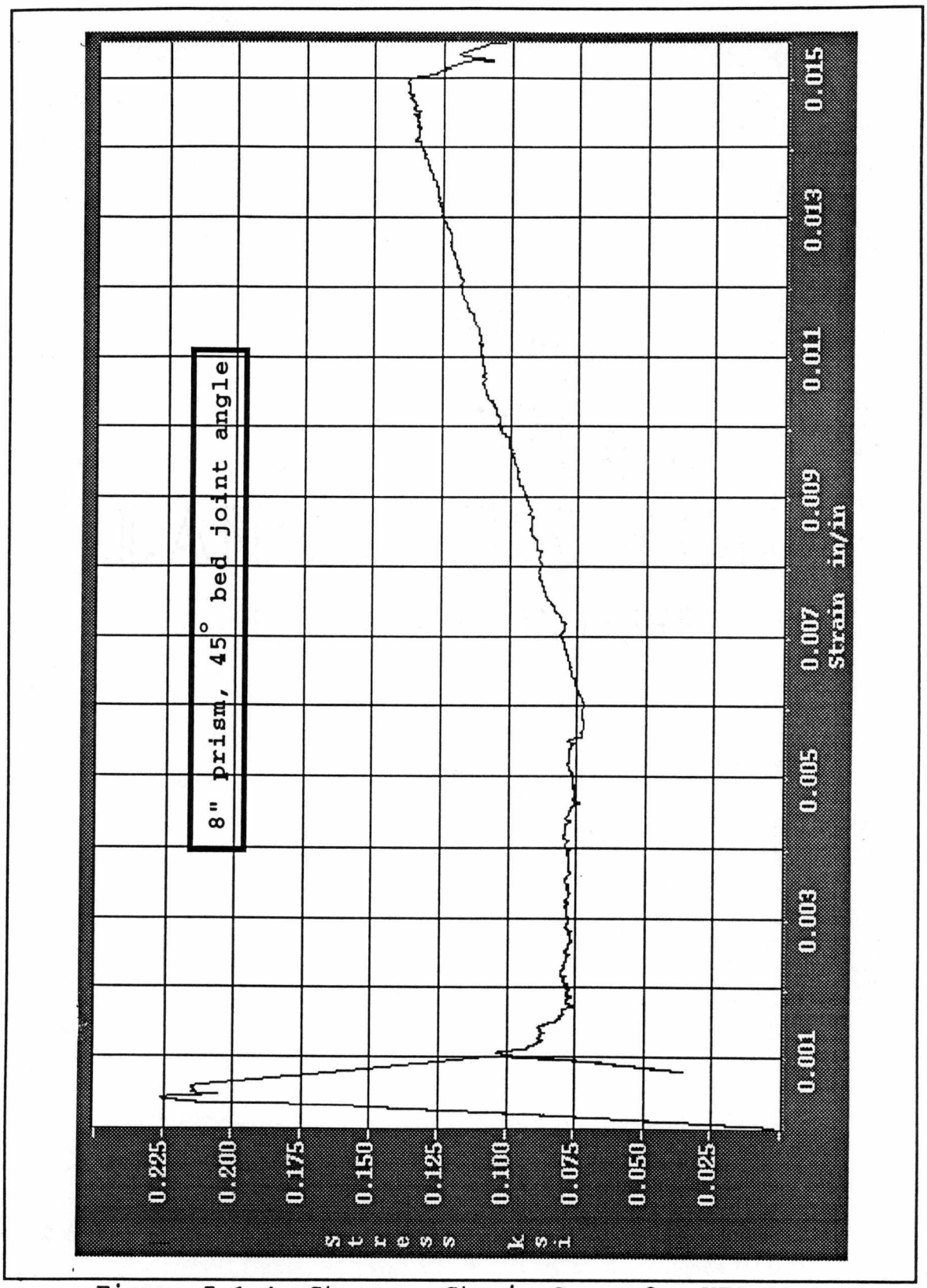


Figure 5.1.4 Stress - Strain Curve for UT8-45-1

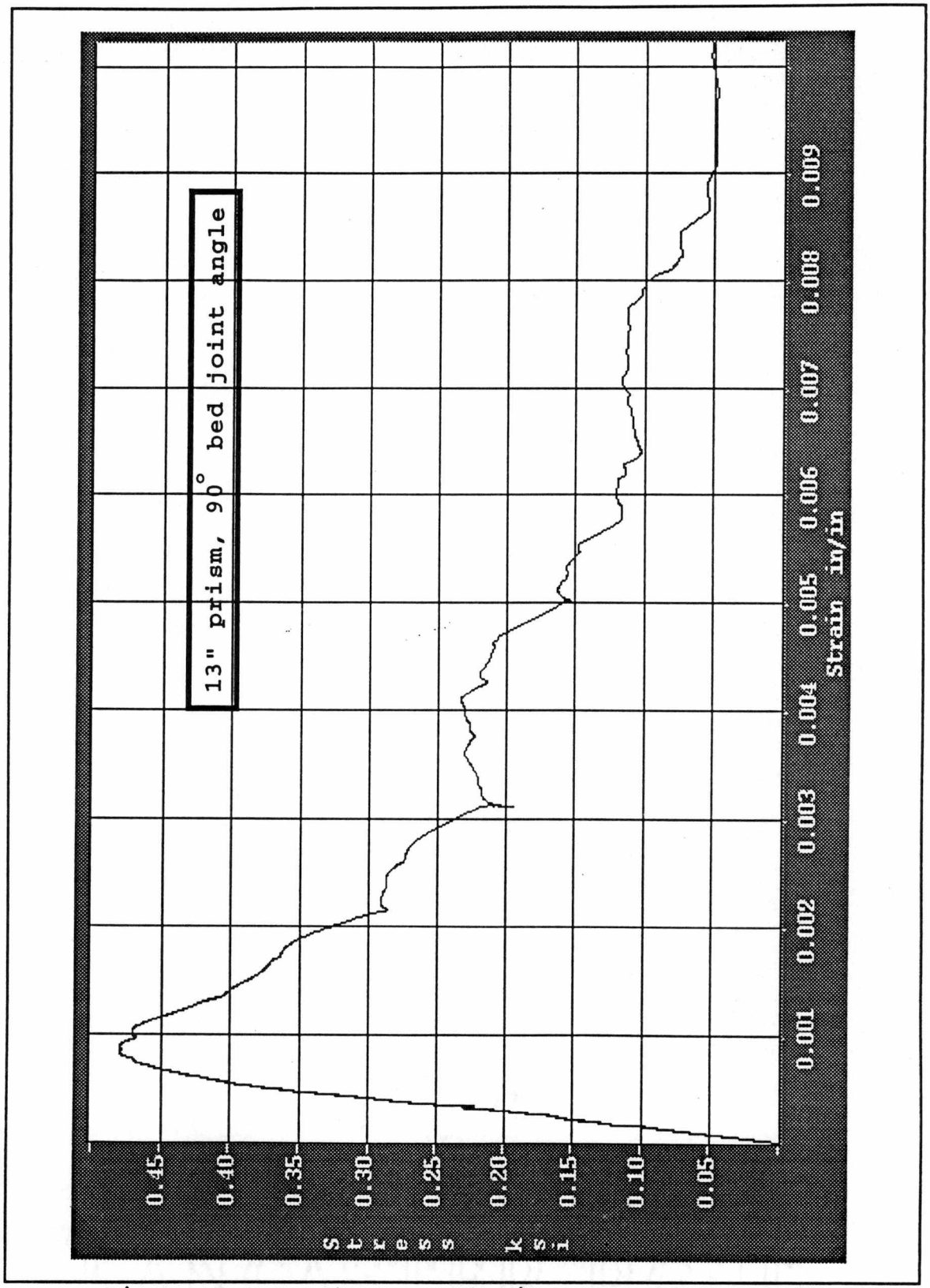


Figure 5.1.5 Stress - Strain Curve for UT13V-1

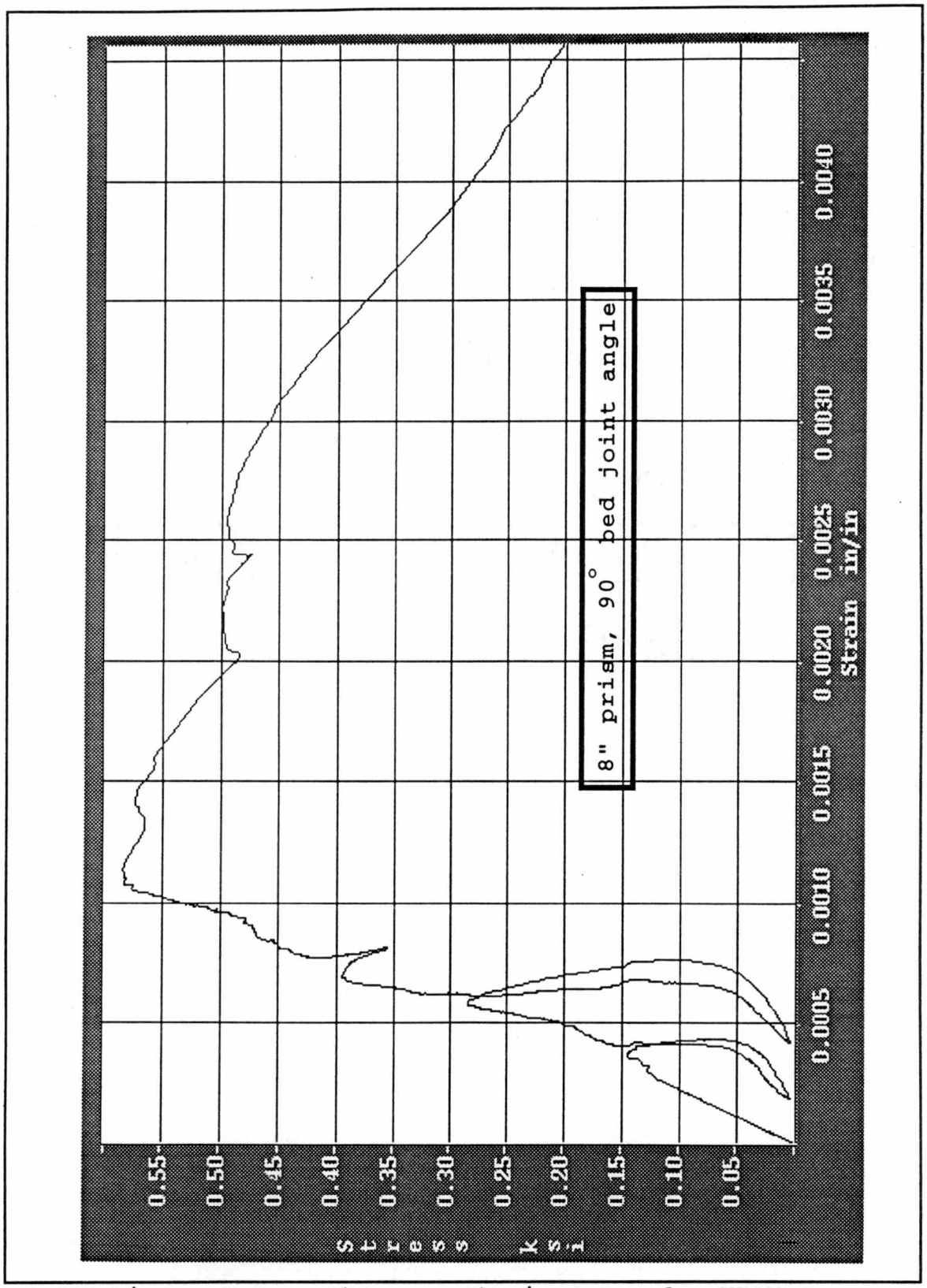


Figure 5.1.6 Stress - Strain Curve for UT8V-4

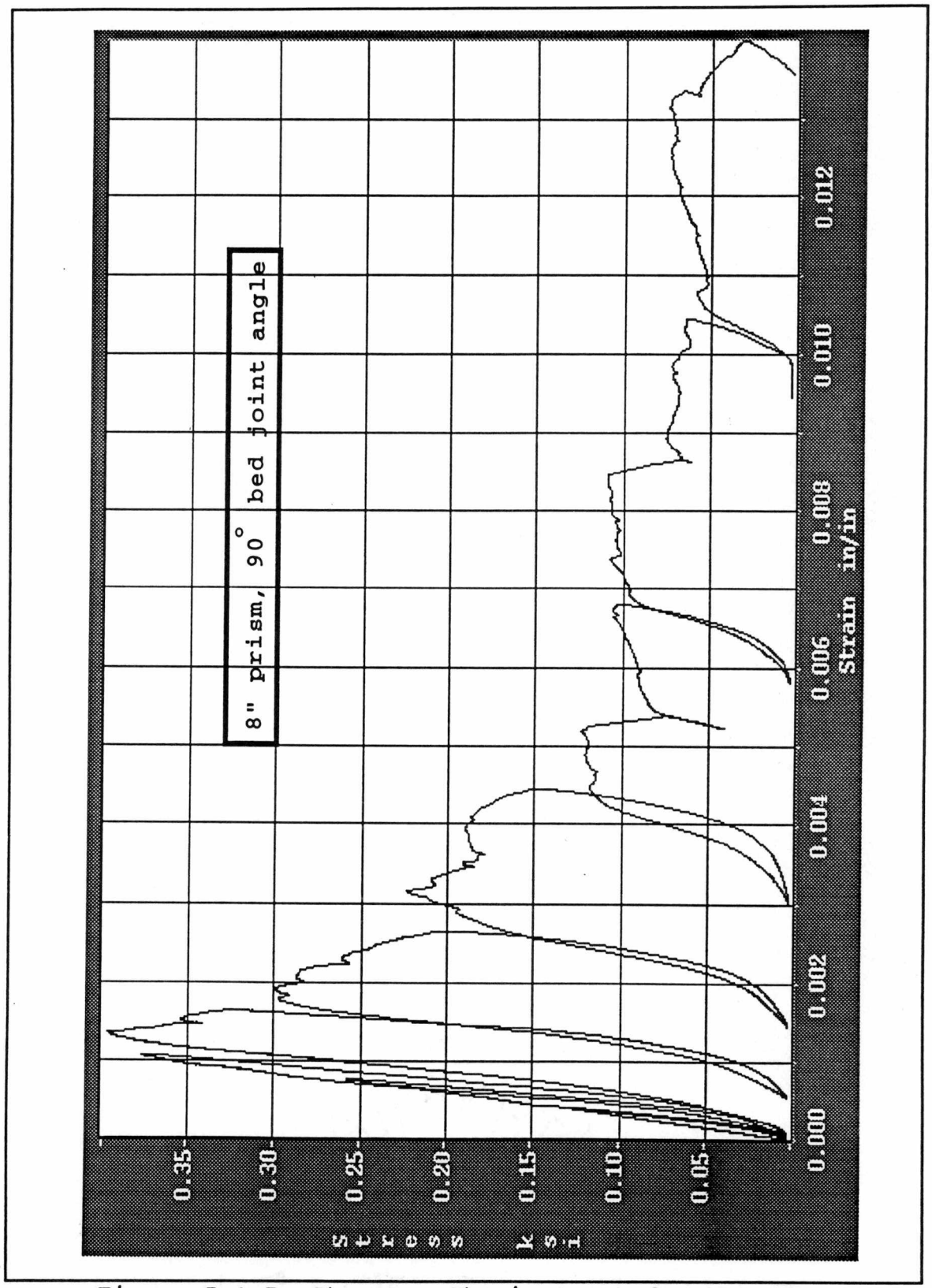


Figure 5.1.7 Stress - Strain Curve for UT8-90-3

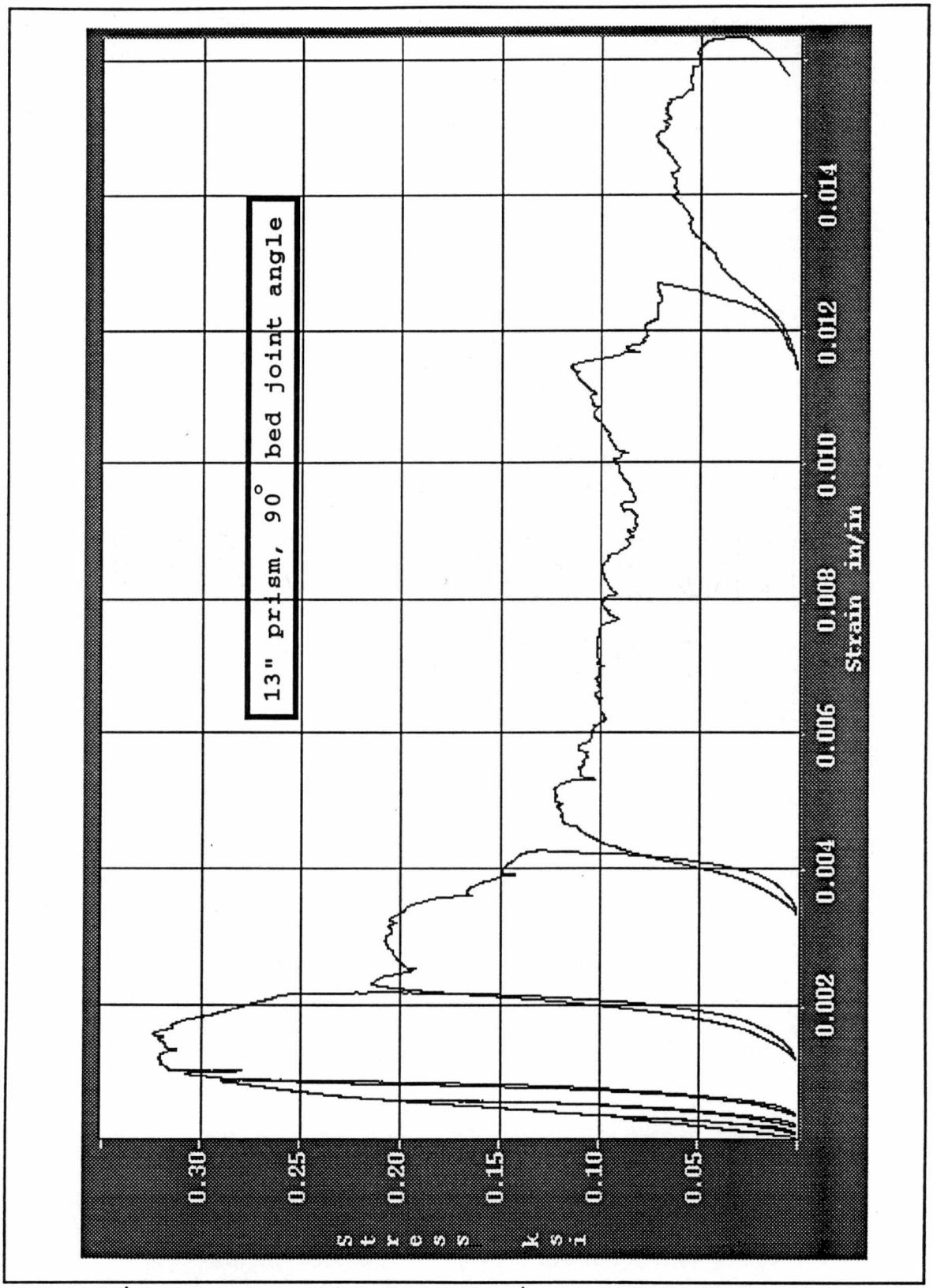


Figure 5.1.8 Stress - Strain Curve for UT13V-3

Figure 5.2.1 Modulus of Elasticity for Clay Tile Prisms

Prism Number	Modulus of Elasticity (ksi)		Comments
	E (5–50%)	E (5–33%)	
UT8H–1	676	694	values obtained from corrected RAM LVDT
UT8H–2	811	783	values obtained from average of panel LVDTs
UT8H–3	802	823	values obtained from average of panel LVDTs
UT8H–4	828	899	values obtained from corrected RAM LVDT
UT8V–1	255	224	values obtained from average of panel LVDTs
UT8V–2	258	290	values obtained from average of panel LVDTs
UT8V–3	306	310	values obtained from corrected RAM LVDT
UT8V–4	441	390	values obtained from average of panel LVDTs
UT13H–1	----	----	LVDTs not working during test
UT13H–2	704	724	values obtained from average of panel LVDTs
UT13H–3	722	767	values obtained from average of panel LVDTs
UT13H–4	766	819	values obtained from average of panel LVDTs
UT13V–1	680	763	values obtained from corrected RAM LVDT
UT13V–2	294	267	values obtained from average of panel LVDTs
UT13V–3	314	279	values obtained from average of panel LVDTs
UT13V–4	351	309	values obtained from average of panel LVDTs
UT8–0–1	782	791	values obtained from average of panel LVDTs
UT8–0–2	775	788	values obtained from average of panel LVDTs
UT8–0–3	702	694	values obtained from average of panel LVDTs
UT8–22–1	435	470	values obtained from average of panel LVDTs
UT8–22–2	702	720	values obtained from average of panel LVDTs
UT8–22–3	526	547	values obtained from average of panel LVDTs
UT8–45–1	516	531	values obtained from average of panel LVDTs
UT8–45–2	594	627	values obtained from average of panel LVDTs
UT8–45–3	768	712	values obtained from average of panel LVDTs
UT8–67–1	940	960	values obtained from average of panel LVDTs
UT8–67–2	661	663	values obtained from average of panel LVDTs
UT8–67–3	240	270	values obtained from average of panel LVDTs
UT8–90–1	482	444	values obtained from average of panel LVDTs
UT8–90–2	216	191	values obtained from average of panel LVDTs
UT8–90–3	344	352	values obtained from average of panel LVDTs

ultimate was reached. In these cases, the corrected control LVDT was used to develop the two modulus values. When the prism underwent a load - unload pattern, it was often necessary to remove one or two cycle loops from the stress - strain curve in order to do a linear fit over the initial portion of the curve.

The average values of elastic modulus for the various prism types are given in figure 5.2.2. The variance was higher for prisms with 22.5°, 45°, 67.5°, and vertical bed joint angles than those prisms with horizontal bed joints. The highest variance occurred in prisms with a bed joint angle of 67° and 90°. The difficulty of providing a consistent head joint may have resulted in the lack of consistency. The difference between the elastic modulus at 50% and 33% was slight with no appreciable change in the variation.

In 10 of the 31 cases reported in figure 5.2.1, the elastic modulus at 50% of ultimate was greater than the elastic modulus at 30% of ultimate. This was observed in 7 of the vertically cored prisms. The apparent increase in stiffness is the result of the head joint being crushed. Because of the difficulty in applying a full head joint, gaps occasionally were observed in the joint. As a result, a lower stiffness was observed as the joint was crushed in the initial loading sequence.

Figure 5.2.3 shows some typical results obtained from relevant past research. The average elastic modulus obtained

Prism Number	Number of Samples	E (5–33%) ksi	V (%)	E (5–50%) ksi	V (%)
8" horizontal	7	782	9.2	768	7.5
8" vertical	7	314	28.4	329	30.4
13" horizontal	4	770	6.2	731	4.4
13" vertical	4	404	59.4	410	44.4
8" at 22.5	3	579	22.2	554	24.5
8" at 45	3	623	14.6	626	20.6
8" at 67.5	3	631	54.9	627	59.2

V = Coefficient of Variation (100*standard deviation/mean)

Figure 5.2.2 Average Elastic Modulus for Clay Tile Prisms

Testing Program	Elastic Modulus (at $\frac{1}{2}f'_m$), ksi
Current Results 8" horizontal	768
Current Results 8" vertical	329
8" horizontal - Tile A (Stang,1926)	457
8" vertical - Tile A (Stang,1926)	846
8" horizontal - Tile B (Stang,1926)	340
8" vertical - Tile B (Stang,1926)	632
8" horizontal (Johnson and Matthys,1973)	720
8" vertical (Johnson and Matthys,1973)	830

Figure 5.2.3 Modulus of Elasticity from Past Research

for the prisms tested with a horizontal bed joint was very close to the results given by Johnson and Matthys (1973). The prisms tested with the tile cores vertical were about one-half as large as those reported by the researchers in figure 5.2.3. This discrepency is mainly the result of the load being applied perpendicular to the head joint in the tests reported herein. The tests for which the data is reported in figure 5.2.3 always applied the load perpendicular to the bed joint.

The strain at ultimate stress was determined from the corrected stress - strain curve. These values were inconsistent. The strains were found to range between 0.00041 in/in for the 45° prism and .00484 in/in for the 8 inch prisms with vertical cores. The values of these strains are shown in figure 5.2.4.

The ratio of the lateral expansion to longitudinal compression (Poisson's ratio) ranged between 0.025 and 1.355. Figure 5.2.5 shows the values of Poisson's ratio for 33% and 50% of ultimate stress. According to Plummer (1962), the ratio for clay tile would probably be in the range of 0.05 to 0.10. The values obtained for the 8" and 13" prisms with a horizontal bed joint had an average ratio of 0.122 at 33% of ultimate and 0.130 at 50% of ultimate. The remaining prisms had consistently large Poisson ratios, with many having a ratio greater than one. However, these values are not the result of lateral expansion of the tile. As the load is applied, cracks form in the mortar which can result in the

Prism Number	Strain at Ultimate Stress	Mean	V (%)
UT8H-1	0.001638	0.001347	23.96
UT8H-2	0.000967		
UT8H-3	0.001259		
UT8H-4	0.001059		
UT8-0-1	0.001236		
UT8-0-2	0.001384		
UT8-0-3	0.001887		
UT8V-1	0.001509	0.002221	65.43
UT8V-2	0.002132		
UT8V-3	0.004839		
UT8V-4	0.001138		
UT8-90-1	0.000987		
UT8-90-2	0.003587		
UT8-90-3	0.001358		
UT8-22-1	0.001159	0.000867	23.12
UT8-22-2	0.001256		
UT8-22-3	0.001655		
UT8-45-1	0.000410	0.001255	41.34
UT8-45-2	0.001785		
UT8-45-3	0.000433		
UT8-67-1	0.001202	0.001357	19.41
UT8-67-2	0.001335		
UT8-67-3	0.002089		
UT13H-1	0.000728	0.000876	89.87
UT13H-2	0.000726		
UT13H-3	0.001152		
UT13H-4	0.000860		
UT13V-1	0.000873	0.001246	6.14
UT13V-2	0.001846		
UT13V-3	0.001530		
UT13V-4	0.000769		

V = Coefficient of Variation (100*standard deviation/mean)

Figure 5.2.4 Strain at Maximum Stress from Stress - Strain Curves

Figure 5.2.5 Poisson's Ratio at 33% and 50% of Ultimate Stress

Prism Number	Poisson's Ratio (at 33% ultimate)	Mean	V (%)	Poisson's Ratio (at 50% ultimate)	Mean	V (%)
UT8H-3	0.0965	0.140	96.05	----	0.164	88.16
UT8H-4	0.0385			0.040		
UT8-0-1	0.376			0.373		
UT8-0-2	0.093			0.115		
UT8-0-3	0.095			0.129		
UT8V-1	0.960	0.830	39.42	1.232	0.955	43.53
UT8V-2	0.543			0.621		
UT8V-3	0.961			1.341		
UT8V-4	0.897			0.950		
UT8-90-1	1.176			1.355		
UT8-90-2	1.039			0.968		
UT8-90-3	0.232			0.220		
UT8-22-1	0.209	0.152	34.20	0.197	0.179	10.06
UT8-22-2	0.138			0.179		
UT8-22-3	0.108			0.161		
UT8-45-1	0.914	0.369	128.53	1.236	0.509	124.96
UT8-45-2	0.143			0.236		
UT8-45-3	0.050			0.055		
UT8-67-1	0.312	0.224	77.08	0.518	0.378	53.53
UT8-67-2	0.025			0.146		
UT8-67-3	0.334			0.470		
UT13H-2	0.144	0.092	56.88	0.134	0.083	55.27
UT13H-3	0.094			0.072		
UT13H-4	0.039			0.044		
UT13V-1	0.107	0.343	51.37	----	0.397	25.77
UT13V-2	0.528			0.515		
UT13V-3	0.397			0.343		
UT13V-4	0.338			0.333		

V = Coefficient of Variation (100*standard deviation/mean)

tiles sliding from their original position. For example, consider the ratio at 33% of 0.914 for UT8-45-1 and 0.143 for UT8-45-2. Cracks existing in the bed joint of UT8-45-1 allowed the tile on the side of the second course to slide, increasing the lateral expansion. In the case of the prisms tested with a vertical bed joint angle, a vertical crack extended the length of the bed joint. As the load was increased, the separation increased as each section began to buckle and deform. The wide variation in the Poisson ratios emphasize the non-homogeneous behavior of masonry tile prisms.

5.3 Constitutive Behavior During Load - Unload Cycling

The effect of loading - unloading - reloading on the system appeared to have little impact on the strength and virgin stiffness of the prism. Plastic deformations are particularly apparent in the post-peak region of the stress - strain curve. For instance, consider the stress - strain curve of prism UT13V-3 in figure 5.1.8. At each unload in the post-peak region, there was an increasing permanent, or plastic, strain. Each reload cycle initially consisted of a curved section at near zero stress which gradually progressed into a linear relationship between the stress and the strain. The change in the strain between near zero stress and the stress where the linear portion of the reload curve began appeared to increase from the first cycle to the last cycle. This is evident in figure 5.1.7. In the later cycles, the linear

portion of the reload curve becomes relatively small compared to the curved portion.

The rebound modulus is defined as the straight line portion of the stress - strain curve after the load has been removed and reapplied to the prism. Figure 5.3.1 shows the locations of the rebound moduli for prism UT8-90-3. A least-squares linear fit was made over the straight portion of the reload for each cycle. The ultimate load for each cycle was also noted. The post-peak rebound modulus for prism UT8-90-3 is shown in figure 5.3.2. As with the pre-peak moduli, the point where the unload began is noted. The pre-peak rebound moduli for several prisms under a cycled load are given in figure 5.3.3. Figure 5.3.4 is the post-peak results, where the peak is the point of ultimate stress.

In the vertically cored prisms, the rebound modulus was typically greater than the modulus of elasticity when the unload occured prior to ultimate. The rebound modulus tended to increase dramatically as ultimate approached. In UT13V-4, the rebound modulus doubled when the unload was taken at 56.6% of ultimate. This sharp increase was observed for only this prism. The other moduli appeared to increase gradually.

The rebound modulus at an unload point of 44% of ultimate for prisms with the cores horizontal was found to be less than the calculated modulus of elasticity. The rebound modulus gradually increased as the cycling approached ultimate.

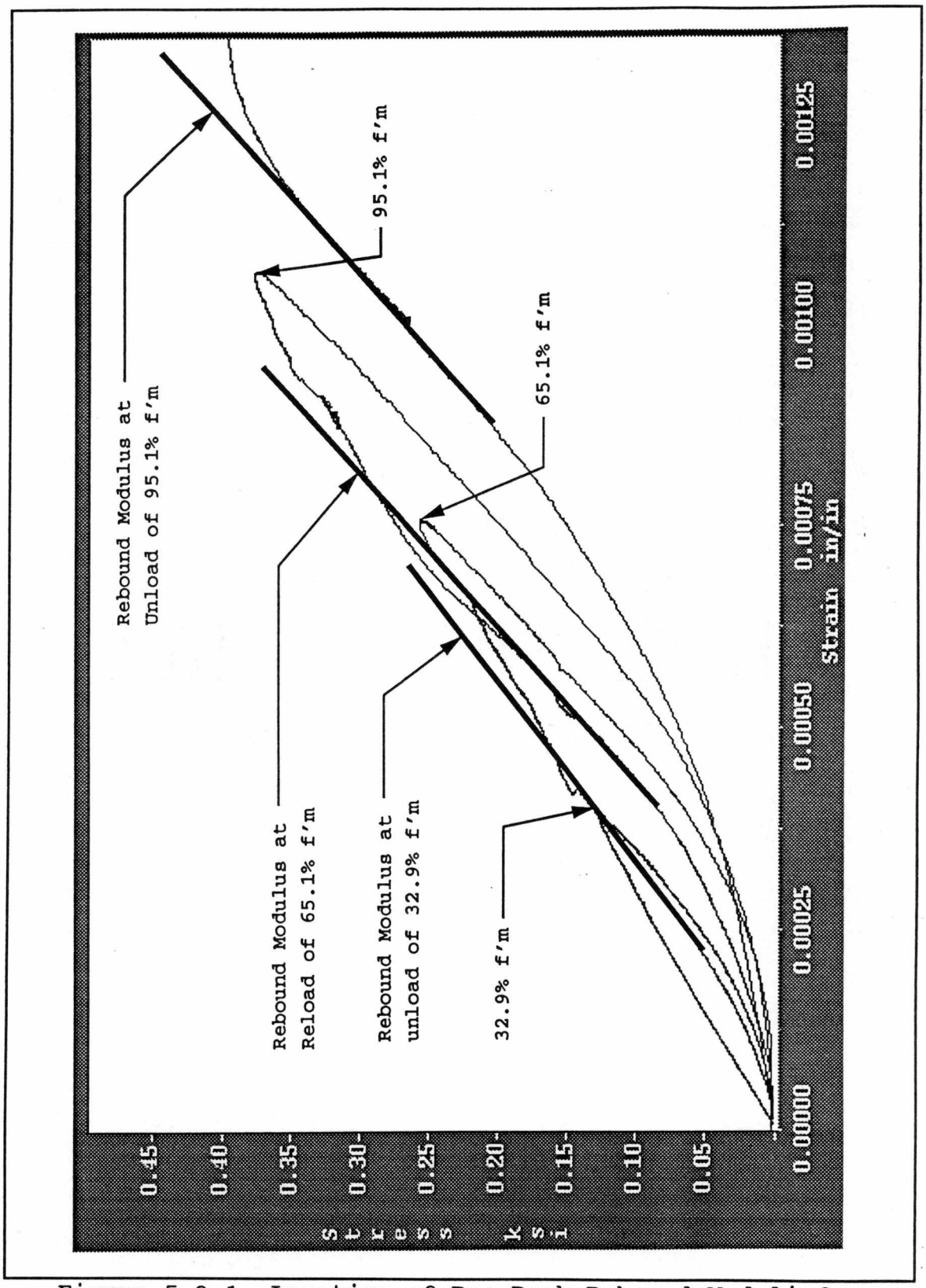


Figure 5.3.1 Location of Pre-Peak Rebound Moduli for Prism UT8-90-3

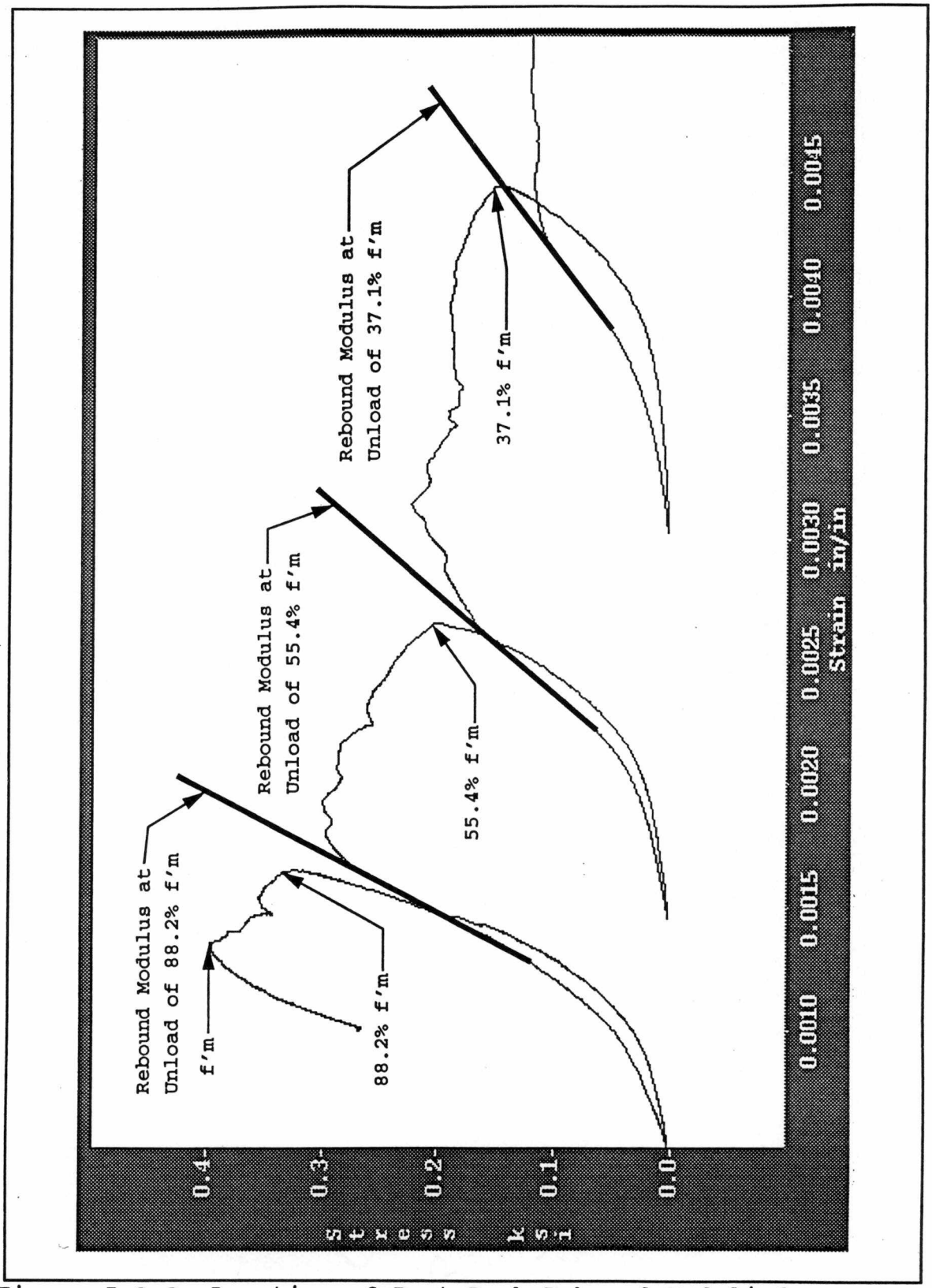


Figure 5.3.2 Location of Post-Peak Rebound Moduli for Prism UT8-90-3

Prism Number	Unload (% ultimate)	Pre-peak Rebound Modulus (ksi)
UT13V-3	28.9	590
	61.0	499
	89.4	437
UT13V-4	26.2	653
	56.6	1269
	83.5	1390
UT8-90-3	32.9	434
	65.1	518
	95.1	535
UT8-90-2	28.7	337
	51.0	337
UT8-0-2	22.4	388
	44.3	463
UT13H-3	43.7	560
	79.1	551
UT8-22-2	24.5	603
	48.4	655
UT8-45-2	38.5	738
	69.9	848

Figure 5.3.3 Pre-Peak Rebound Modulus

Prism Number	Unload (% ultimate)	Post-Peak Rebound Modulus (ksi)
UT13V-3	77.9	517
	45.9	125
UT13V-4	80.7	450
	40.4	89
UT8-90-3	88.2	418
	55.4	236
	37.1	158

Figure 5.3.4 Post-Peak Rebound Modulus

The prisms with a bed joint angle of 22.5° reacted in the same manner as the horizontally cored prisms. The rebound modulus at an unload of 25% of ultimate, however, was closer to the calculated modulus of elasticity than the horizontally cored prisms' rebound modulus.

Prisms with bed joint angles of 45° and 67.5° reacted similarly to the vertically cored prisms. The rebound modulus tended to be greater than the elastic modulus. As the unloading point approached ultimate, the rebound modulus gradually increased.

The post-peak rebound modulus could only be observed in the vertically cored prisms. Because of the dramatic failure pattern in the other prism types, very little load could be applied beyond ultimate. The rebound modulus was slightly greater than the elastic modulus if the prism was unloaded just past ultimate. The rebound modulus dropped rapidly in the post-peak portion of the stress - strain curve. However, the amount of plastic strain continued to increase.

5.4 Logarithmic Relationship Of Stress - Strain Curve

It has been suggested by several people including Romano et al. (1992) and Giovanni and Roberto (1987) that the stress - strain curves for masonry prisms under a uniaxial load are linear in log - log space. As an example, the stress - strain curve for UT8V-3 is shown in figure 5.4.1. The dashed line is the least-squares linear fit for the curve up to ultimate

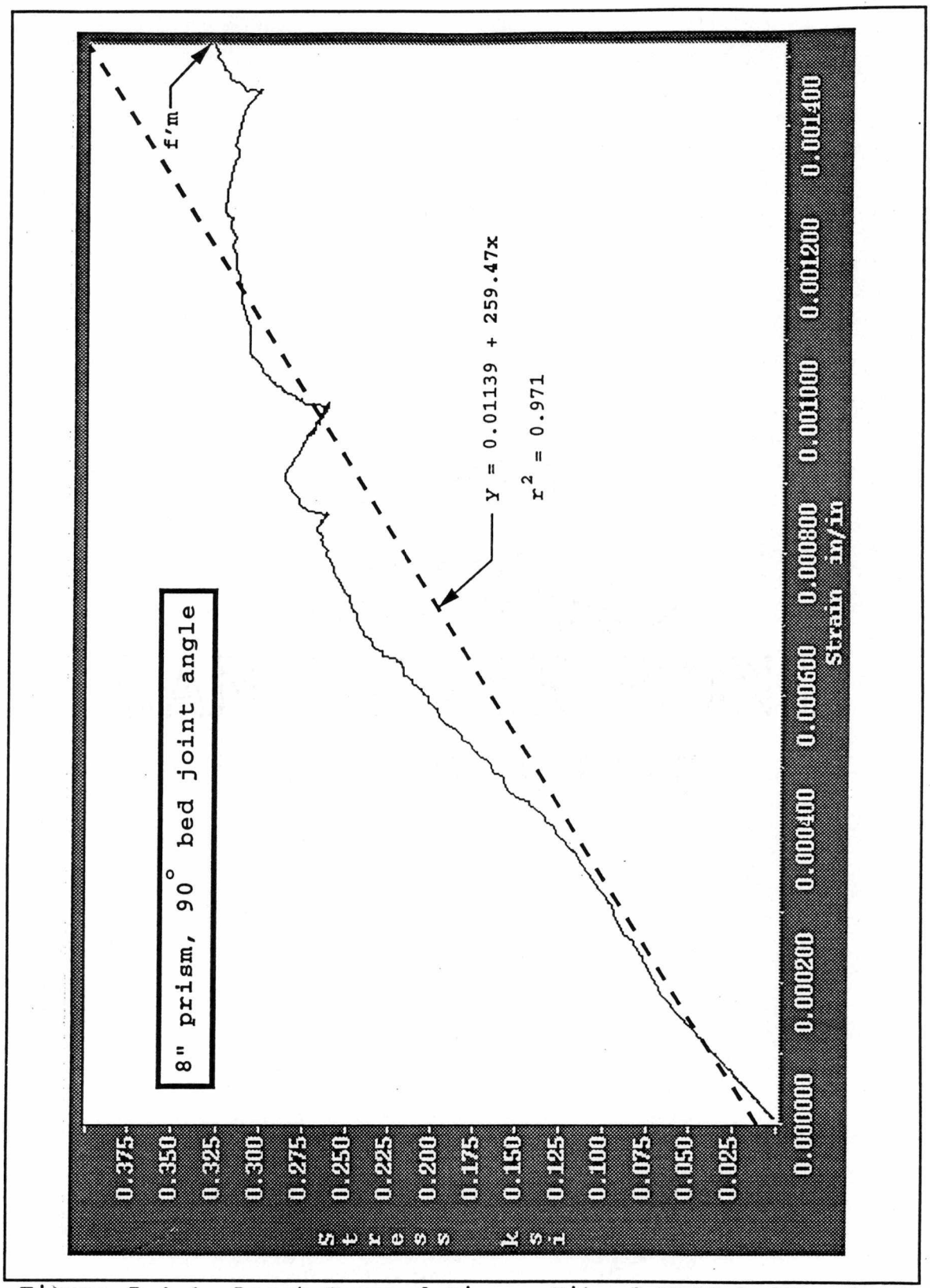


Figure 5.4.1 Least-Squared Linear Fit of UT8V-3 (Standard Space)

stress. As a reference of correlation between the stress - strain data and the linear fit, r^2 was calculated to be 0.971. Figure 5.4.2 is a log-log plot of the same stress - strain curve. A least-square linear fit of the log-log plot produced an r^2 of 0.998.

Figure 5.4.3 shows the least-squares linear fit coefficients for the standard plot and the log - log plot. Average values of the log-log constitutive relation are given in figure 5.5.4. It is apparent that the logarithmic plot of the stress - strain curve gives an improved model. The most dramatic improvement on the linear fit was in prism UT45-2 where r^2 went from 0.802 for the standard plot to 0.984 for the logarithmic plot.

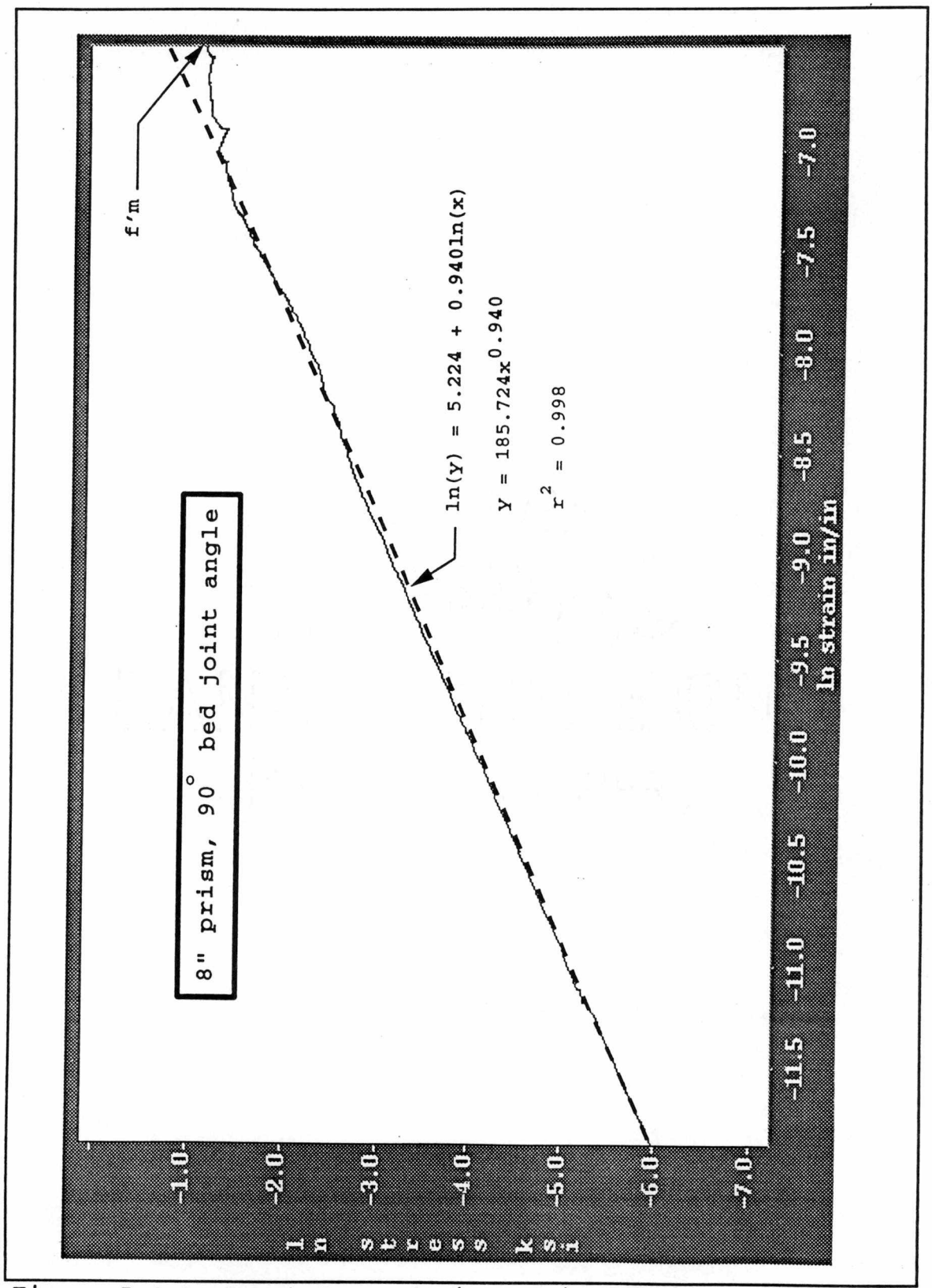


Figure 5.4.2 Least-Squared Linear Fit of UT8V-3 (Log - Log Space)

Prism Number	Standard Plot (ksi) stress = a(strain) + b			Logarithmic Plot (ksi) stress = b(strain)^a		
	a	b	r^2	a	b	r^2
UT8H-1	554	0.026	0.993	0.970	520	0.998
UT8H-3	754	0.009	0.993	0.993	743	1.000
UT8H-4	750	0.019	0.995	0.983	704	0.999
UT8V-1	314	-0.004	0.992	1.041	399	0.998
UT8V-2	214	0.017	0.941	0.991	240	0.996
UT8V-3	259	0.011	0.971	0.940	186	0.998
UT8V-4	536	-0.015	0.987	1.030	612	0.998
UT8-0-1	762	0.005	0.999	0.997	756	1.000
UT8-0-2	802	-0.003	0.990	1.005	822	0.999
UT8-0-3	542	0.018	0.995	0.955	420	0.999
UT8-22-1	423	0.011	0.988	1.002	450	0.999
UT8-22-2	678	0.022	0.979	1.006	775	0.997
UT8-22-3	440	0.021	0.988	0.966	374	0.998
UT8-45-1	571	-0.003	0.992	1.018	631	0.999
UT8-45-2	238	0.048	0.802	0.898	190	0.984
UT8-45-3	617	0.011	0.955	0.984	607	0.993
UT8-90-1	433	0.016	0.971	0.982	406	0.996
UT8-90-2	156	0.035	0.922	0.967	157	0.996
UT8-90-3	343	0.001	0.989	1.001	348	1.000
UT13H-2	543	0.010	0.980	0.958	419	0.998
UT13V-1	686	0.006	0.986	1.002	724	0.999
UT13V-2	208	0.022	0.937	0.948	171	0.993
UT13V-3	276	0.017	0.950	0.993	298	0.996
UT13V-4	391	0.002	0.977	1.027	482	0.997

Figure 5.4.3 Results of Least-Squared Linear Fit for Clay Tile Prisms

Prism Number	Number of Samples	Average Coefficients of Log-Log Plot			
		a	V (%)	b	V (%)
8" horizontal	6	0.984	1.9	661	23.6
8" vertical	7	0.993	3.5	335	47.0
13" horizontal	1	0.958	0.0	419	0.0
13" vertical	4	0.993	3.3	419	57.4
8" at 22.5	3	0.991	2.2	533	40.0
8" at 45	3	0.967	6.4	476	52.1

V = Coefficient of Variation (100*standard deviation/mean)

Figure 5.4.4 Average Coefficients for Log-Log Plot

Chapter 6

CONCLUSIONS

Prisms constructed of terra cotta structural clay tiles were tested under a uniaxial compressive load. Much of the design of the testing program was based on the findings described in the literature review. Each prism was constructed with four courses of tiles to reduce the effect of end constraint. Four inch thick bearing plates were utilized to prevent stress concentrations at the top of the prism. Finally, the top and bottom of the prism were capped with hydrostone which had a high strength relative to the mortar.

The orientation of the bed joint had a major effect on the compressive strength of the prisms. This was evident in the modes of failure exhibited in prisms with bed joints of 0°, 22.5°, 45°, 67.5°, and 90° relative to the horizontal. The prisms with bed joints of 0° and 22.5° resulted in crushing failure. Prisms with bed joint angles of 45° and 67.5° tended to produce sliding failures along the bed joint. The strength was controlled by the friction between the bed joint and the tile. The tiles in the prisms with 90° bed joints tended to buckle as the bed joint split and the head joint was crushed.

The 8" prisms tested with a horizontal bed joint were found to have the highest compressive strength based on the net and gross areas. The average strength of 810 psi based on

the gross area was almost twice the strength of that obtained for the prisms with the bed joint vertical. As the bed joint angle was increased from 22.5° to 67.5°, the strength decreased. This was the result of the increasing influence of sliding along the bed joint.

The 13" prisms had strengths lower than the 8" prisms. Contrary to what was observed in the 8" prisms, the vertical cored prisms had higher strengths than the horizontally cored prisms, due to the practice of alternating the 8" and 4" tile courses along the height of the prism. It is possible that a higher strength would be observed if the horizontally cored prism was constructed so that the 8" tiles and the 4" tiles did not alternate. This construction would require some type of tie between the tiles to obtain composite action.

Comparison with past research revealed that earlier results had little in common with the strengths found in this program. This finding underscores the need to do compressive tests on prisms of similar construction to the walls being analyzed to determine the compressive strength. The results for the 0° bed joint prisms had the best correlation with other research performed, due to the similarity in construction practices. In prisms with a 90° bed joint angle, the bed joints and head joints in prisms tested in other programs were in opposite positions to the prisms tested in this program. This orientation resulted in lower strengths for the vertically cored prisms in this program. The difficulty in

obtaining good head joints along the thin face shells led to premature crushing in the head joints.

The modulus of elasticity obtained in these tests compared reasonably well with past findings for the horizontally cored prisms. The results for the vertically cored prisms were less than half the elastic moduluii observed in past research, due to the same factors that caused the lower unit strength. The average modulus of elasticity was 768 ksi and 329 ksi for the horizontal and vertical prisms, respectively.

There appeared to be little relationship between the strain at ultimate stress and the ultimate stress. For example, in the horizontally cored prisms, the strains varied between 0.000967 and 0.001887 with a coefficient of variation of 24%.

The ratios between the lateral and transverse strains were quite high, except for the horizontally cored prisms. The 8" prism had a Poisson's ratio of 0.14 at 33% of ultimate and 0.16 at 50% of ultimate. The 13" prisms had a Poisson's ratio of 0.09 at 33% ultimate and 0.08 at 50% ultimate. The remaining prism types had extremely high ratios because tiles tended to slide in the 45° and 67.5° prisms, creating large lateral displacements. In the 90° prisms, the bed joint split, and the measurement of the lateral expansion included the increasing separation along the joint. Thus, the lateral

measurements were measurements of crack openings, not elastic deformations.

The loading - unloading - reloading pattern appeared to have very little effect on the prism strength and constitutive properties. In fact, the strength of prism UT8V-4 which was subjected to unloading had the highest strength of any of the other prisms. This was unexpected, but it does demonstrate the lack of influence in cycling the load.

The stress - strain curve up to ultimate is best represented by an exponential relationship. Plotting the stress - strain curve in log - log space produces a good linear fit, with a high r^2.

BIBLIOGRAPHY

BIBLIOGRAPHY

Atkinson, R.H. and Yan, G.G. (1990). "Results of a Statistical Study of Masonry Deformability." The Masonry Society Journal, Volume 9, No. 1, pp. 81-94.

Building Code Requirements for Masonry Structures (ACI 530-88/ASCE 6-88), American Concrete Institute, 1988.

Flanagan, R.D. and Bennett, R.M. (1992). "Structural Testing of Hollow Clay Tile Units." Technical Report Y/EN-4536/V1, Martin Marietta Energy Systems,Inc., Oak Ridge, TN.

Foster, P. and Bridgeman, D. (1973). "Prism Tests for the Design and Control of Brick Masonry." The New Zealand Pottery and Ceramics Research Association (Inc.), Technical Report No. 22.

Francis, A.J., Horman, C.B., and Jerrems, L.E. (1971). "The Effect of Joint Thickness and Other Factors on the Compressive Strength of Brickwork." Proceedings of the Second International Brick Masonry Conference, British Ceramics Research Association, pp. 31-37.

Giovanni, M. and Roberto, G. (1987). "Reliability of Three Nonlinear Constitutive Laws in Predicting Masonry Deformations." Proceedings of the Fourth North American Masonry Conference, 22A:1-22A:14.

Hamid, A.A. and Chukwunenye, A.D. (1986). "The Compression Behavior of Concrete Masonry Prisms." Journal of Structural Engineering, ASCE, 112(3), pp. 605-614.

Hamid, A.A., and Drysdale, R.G. (1980). "Concrete Masonry Under Combined Shear and Compression Along the Mortar Joints." Journal of the American Concrete Institute, Volume 77(5), pp. 314-320.

Hegemier, G.A., Krishnamoorthy, G., Nunn, R.O., and Moorthy, T.V. (1978). "Prism Tests for the Compressive Strength of Concrete Masonry." North American Masonry Conference, 18:1 - 18:17.

Johnson, F.B. and Matthys, J.H. (1973). "Structural Strength of Hollow Clay Tile Assemblages." Journal of the Structural Division, ASCE, 99(ST2), pp. 259-275.

Khattab, M.M. and Drysdale, R.G. (1992). "Tests of Concrete Block Masonry Under Biaxial Tension - Compression." Proceedings, Sixth Canadian Masonry Symposium, pp. 645-656.

Kingsley, G.R., Noland, J.L., and Schuller, M.P. (1992). "The Effect of Slenderness and End Restraint on the Behavior of Masonry Prisms: A Literature Review." The Masonry Society Journal, Volume 10, No. 2, pp. 65-74.

Krefeld, W. (1938). "The Effects of Shape of Specimens on the Apparent Compressive Strength of Brick Masonry." Proceedings of American Society for Testing and Materials, Volume 38, Part I, pp. 363-370.

Mayes, R.L. and Clough, R.W. (1975). "A Literature Survey - Compressive, Tensile, Bond, and Shear Strength of Masonry." Earthquake Engineering Research Center Report 75-15, University of California, Berkeley, Ca.

Monk Jr., C.B. (1967). "A Historical Survey and Analysis of the Compressive Strength of Brick Masonry." Structural Clay Products Research Foundation, Research Report No. 12.

Page, A.W. and Shrive, N.G. (1988). "A Critical Assessment of Compression Tests for Hollow Block Masonry." Masonry International, Volume 2, No. 2, pp. 64-70

Priestley, M.J.N. and Elder, D.M. (1982). "Seismic Behavior of Slender Concrete Masonry Shear Walls." Research Report ISSN 0110-3326, Dept. of Civil Engineering, University of Canterbury, Christchurch, New Zealand.

Romano, F., Ganduscio, S., and Zingone, G. (1992). "Stability of Masonry with Nonlinear Stress-Strain Relationship." Masonry International, Vol. 6, No. 2, pp. 69-74.

Specifications for Masonry Structures (ACI 530.1-88/ASCE 6-88), American Concrete Institute, 1988.

Stang, A.H., Parsons, D.E., and Foster, H.D. (1926). "Compressive and Transverse Strength of Hollow - Tile Walls." National Bureau of Standards Technologic Paper 311, Volume 20, pp. 317-353.

Structural Clay Products Institute (1967). "Compressive, Transverse, and Racking Strength Tests of Four - Inch Structural Clay Facing Tile Walls." Structural Clay Products Research Foundation , Report No. 11.

Structural Clay Products Research Foundation (1965). "Compressive, Transverse, and Racking Tests of 4 Inch Brick Walls." SCPRF, Research Report No. 9.

Structural Clay Products Research Foundation (1964). "Small Scale Specimen Testing - National Testing Program." SCPRF, Research Report No. 1.

U.S. Department of Commerce (1926). "Compression Tests on Brick Masonry." Building Code Committee, U.S. Department of Commerce, March.

Uniform Building Code, International Conference of Building Officials, Whittier, CA., Chapter 24, 1988 Edition.

Watstein, D. and Allen, M. (1971). "Structural Performance of Clay Masonry Assemblages Built with High - Bond Organic Modified Mortar." Proceedings of Second International Brick Masonry Conference, British Ceramic Association, pp. 99-112.

Whittemore, H.L. and Hathcock, B.D. (1923). "Some Compressive Tests of Hollow - Tile Walls." U.S. Bureau of Standards Technologic Paper No. 238, Volume 17, pp. 513-527.

Whittemore, H.L., Stang, A.H., and Parsons, D.E. (1938). "Structural Properties of Six Masonry Wall Constructions." U.S. National Bureau of Standards, Building Materials, and Structures, Report BMS5.

APPENDICES

APPENDIX A

(Sample Data Sheets)

TEST PERSONNEL: PRISM TESTING

Test Date _____

Test Prism No. _____

Test Director _____

MM-ES Technical Contact _____

MTS System Operator _____

Data Acquisition Operator _____

Assistants

_____
_____
_____
_____
_____

Attendees

_____
_____
_____
_____
_____
_____
_____
_____
_____
_____
_____
_____
_____
_____
_____
_____

PRISM COMPRESSION TEST DATA SHEET

Prism Test Number _____
Date Made _____
Date Tested _____

Prism Type
___ A (8" - cores horizontal)
___ B (8" - cores vertical)
___ C (13" - cores horizontal)
___ D (13" - cores vertical)

Prism Dimensions

Width (in.)		Thickness (in.)		Height w/cap (in.)	
Top		Top		Left	
Middle		Middle		Center	
Bottom		Bottom		Right	
Average		Average		Average	

Cap Thickness: Top _____ Bottom _____

Prism Weight: Total _____
Tare _____
Prism _____

Prism Ultimate Load _____

Testing Comments:

DATA ACQUISITION CHANNEL NUMBERS: PRISM COMPRESSION TEST

Sensor	Channel No.
Load Cell	000
Upper Bearing Plate LVDT - Vertical (Control, AC)	001
Doorbell	002
Side Left LVDT - Horizontal (13" Prism only)	006
Side Right LVDT - Horizontal (13" Prism only)	007
Front Face Left LVDT - Vertical	008
Front Face Center LVDT - Vertical	009
Front Face Right LVDT - Vertical	010
Front Face center LVDT - Horizontal	011
Back Face Left LVDT - Vertical	012
Back Face Center LVDT - Vertical	013
Back Face Right LVDT - Vertical	014
Back Face Center LVDT - Horizontal	015

LVDT PLACEMENT: PRISM COMPRESSION TEST

Prism No. _____

LVDT Location	Size	Serial No.	MEGADAC Channel No.	Gage Length (in)
Upper Bearing Plate - Vertical	± 0.2"		001	
Side Left - Horiz. (13" only)	± 1.0"		006	
Side Right - Horiz. (13" only)	± 1.0"		007	
Front Face Left - Vertical	± 1.0"		008	
Front Face Center - Vertical	± 1.0"		009	
Front Face Right - Vertical	± 1.0"		010	
Front Face Center - Horizontal	± 1.0"		011	
Back Face Left - Vertical	± 1.0"		012	
Back Face Center - Vertical	± 1.0"		013	
Back Face Right - Vertical	± 1.0"		014	
Back Face Center - Horizontal	± 1.0"		015	

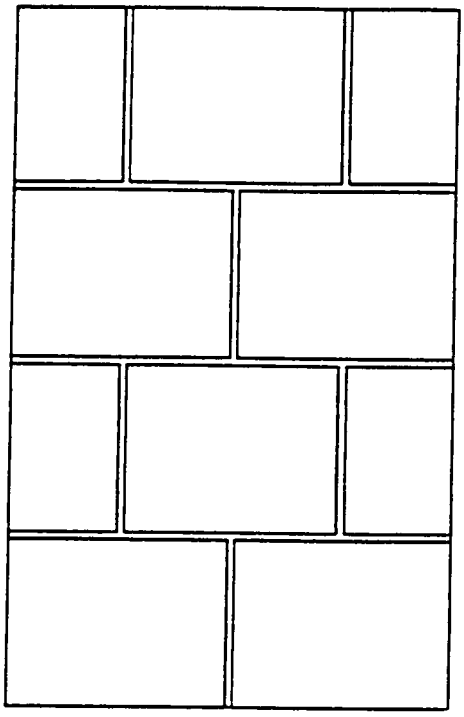
CRACK AND FAILURE PATTERNS

Prism Test Number _____

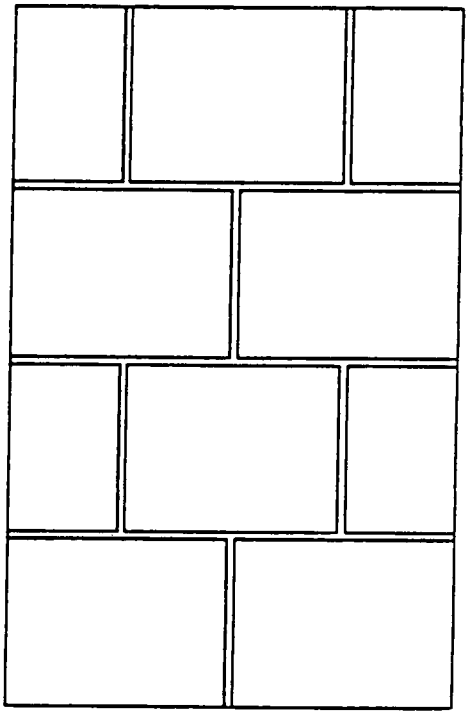
Cracks Mapped By _____

Test Event _____

Front View



Back View



Type A Prism

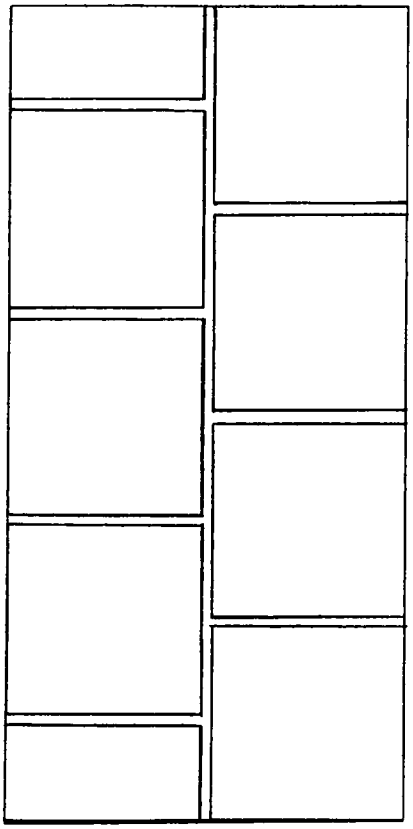
CRACK AND FAILURE PATTERNS

Prism Test Number _____

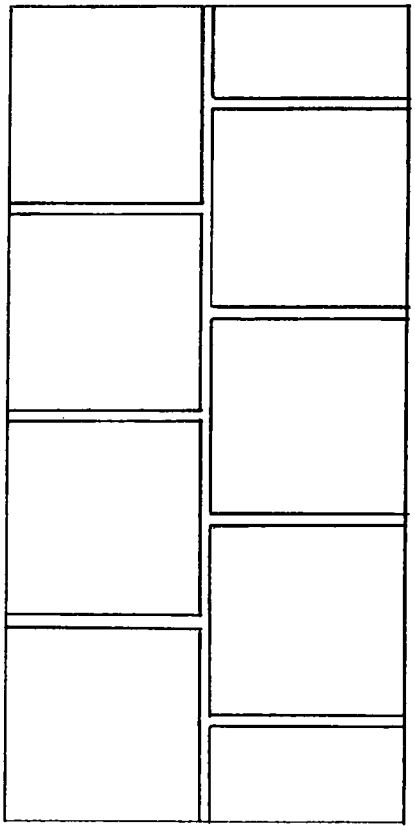
Cracks Mapped By _____

Test Event Date _____

_____ VIEW



_____ VIEW

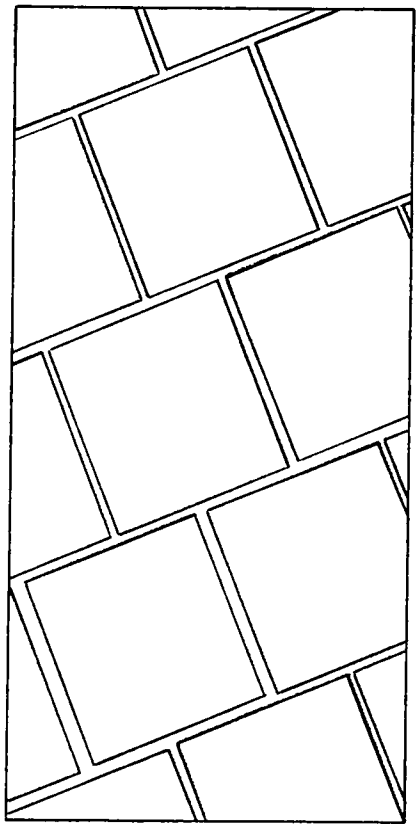


VERTICAL PRISMS

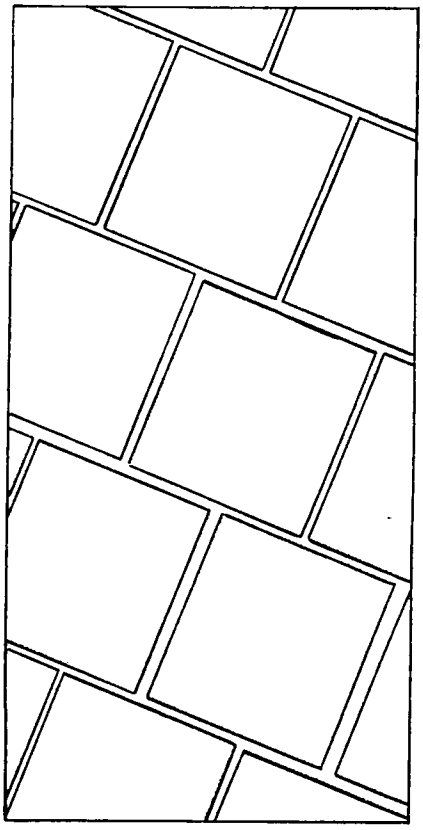
Crack and Failure Patterns

Prism Test Number _____
Cracks Mapped By _____
Test Event Date _____

_____ View



_____ View

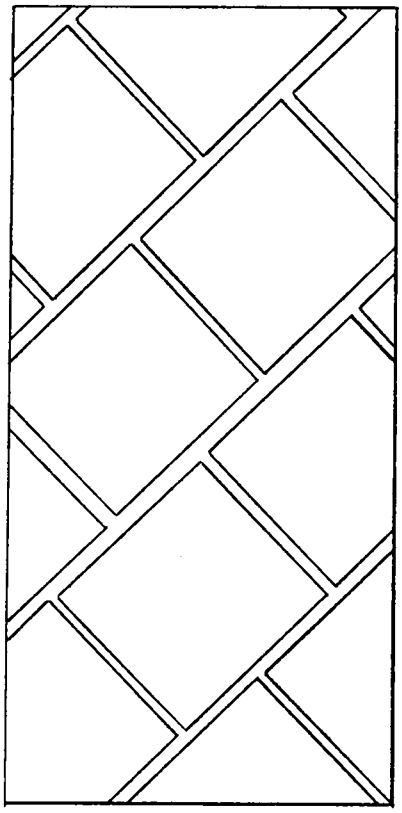


Prism with Bed Joint at 22.5°

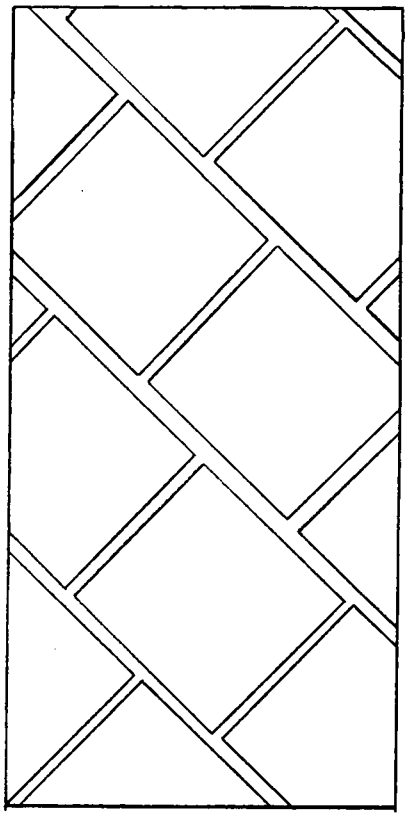
Crack and Failure Patterns

Prism Test Number _____
Cracks Mapped By _____
Test Event Date _____

_____ View



_____ View

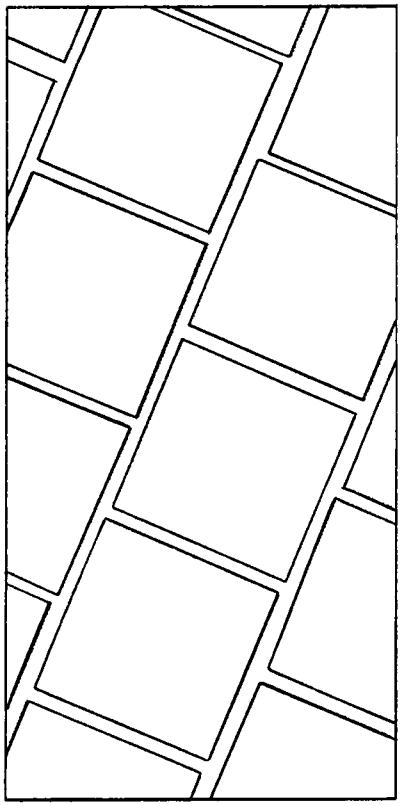


Prism with Bed Joint at 45°

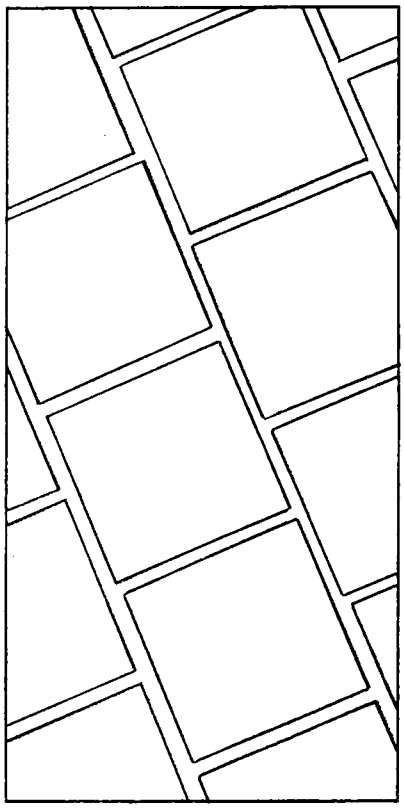
Crack and Failure Patterns

Prism Test Number _____
Cracks Mapped By _____
Test Event Date _____

_____ View



_____ View



Prism with Bed Joint at 67.5°

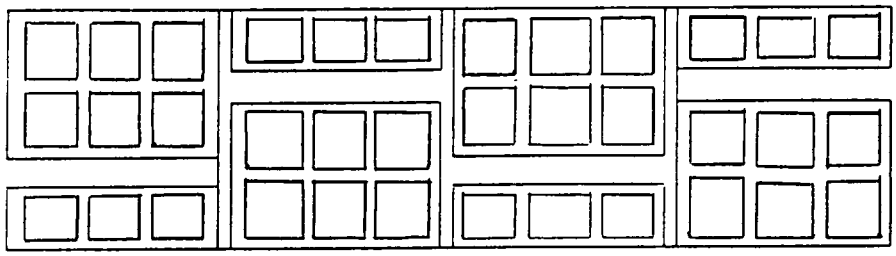
CRACK MAP

Test Date _____

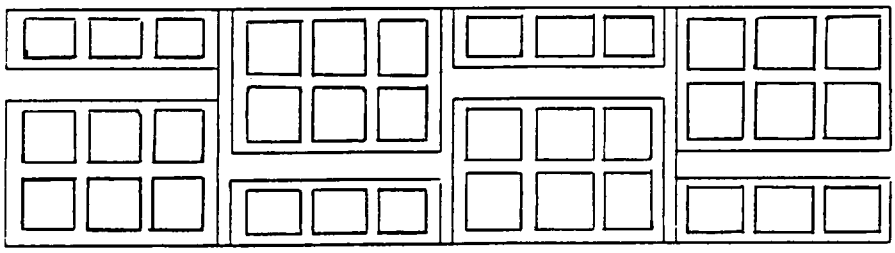
Cracks Mapped By _____

Test Prism Number _____

Side View

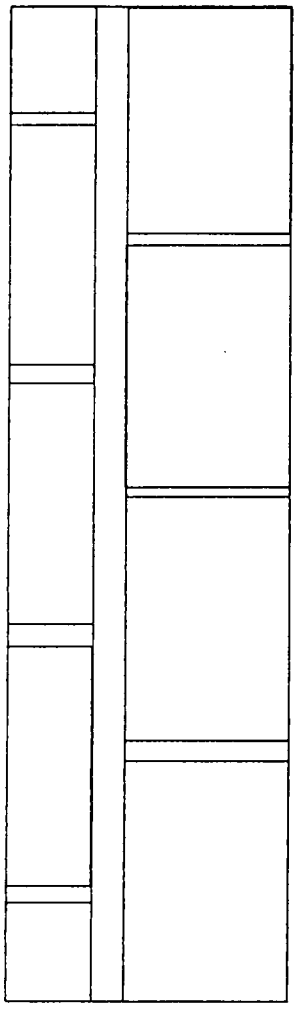


Side View

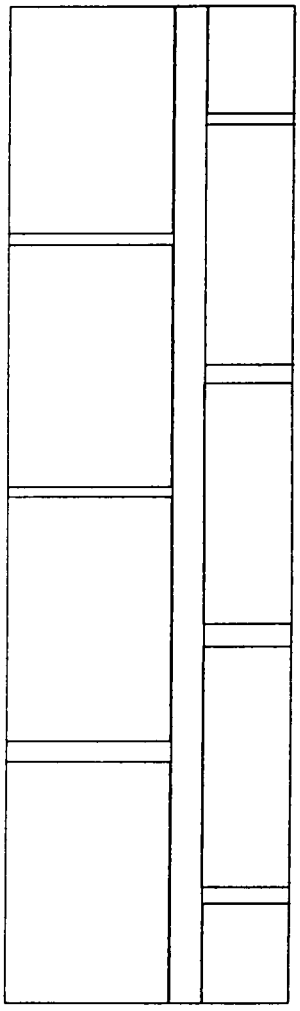


Crack Map for 13" prism

Left Side View



Right Side View



MORTAR COMPRESSIVE TESTING - ASTM C 780

Test Prism No.: _____

Specimen Data:
Date Made: _____
Samples Made by: _____
Mortar Type: _____
Date Specimens put in Moist Room: _____

Test Data:

	30-Day Test	Test Date Data	
Date			
Age of Samples			
Tested By			
Recorded By			
Ultimate Strength (Pounds)			
Batch A			
Batch B			
Average			

APPENDIX B

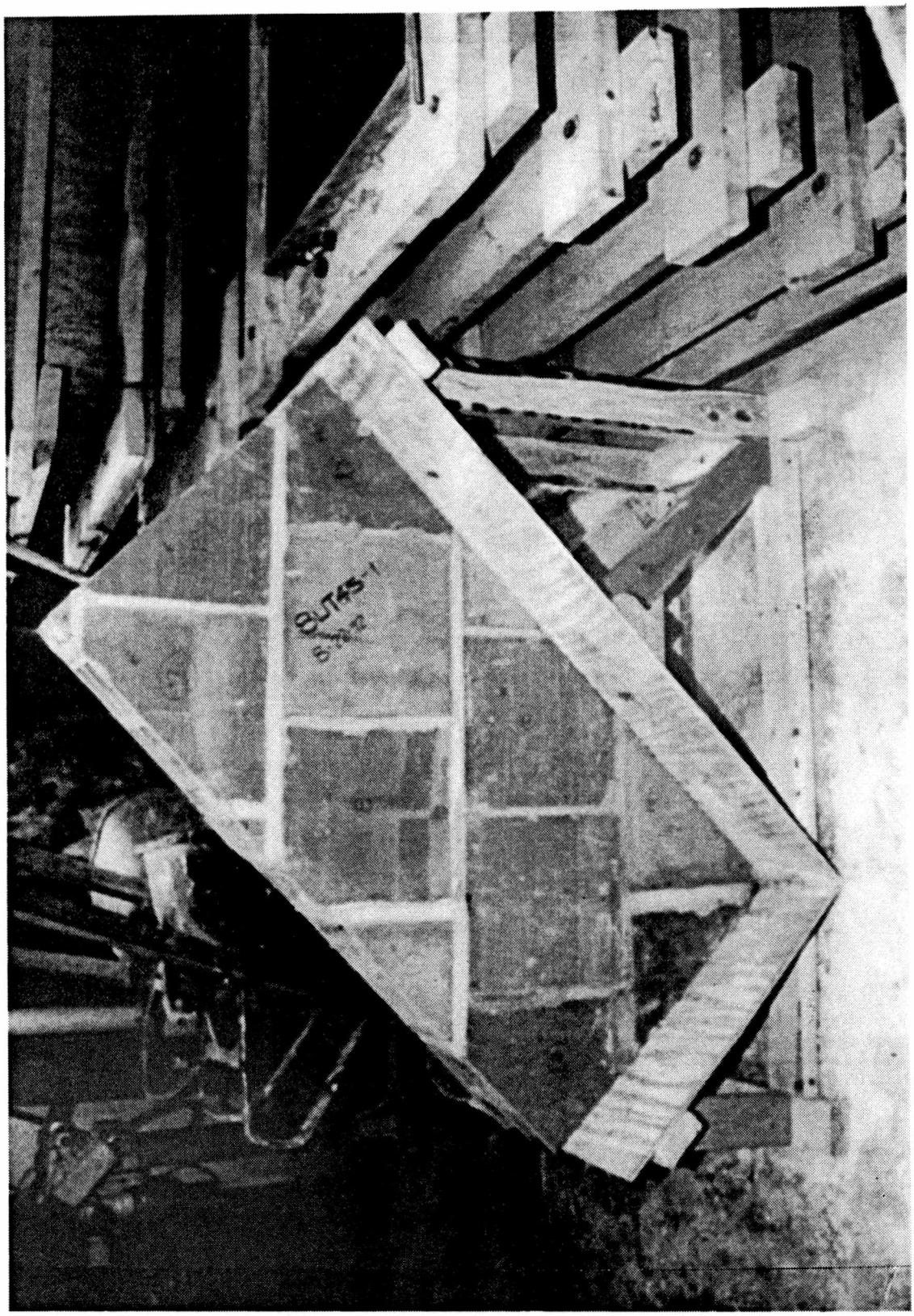
(Fortran Program for Control Data Modification)

```
*
*     ************************************************************************
*     This program takes data from the LVDT mounted to the ram and adjusts
*     the values to account for the initial offset and the machine flexibility.
*
*     The machine flexibility is adjusted using the average elastic modulus
*     of up to six external LVDTs.
*
*     The corrected stress-strain values are then written in ASCII format
*     compatable with DADISP.
*
*     Written by Kurt A. Boyd
*     ************************************************************************
*
*     N = total number of data points collected
*     MP = number of data points to f'm
*     MP5 = number of data points to 50% of f'm
*     MP2 = number of data points to 20% of f'm
*     ELVDT = average modulus for panel LVDTs taken at 50% ultimate
*     DATAP = original stress-strain data of control LVDT
*
*
*     Input original data points from LVDTs
*
      Real ELVDT
      Integer N,MP,MP5,MP2
      Real DATAP(11894,2) , NDATA(11894,2) , NNDATA(11894,1)
      Character*30 filein, fileout
      Print *, 'Enter the Input Filename'
      Read 10, filein
      Open (7,file=filein)
      Print *, 'Enter the Output Filename'
      Read 10, fileout
      Open (8,file=fileout)
      Read(7,1000)N
      Read(7,1000)MP
      Read(7,1000)MP5
      Read(7,1000)MP2
      Read(7,2000)ELVDT
      Read(7,2000)ERAM
   10 Format(A)
 1000 Format(I5)
      Do 100 I = 1,N,1
        Read(7,*) DATAP(I,1) , DATAP(I,2)
  100 Continue
 2000 Format(F7.2)
*
*     Adjust for the initial offset
*
      DEPS = DATAP(MP2,2)-(DATAP(MP2,1)/ERAM)
      Do 200 I=1,N,1
        NDATA(I,2) = DATAP(I,2)-DEPS
        NDATA(I,1) = DATAP(I,1)
  200 Continue
*
*     Correct for the initial linear portion of stress-strain curve
*
      Do 300 I = 1,MP2,1
        NDATA(I,2) = NDATA(I,1)/ERAM
  300 Continue
*
*     Calculate difference due to machine stiffness
*
      EMACH = 1/((1/ERAM)-(1/ELVDT))
*
*     Correct curve strains due to machine stiffness
```

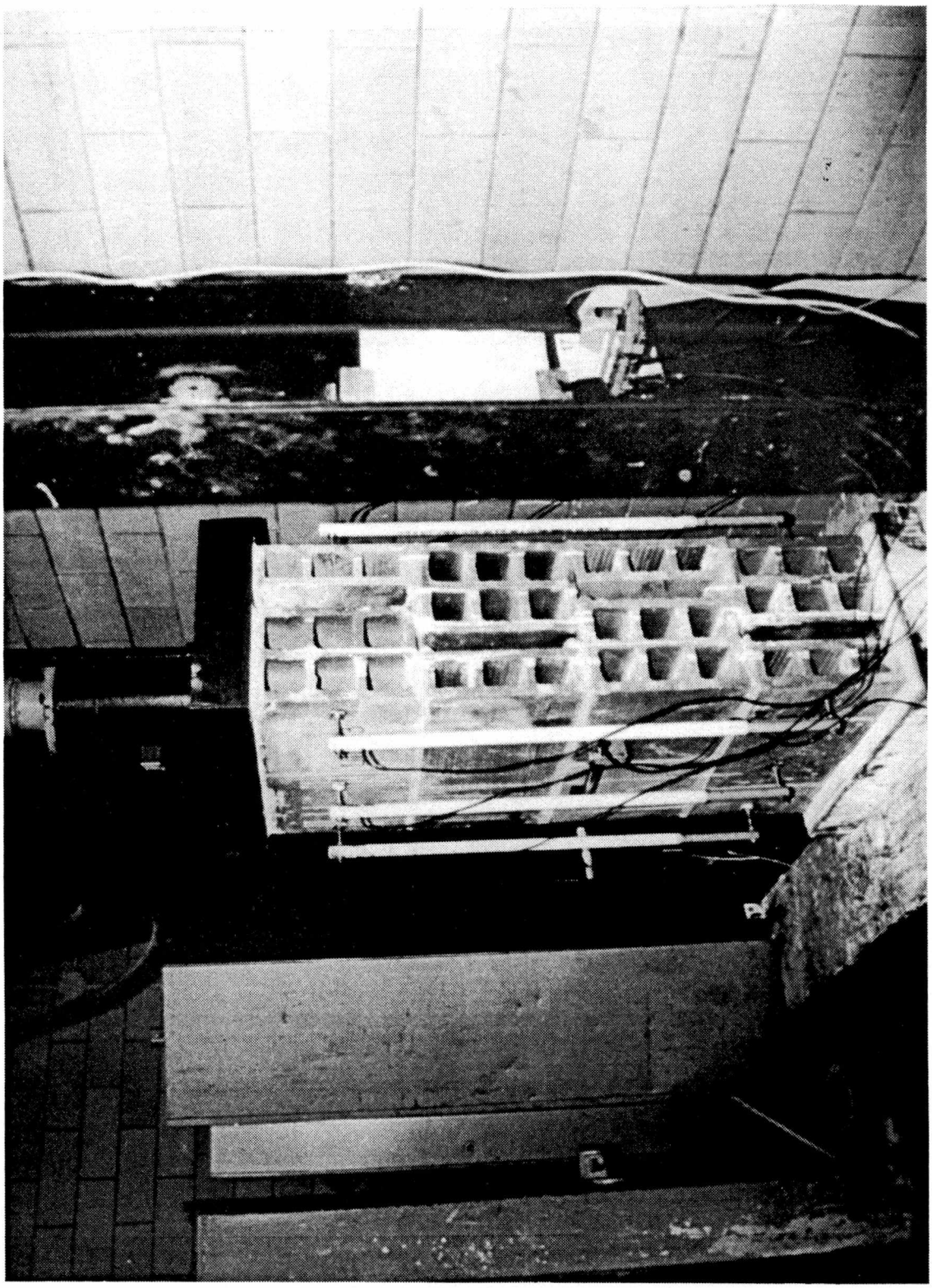
```
*
      Do 400 I=1,N,1
        NNDATA(I,1) = (NDATA(I,2) - (NDATA(I,1)/EMACH))
  400 Continue
*
*     Write statements compatable with DADISP input
*
      Write(8,4000)
      Write(8,4100)
      Write(8,4200)
      Write(8,4500)
      Write(8,4600)
      Write(8,4700)
      Write(8,4800)
      Write(8,4900) N
      Write(8,5100)
      Write(8,5200)
      Write(8,5300)
      Do 600 I=1,N,1
        Write(8,5400) NDATA(I,1),NNDATA(I,1)
  600 Continue
 4000 Format('DATASET TRUE8_90_3')
 4100 Format('VERSION N')
 4200 Format('COMMENT Prism Test')
 4500 Format('FILE_TYPE ASCII')
 4600 Format('STORAGE_MODE INTERLACED')
 4700 Format('INTERVAL 0.100000')
 4800 Format('NUM_SIGS 2')
 4900 Format('NUM_SAMPS ',I5)
 5100 Format('VERT_UNITS ksi')
 5200 Format('HORZ_UNITS in/in')
 5300 Format('DATA')
 5400 Format(' ',f8.6,' ',E13.6)
      Stop
      End
```

APPENDIX C

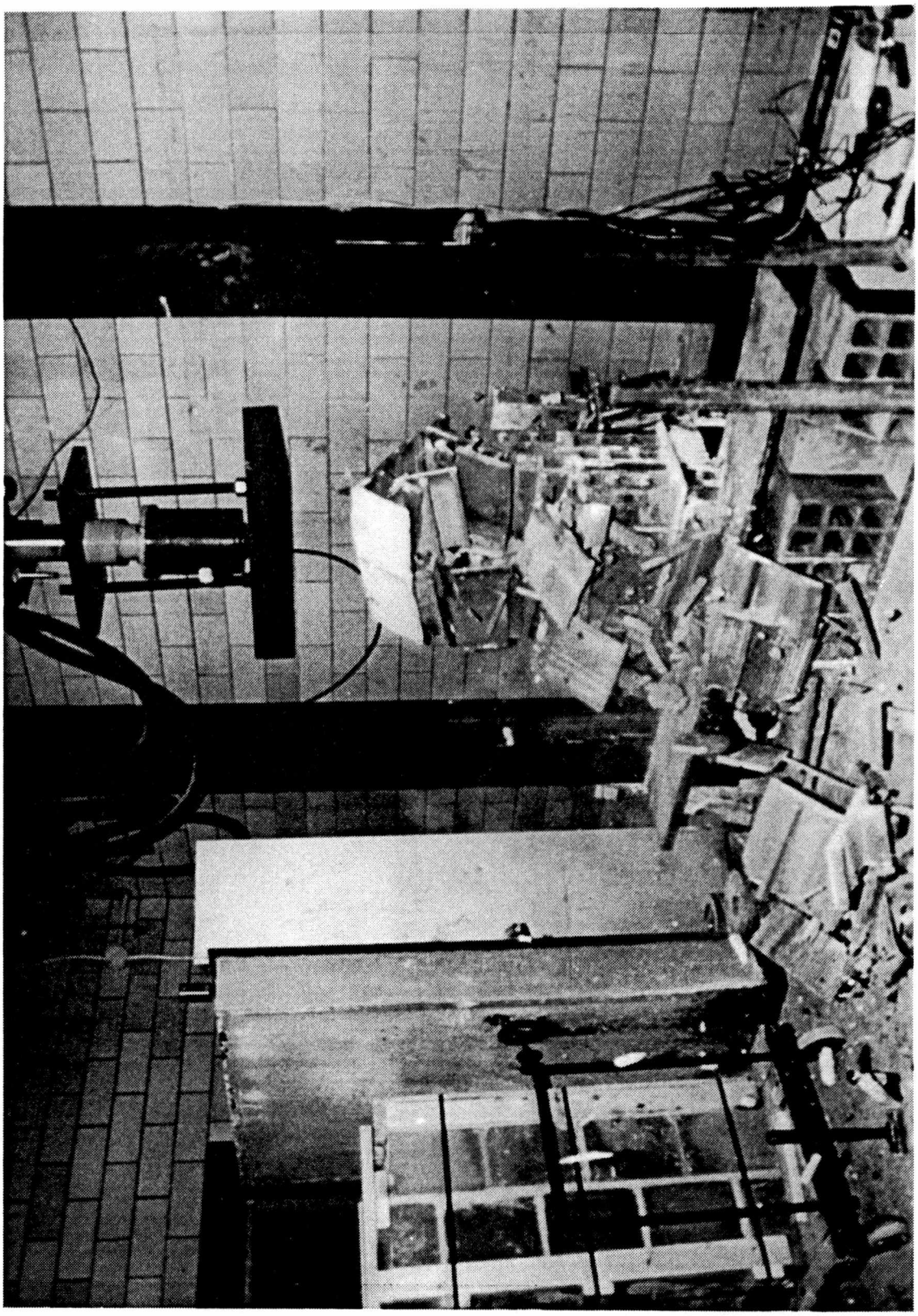
(Photographs)



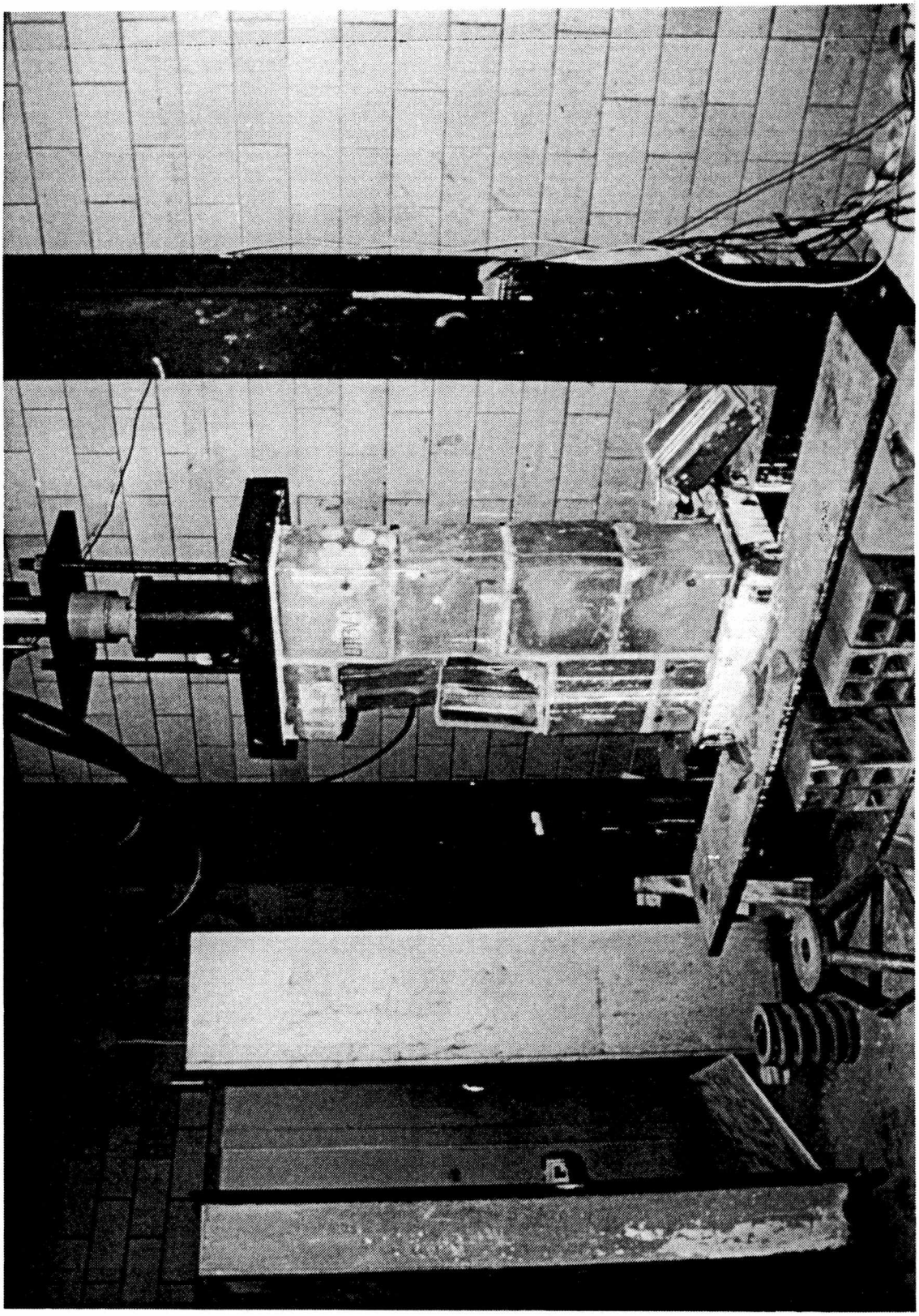
Form for Construction of Prism with 45° Bed Joint Angle



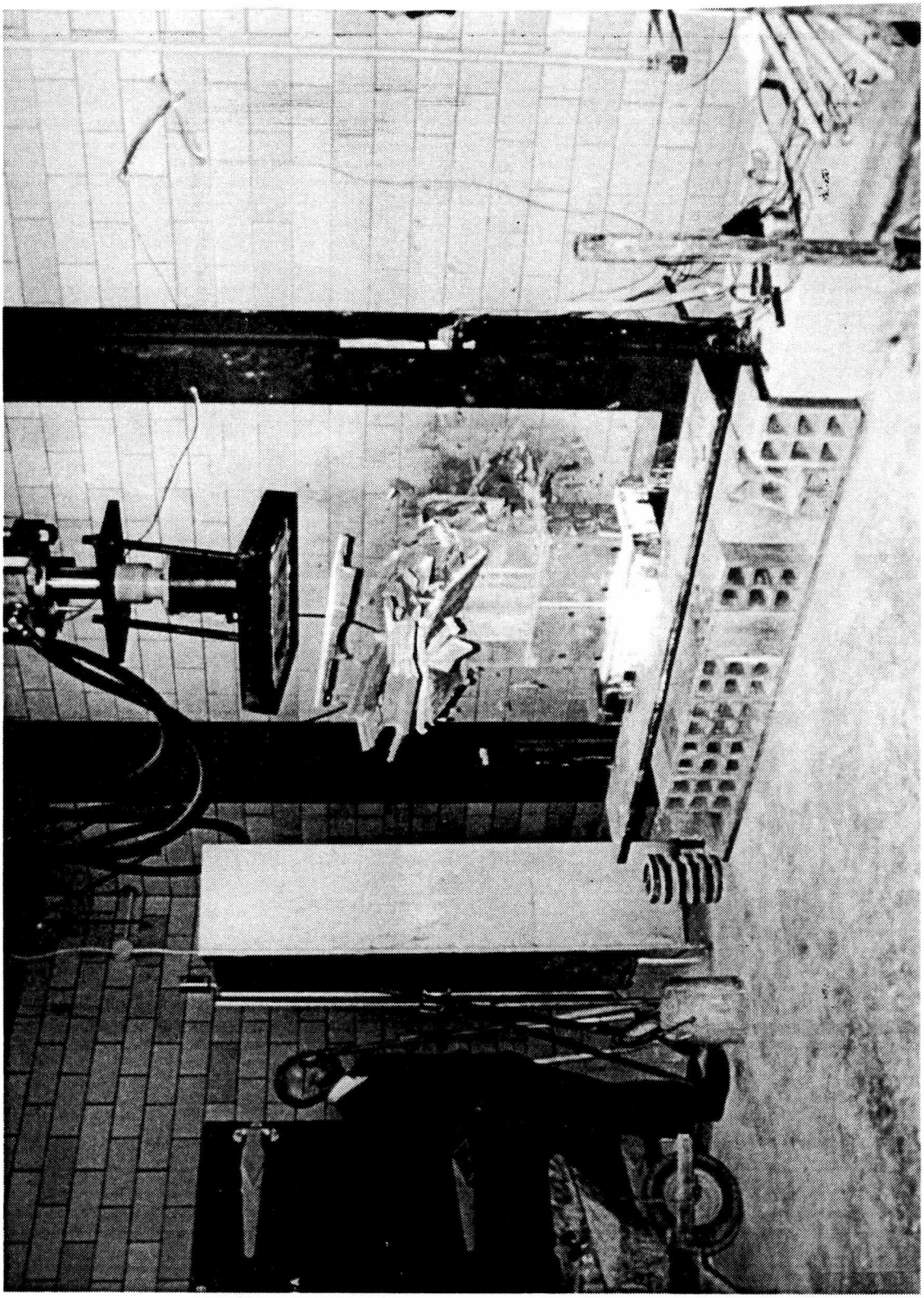
Panel LVDTs on 13" Prism with a Horizontal Bed Joint



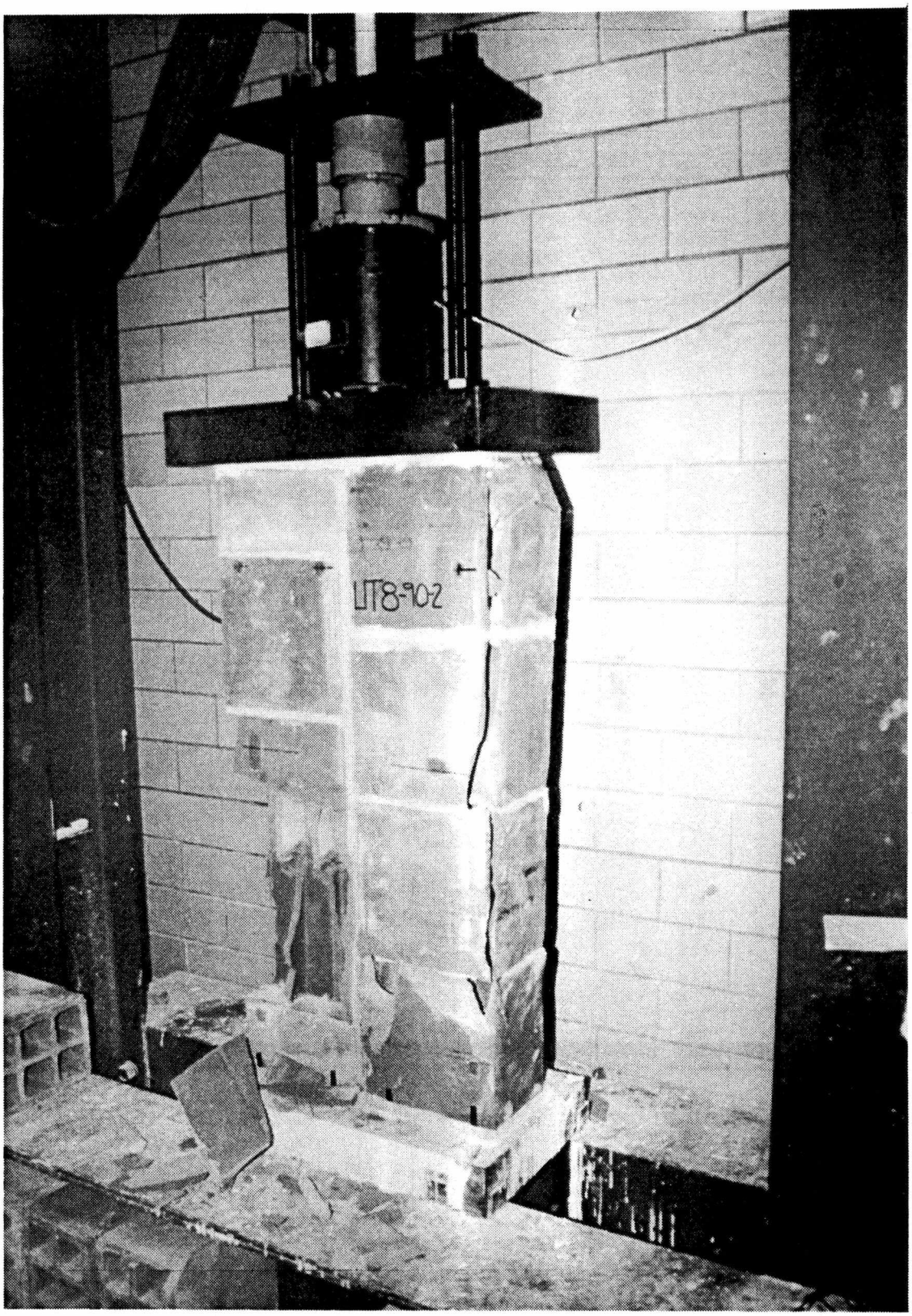
Failure of 13" Prism with a Horizontal Bed Joint



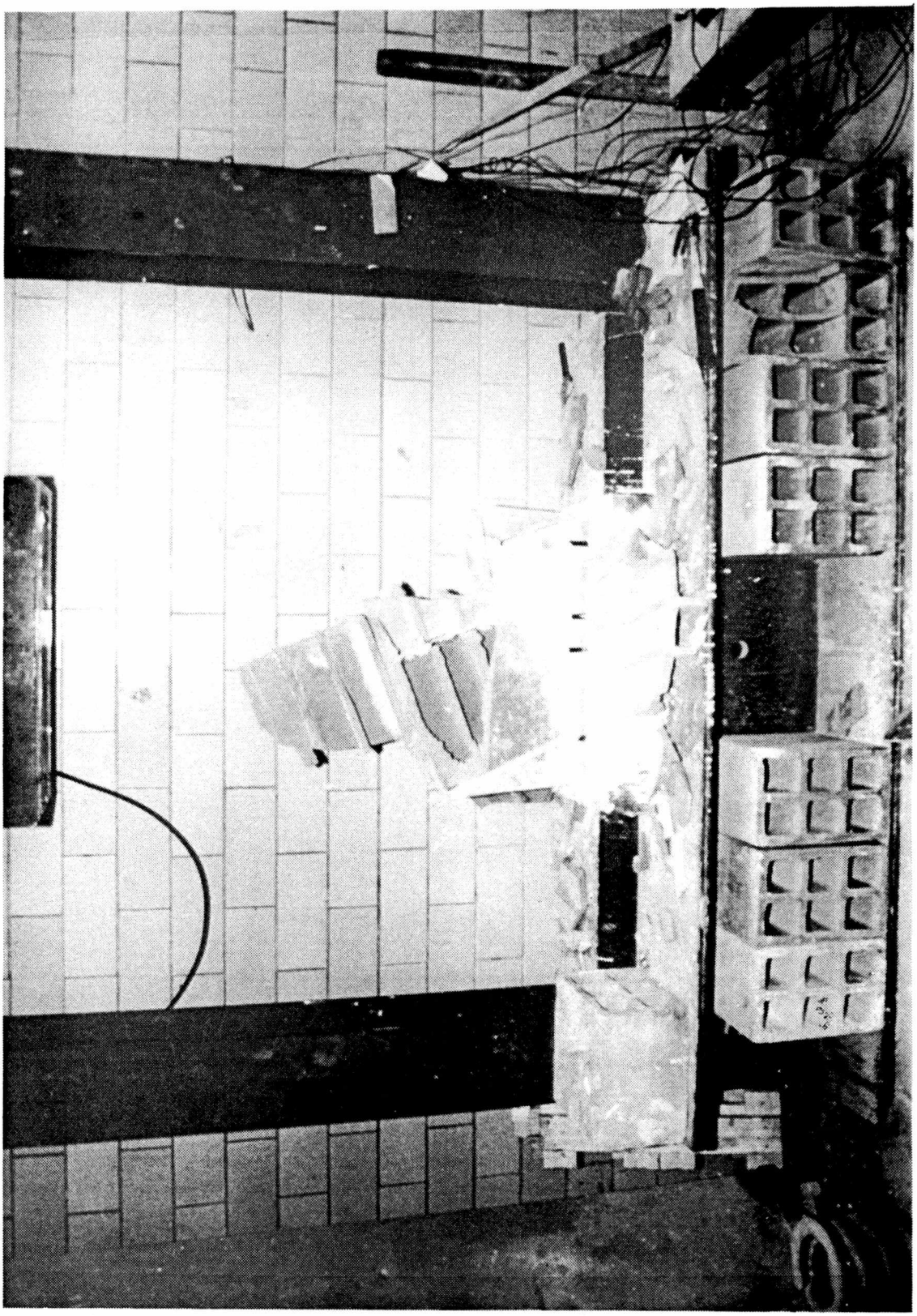
Failure of a 13" Prism with a Vertical Bed Joint



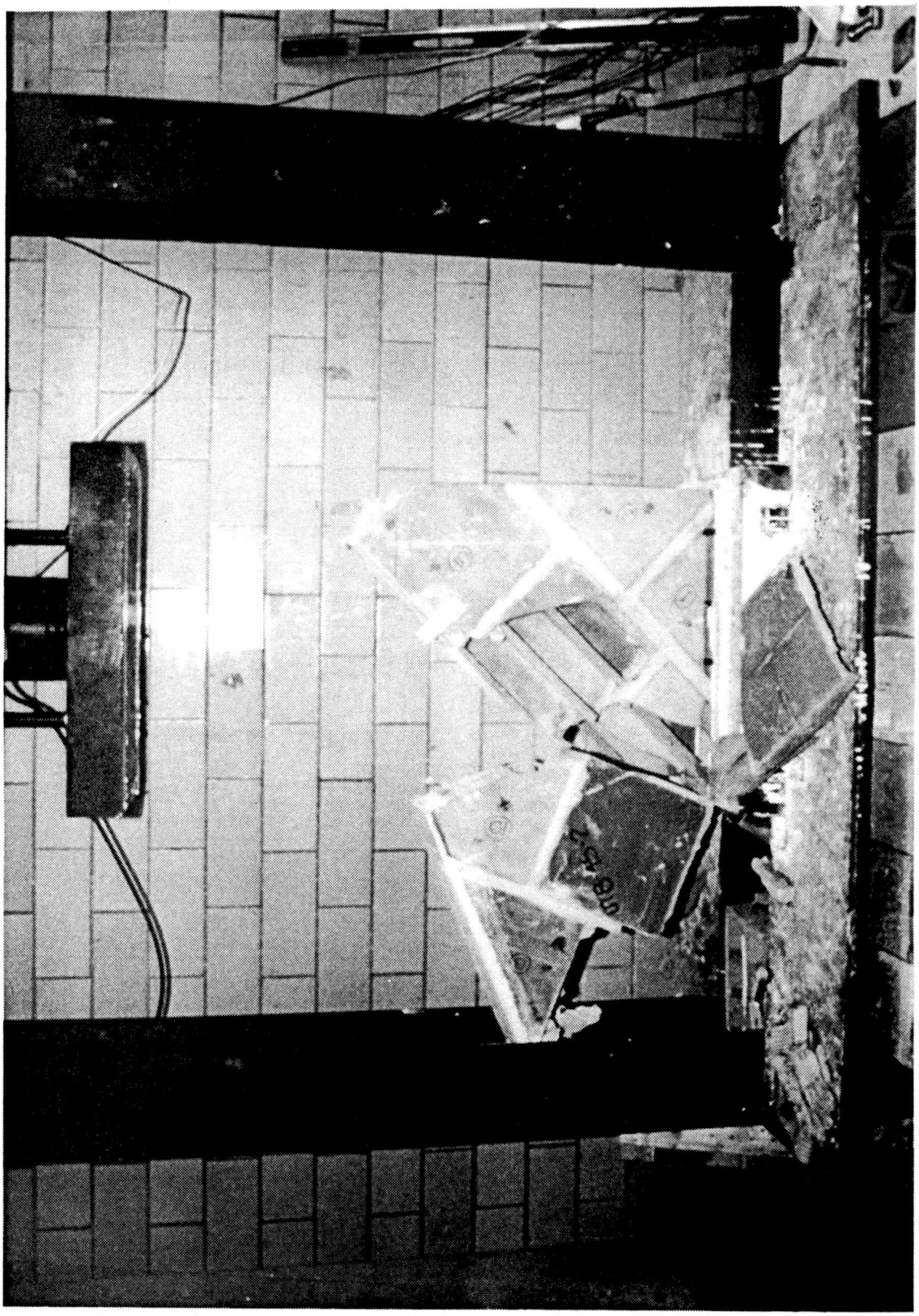
Failure of a 8" Prism with a Horizontal Bed Joint



Failure of a 8" Prism with a Vertical Bed Joint



Failure of a 8" Prism with a Bed Joint Angle of 22.5°



Failure of a 8" Prism with a Bed Joint Angle of 45°



Failure of a 8" Prism with a Bed Joint Angle of 67.5°

VITA

Kurt Allison Boyd was born October 15, 1964 in Chattanooga, Tennessee. He attended McCallie Preparatory High School in Chattanooga, and graduated in 1983. The same year he entered The University of Tennessee at Chattanooga and received a Bachelor's degree in mathematics in 1987. The following semester he began working on his second degree in Civil Engineering. In 1991 he received a B.S degree in Civil Engineering from The University of Tennessee - Knoxville. After working for Trinity Industries in Birmingham, Alabama for one year, he returned to The University of Tennessee - Knoxville and received an M.S. degree in Civil Engineering in 1993.